

Aus dem Bereich
Theoretische Medizin und Biowissenschaften
Fachrichtung Medizinische Biochemie und Molekularbiologie
Der Medizinischen Fakultät
Der Universität des Saarlandes, Homburg (Saar)

Consequences of HIV-1 multifinfection of single cells

Dissertation

zur Erlangung des Grades eines Doktors der Naturwissenschaften
der Medizinischen Fakultät
der UNIVERSITÄT DES SAARLANDES

2010

vorgelegt von

Dipl. Biol. Javier Pablo Martínez

Geboren am: 04. Oktober 1977 in La Plata, Buenos Aires, Argentina.

Gedruckt mit Unterstützung des
Deutschen Akademischen Austauschdienstes, 2010.

Para Papá, Mamá y Dana.

Index	Page
1. Zusammenfassung / Summary	1
1.1 Zusammenfassung	1
1.2 Summary	2
2. Introduction	4
2.1 HIV causes AIDS	4
2.1.1 Structure of HIV-1	5
2.1.2 Replication of HIV-1	9
2.1.3 Course of HIV-1 Infection	13
2.2 Genetic variability of HIV-1	17
2.2.1 HIV-1 classification	17
2.2.2 Error mechanisms of HIV-1	19
2.2.3 Multinfection in HIV-1	20
2.2.4 Robustness of HIV-1	22
2.3 Epistasis	23
2.3.1 Definition of Epistasis	23
2.3.2 Types of epistatic interactions	25
2.3.3 Epistasis in the context of HIV	26
2.4 Phenotypic Mixing	29
2.5 Objectives	33
3. Materials and Methods	36
3.1 List of chemical reagents	36
3.2 Experimental design	37
3.2.1 Approach to quantify relative fitness of HIV-1 RT mutants	37
3.2.2 Approach to quantify phenotypic mixing effects on fitness	39

3.3 Plasmids	40
3.4 Cells and Bacteria	41
3.4.1 Cell lines	41
3.4.2 Bacterial strains	42
3.5 Cell culture	42
3.5.1 Buffers and media	42
3.5.2 Suspension cells	44
3.5.3 Adherent cells	44
3.5.4 Cell counting	44
3.5.5 Freezing and thawing cells	45
3.5.5.1 Freezing cells	45
3.5.5.2 Thawing cells	45
3.5.6 Mycoplasma test	46
3.6 Isolation of PBMC from “Buffy coats”	48
3.7 Generation of wild type and drug-resistant HIV mutants	49
3.7.1 Site-directed Mutagenesis PCR	49
3.7.2 Isolation of PCR products from agarose gels	52
3.7.3 Cloning	53
3.7.3.1 Ligation of PCR fragments into pGEM-T	54
3.7.3.2 Transformation of E. coli ER2925	55
3.7.3.3 Plasmid isolation with the alkaline method	57
3.7.3.4 Sub-cloning into the HIV vector pTN7-Stopp	58
3.7.4 Production of HIV pseudovirus stocks	60
3.7.4.1 Transfection and collection of virus stocks	61
3.7.4.2 Titration and storage of virus stocks	62
3.7.4.3 p24 quantification	64
3.8 Antiviral drugs	65
3.8.1 Zidovudine (AZT, Sigma)	65
3.8.2 Enfuvirtide (T20, Roche)	65
3.8.3 Range of drug concentrations	66
3.9 Pseudotype infections and determination of relative fitness	66
3.10 Renilla luciferase Assay	67
3.11 Statistical analysis	69

4. Results	72
4.1 The fitness ranking of individual mutants explains the complex pattern of epistatic interactions in HIV-1	72
4.1.1 Selection of a HIV-1 mutation pathway for the analysis of epistatic interactions	72
4.1.2 Generation of AZT-resistant mutants of HIV-1, fitness determination and epistasis calculations	74
4.1.3 The fitness ranking of AZT-resistant HIV-1 RT mutants corresponds to their frequency distribution in AZT-treated patients	76
4.1.4 The HIV-1 AZT-resistance pathway is characterized by strong and varying epistasis between the RT mutations at amino acids 41 and 215	79
4.1.5 The epistatic interactions between the mutations changed upon increasing drug pressure and differed between the target cells used	81
4.1.6 Epistasis affects the relative abundance of drug-resistant HIV-1 mutants	81
4.2 Phenotypic mixing modulates the infectivity and fitness of HIV drug-resistant variants	85
4.2.1 Selection of variants for the analysis of phenotypic mixing effects	85
4.2.2 Drug resistance and fitness is modulated by phenotypically mixed HIV Reverse Transcriptases	86
4.2.3 Incorporation of Enfuvirtide (T20)-resistant envelopes do not affect trimer function but alter the infectivity of phenotypically mixed virions	89
4.2.4 AZT and T20 in combination altered the fitness distribution of phenotypically mixed double-resistance variants	92
5. Discussion	95
5.1 On the impact of epistatic interactions in HIV	95
5.2 On the impact of phenotypic mixing in HIV	99
6. References	105

7. Appendix	117
7.1 Table A1	117
7.2 Table A2	120
7.3 Table A3	123
7.4 Table A4	126
7.5 Table A5	127
7.6 Table A6	128
8. Acknowledgments	129
9. Curriculum Vitae	130

1. Zusammenfassung / Summary

1.1 Zusammenfassung

Das humane Immundefizienzvirus (HIV) weist eine hohe genetische Variabilität auf, besitzt aber einen sehr stabilen Phänotyp. Sowohl die hohen Mutations- und Rekombinationsraten, als auch die Fähigkeit zur Mehrfachinfektion von Einzelzellen tragen zur Variabilität bei. Diese ermöglicht es HIV, der Inhibition z.B. durch antivirale Medikamente zu entgehen. Da Mutationen allerdings vor allem eine nachteilige Wirkung auf das Virus haben, muss HIV eine Balance zwischen Replikationsfehlern und Funktionalität bewahren. Dies könnte zum einen durch Fitnessinteraktionen zwischen Mutationen, zum anderen durch phänotypische Mischung geschehen. Durch eine hoch auflösende Fitnessanalyse entlang eines wichtigen HIV-Resistenzentwicklungspfades sowie durch die Quantifizierung des Einflusses der Epistase auf Mutationshäufigkeit und das Ausmaß der phänotypischen Mischung, bietet die vorliegende Doktorarbeit neue Einsichten in beide Phänomene.

Die Muster der epistatischen Interaktionen zwischen den einzelnen Mutationen sind komplex und abhängig von Faktoren wie die An- oder Abwesenheit von antiviraler Medikation oder dem zu infizierenden Zelltyp. Abhängig von diesen Parametern können einige der Interaktionen einen Verlust an Fitness kompensieren und die Epistase kann einen großen Einfluss auf die relativen Mutantenhäufigkeiten haben. In anderen Fällen war der beobachtete Effekt gering. Bedenkt man die starke Abhängigkeit gegenüber diesen unterschiedlichen Faktoren, so scheint die Epistase als

genereller Mechanismus der Abpufferung von Fitnessverlusten eine ineffiziente Robustness-Strategie zu sein. Die Fitness und Infizierbarkeit der phänotypisch-gemischten Varianten sank mischungsabhängig von den reinen Phänotypen her ab. Daraus lässt sich schließen, dass die Genprodukte der Mutationen im Virion keinen drastischen Einfluss auf den resultierenden Phänotyp haben. Dies führt zu der Annahme, dass die phänotypische Mischung *in vivo* zur HIV-Robustheit beitragen kann. Um dies weiter zu untersuchen werden die Fitness- und Infektionwerte, die im Zuge dieser Arbeit bestimmt wurden, in ein mathematisches Modell zur HIV-Evolution eingegeben. Dies wird zu einem besseren quantitativen Verständnis der Konsequenzen von HIV-Multiinfektionen führen.

1.2 Summary

The human immunodeficiency virus (HIV) has an extraordinary genetic diversity but a remarkably robust phenotype. High mutation and recombination rates plus its ability to multinfest single-cells contribute to this diversity and allow HIV to evade selection pressures such as antiviral drug treatments and vaccines. Because mutations are usually deleterious, HIV has to keep a balance between replication errors and functionality. This may be exerted by fitness interactions between mutations and phenotypic mixing. This thesis work provides new insights into these two phenomena by high-resolution fitness analysis along an important HIV drug-resistance mutation pathway and quantifying the impact of epistasis on mutant frequencies and the size of the phenotypic mixing effect. The pattern of epistatic interactions between the specific mutations is complex and dependent on environmental

factors such as the presence and absence of drugs and the host cells used. Depending on those conditions some interactions can compensate fitness losses and epistasis can have a large effect on the relative mutant frequencies while in other cases the effect was small. Given the strong dependency on such environmental factors, epistasis as a general buffering mechanism for fitness losses might be rather inefficient. Overall, the fitness and infectivity of the phenotypically mixed variants decreased gradually between the pure phenotypes in a ratio-dependent manner, suggesting that the incorporation of certain mutant products inside the virions does not change drastically the function of the resulting phenotype. This supports the notion that phenotypic mixing might contribute as a strategy of viral robustness *in vivo*. To further address this issue, the fitness and infectivity values generated from the experiments performed during this thesis work will be feed into a complete mathematical model of HIV evolution. This will help to better understand the consequences of multifinfection in HIV in quantitative terms.

2. Introduction

2.1 HIV causes AIDS

The Human Immunodeficiency Virus (HIV) is one of the most important human pathogens. HIV causes Acquired Immune Deficiency Syndrome (AIDS) of the host by progressively destroying CD4⁺ T helper cells (Norris and Rosenberg 2002), as well as causing oncological and neurological diseases (Salami, Ogunmodele et al. 2009; Saloura, Grivas et al. 2009).

AIDS was first described in 1981 in homosexual men suffering from abnormal opportunistic infections (Gottlieb, Schroff et al. 1981). The ethiological agent was isolated in 1983 from the lymph node of a patient with immune failure and it was called Lymphadenopathy Associated Virus (Barre-Sinoussi, Chermann et al. 1983). In 1986 the virus was renamed HIV (Coffin, Haase et al. 1986).

Today, the infection has become a worldwide epidemic with estimates of around 30 to 36 million infected people, the majority of them living in the Sub-Saharan region of Africa (WHO Report, UNAIDS/09.36E/JC1700E) (Figure 1). Despite the more than 30 years of research, there is still no effective vaccine and current anti-viral therapies fail to eradicate the virus from the infected host. Therefore, and even when prevention programs are showing signs of success, HIV continues to be a major health concern worldwide.

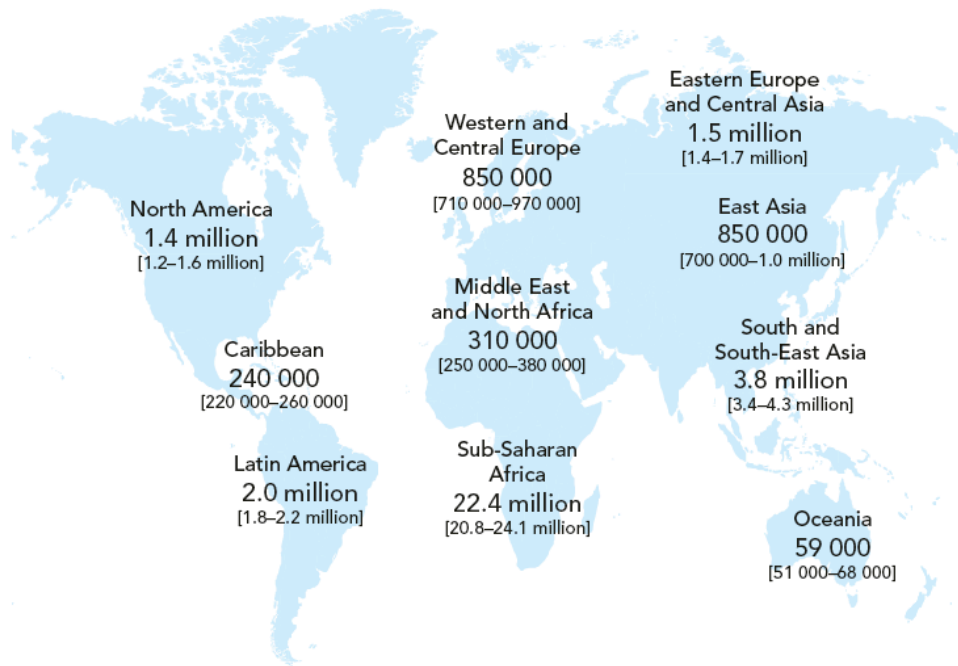


Figure 1. Adults and children estimated to be living with HIV, end of 2008. (Adapted from WHO Report, UNAIDS/09.36E/JC1700E)

2.1.1 Structure of HIV-1

The HIV Type 1 and Type 2 are classified as lentiviruses belonging to the family Retroviridae (Tang, Kuhlen et al. 1999). The infectious particles show a spherical structure with a diameter of about 100 nm (Figure 2A). The viral membrane is built by the host cell cytoplasmic membrane in association with viral envelope proteins. The matrix proteins (MA) are connected with the viral membrane by amino terminal myristyl acids forming an isometric structure (Figure 2B). The viral genome is carried inside the capsid formed by p24, one of the group specific antigen proteins (Gag). The genome is also associated with the nucleocapsid proteins (NC). The capsid is connected to the virion core by the p6 protein and contains the enzymatic proteins reverse transcriptase (RT), integrase (IN) and protease (PR) (Figure 2B).

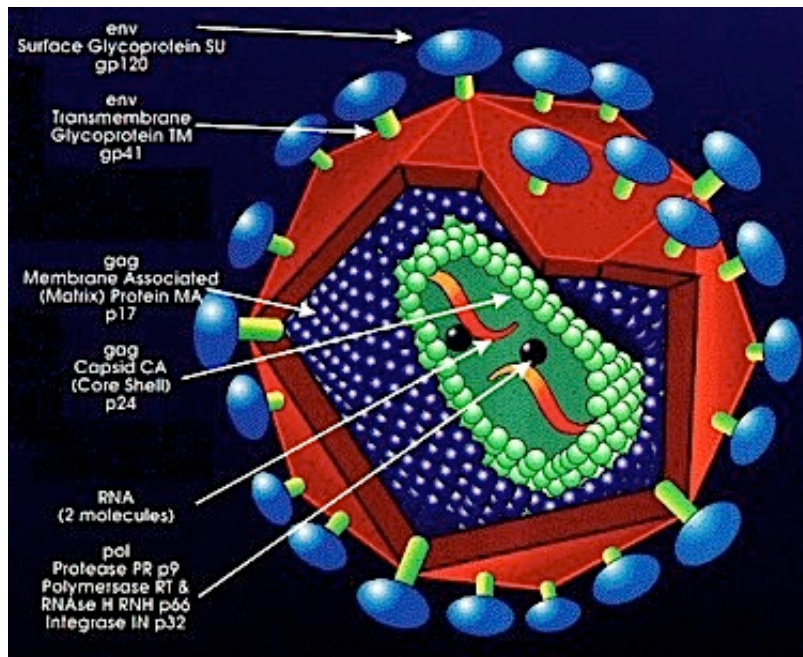
A**B**

Figure 2. The HIV particle. A) Electron microscopy picture of HIV virions emerging from a host cell. B) Schematic representation of the HIV virion showing its most important components.

The HIV-1 genome is around 10 kb in size, and is encoded by two copies of single-stranded RNA consisting of a 5' cap structure and a 3' polyadenylation

signal. Figure 3 shows a schematic summary of the genome, transcripts and proteins of HIV. The genome encodes for proteins Gag (group specific antigens), Pol (enzymatic activities), Env (envelope glycoproteins) and additional regulatory and accessory proteins (Frankel and Young 1998). The coding regions are flanked by regulatory control sequences termed long terminal repeats (LTR) (Coffin 1979). These repetitive sequences consist of three different regions termed U5 (unique), R (repeated) and U3 (unique), which are located at the 5' end and the 3' end in the provirus genome. The LTR bears all *cis*-active sequences as well as elements of the promoter and enhancer sequences controlling viral gene expression. In addition, both LTRs are essential for the process of reverse transcription and integration of the viral DNA into the host cell genome (Nisole and Saib 2004).

The retroviral *gag* gene encodes for a precursor protein of 55 kDa synthesized on ribosomes in the cytoplasm of the host cell. During maturation of the virus, *gag* is processed by the viral protease into the matrix protein (MA), the capsid protein (p24), the nucleocapsid protein (NC) and p6 (Ganser-Pornillos, Yeager et al. 2008). The NC protein forms together with the viral RNA a ribonucleo-protein complex by the interaction with a leader sequence termed ψ -region on the RNA genome. By this mechanism it supports the assembly of the RNA genome and the tLys-RNA primer to initiate the reverse transcription of the genomic RNA (Nisole and Saib 2004). The *pol* genes, encoding for the viral PR, RT and IN, are processed as a single precursor protein together with the *gag* proteins (Nisole and Saib 2004).

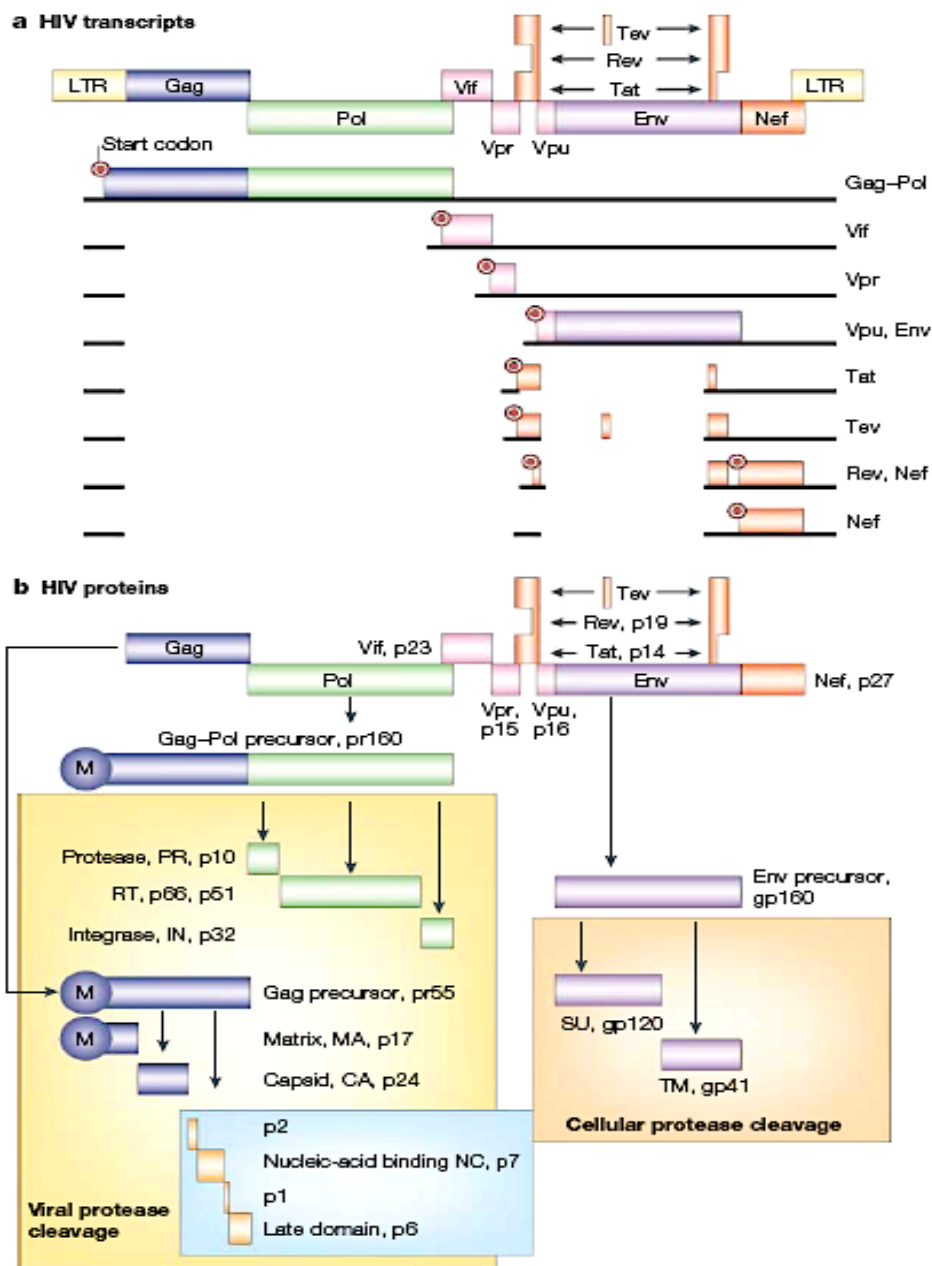


Figure 3. Scheme of the HIV genome, transcripts and proteins. (A) HIV transcripts. Integrated into the host chromosome, the 10-kb viral genome contains open reading frames for 16 proteins that are synthesized from at least ten transcripts. Black lines denote unspliced and spliced transcripts, above which coding sequences are given, with the start codons indicated. Of these transcripts, all singly spliced and unspliced transcripts shown above those encoding the transcriptional transactivator (Tat) require regulator of virion gene expression (Rev) for their export from the nucleus to the cytoplasm. The RNA target for Rev, the Rev response element (Barre-Sinoussi, Chermann et al. 1983), is located within the gene encoding envelope protein (Env). **(B)** HIV proteins. Group-specific antigen (Gag) and

Gag–Pol (polymerase) polyprotein precursors are processed by the viral protease into nine subunits: protease (PR), reverse transcriptase (RT), which contains RNase H, integrase (IN), matrix (MA), capsid (CA), p2, nucleocapsid (NC), p1 and p6 (shown in the yellow box). Env is cleaved by the cellular protease furin into the surface (SU) gp120 and the transmembrane (TM) gp41 moieties (shown in the orange box). Tat is the main transcriptional regulator of the long terminal repeat (Cornell, Technau et al.). Its RNA target, the transactivation response (TAR) element, is present at the 5' end of all viral transcripts. Rev is the main nuclear-export protein and it regulates the shift between early and late viral gene expression. The viral-infectivity factor (Vif), viral protein r (Vpr), viral protein u (Vpu) and negative effector (Nef) proteins are known as accessory proteins because they are dispensable for viral growth in some cell-culture systems. Nevertheless, they have essential roles in viral replication and progression to AIDS *in vivo*. Arrows below polyprotein precursors point in the direction of their processing to mature proteins. Tev contains Tat, Env and Rev sequences and functions as Tat and Rev. **Figure taken from (Peterlin and Trono 2003).**

2.1.2 Replication of HIV-1

The early phase of HIV-1 infection (Figure 4) is marked by the recognition and adsorption of the virus to the host cell membrane mediated by the cellular receptor CD4 as well as the co-receptors CXCR4 or CCR5 (Doms and Moore 2000). During the attachment process, gp120 mediates the contact to the host cell by binding to the CD4 receptor and by an interaction with one of the secondary cellular co-receptor. The co-receptor binding is essential for the infection of CD4⁺ T helper cells (McDougal, Nicholson et al. 1986) and permits either the infection of cells by binding to CXCR4 or by binding to CCR5 (Alkhatib, Combadiere et al. 1996; Feng, Broder et al. 1996). The binding of gp120 to CD4 induces a change of conformation within the trimeric Env protein (Salzwedel and Berger 2000) that leads to the exposition of the viral co-receptor binding site (Kwong, Wyatt et al. 1998). This conformational change exposes a viral fusion peptide present in the

transmembrane (TM) unit of the protein, allowing the viral membrane to fuse with the host cell membrane (Kliger, Peisajovich et al. 2000).

After fusion of the virus with the host cell membrane, the HIV-1 RT catalyzes the transcription of both genomic RNA strands into one double-stranded DNA molecule in the cellular cytoplasm. In addition, the RT bears an RNase H activity allowing degradation of RNA from DNA-RNA hybrid strands. The viral DNA associates with components of the so-called preintegration complex (IN, MA, RT) and is transported to the nucleus where the viral integrase cleaves the 5' and the 3' LTR of the double stranded viral DNA at their 3' ends. Via the resulting ends, the viral DNA is integrated into the host cell genome. The late phase of the HIV infection cycle starts with the transcription of the regulatory genes *tat* and *rev*, and the accessory genes. The Tat protein stabilizes the elongation of viral mRNA and is an important regulatory element of HIV-1. In early stages of the infection cycle, Tat accumulates and binds to the TAR (trans-activating response) element on the newly synthesized mRNA (Peterlin and Trono 2003). This leads to the phosphorylation of the cellular RNA-polymerase II and finally to the stabilization of viral transcriptional elongation (see below). The Rev protein participates in the transport mechanism of viral mRNA from the nucleus to the cytoplasm. For this it binds to the Rev-response element (Barre-Sinoussi, Chermann et al. 1983) located on the mRNA encoding for the *env* gene. In this way, Rev serves as a regulator separating the translation of early genes, which depend on multi-spliced mRNA (i.e. *Tat*, *Rev* and *Nef*), from the translation of late genes (*Gag*, *Pol*, *Env* and some accessory proteins) which depend on single and un-spliced mRNA.

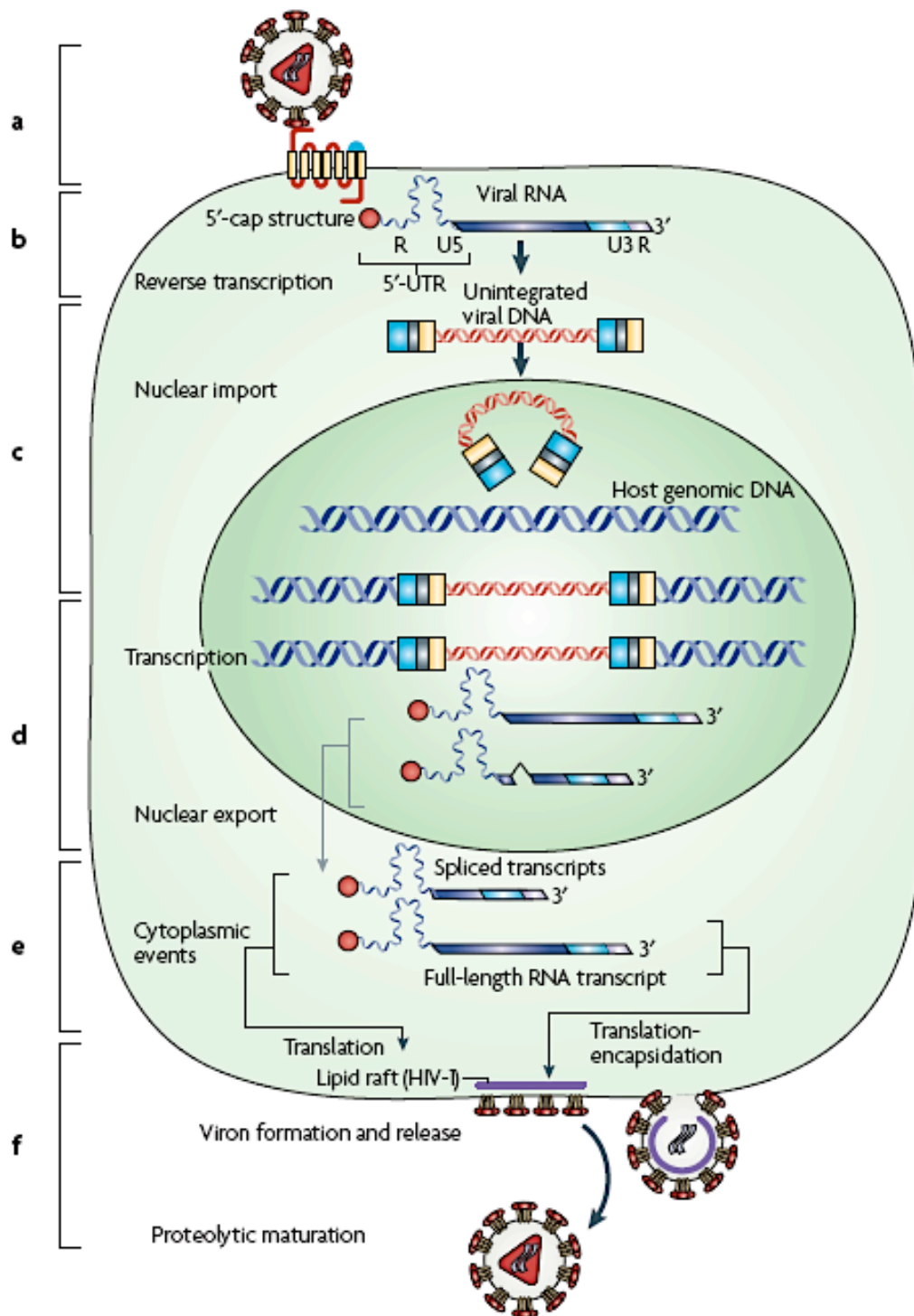


Figure 4. The infection cycle of HIV. The life cycle of HIV can be broadly divided into six essential steps, which are shown here in the figure: interaction, adsorption and entry into the cell (a); reverse transcription of RNA into DNA (b); integration (c); transcription, splicing and nuclear export (d); translation and encapsidation (e); and viral assembly and budding (f). **Figure taken from (Balvay, Lopez Lastra et al. 2007).**

In this late phase, the gp160 protein is transported to the ER and post-translational processes are initiated i.e. glycosylation and cleavage of gp160. The resulting trimer of non-covalently bound gp120 and gp41 is transported to the cell surface by Golgi vesicles. The gag polyprotein is translated from an unspliced mRNA and attaches to the Gag/Pol fusion proteins. After viral assembly, the virus is directed to the cellular membrane for release or, as described recently, to the endosomes of the infected cells (Kramer, Pelchen-Matthews et al. 2005). The final maturation of the infectious particle occurs outside the host cell when the viral protease cleaves the HIV polyprotein products (Ganser-Pornillos, Yeager et al. 2008)

At least five different accessory proteins are known with distinct impacts on viral pathogenesis, evasion from the host immune response and on viral replication. The so-called negative factor protein (Nef) is an early phase protein that accumulates in the cytosol of the infected host cell. It actually increases viral replication and at the same time it decreases the expression of CD4 molecules on the host cell membrane by clathrin-mediated endocytosis (Daecke, Fackler et al. 2005). Thus CD4-Env complexes at the cell surface are prevented and the probability of a secondary HIV-1 infection of that particular host cell is reduced. Furthermore Nef downregulates the major histo-compatibility complex II (MHC-II) protein levels on infected cells and interacts with a variety of different cellular proteins. The viral infectivity factor (Vif) is encoded in a reading frame between the *pol* and the *env* gene. Vif mediates the proteasome depending degradation of a cellular deoxycytidine deaminase (APOBEC3G) and thus allows the production of

infectious viral particles in non-permissive cells (Mehle, Strack et al. 2004). The Vpr (virion associated protein r) binds to the nucleus import complex composed of nucleoporin and importin and it participates in the transport of the preintegration complex towards the nucleus. In addition the Vpr influences the host cell cycle by arresting it in the G2 phase. The Vpu (viral protein U) interacts with CD4 molecules in the ER and triggers their degradation to the ubiquitine-proteasome pathway, preventing generation of CD4-env complexes in the ER. Vpu is also necessary for releasing HIV particles from the cell surface (Wildum, Schindler et al. 2006; Schindler, Rajan et al. 2010). Vpu enhances the release of HIV-1 virions from infected cells by counteracting the function of the host cell factors involved in release restriction Task-1 (Hsu, Seharaseyon et al. 2004), UBP (Callahan, Handley et al. 1998) and the more recently described BST-2, also known as Tetherin (Neil, Sandrin et al. 2007; Van Damme, Goff et al. 2008).

2.1.3 Course of HIV-1 Infection

HIV mainly infects CD4⁺ T helper cells, which are a key cell type in fighting infectious agents. The pattern of disease progression in HIV infection is generally divided into 3 phases: (a) primary infection, (b) clinical latency, and (c) AIDS (Pantaleo and Fauci 1996). Such a course of infection is characteristic of the so-called typical progressors who represent the majority of HIV-infected individuals (**Figure 5**). The average time from initial infection to AIDS progression in typical progressors is eight to ten years (Buchbinder, Katz et al. 1994). Based on studies involving large cohorts of HIV-infected individuals, three additional subgroups have been identified. These include

subjects who have an unusually rapid progression of disease (i.e. rapid progressors) (Phair 1994), those who do not experience progressive disease for many years following primary infection (i.e. long-term nonprogressors) (Buchbinder, Katz et al. 1994; Cao, Qin et al. 1995), and those who progress to AIDS within a time frame similar to typical progressors, but in whom both clinical and laboratory parameters remain stable for an unusually long period of time once disease progression has occurred (i.e. long-term survivors) (**Figure 5**) (Zucconi, Jacobson et al. 1994). It has recently been described a subtype of this group, the so-called elite controllers, who are able to avoid immunodeficiency without the need for antiviral therapy (Deeks and Walker 2007).

Primary infection may be associated with a mononucleosis-like clinical syndrome (Clark, Saag et al. 1991). Due to the lack of specificity and the variable severity of the clinical syndrome, primary infection generally goes unnoticed. However, upon retrospective analysis of the clinical history, it is estimated that 50–70% of HIV-infected individuals experience a clinical syndrome of varying severity during primary infection (Clark, Saag et al. 1991).

Typical Progressors

The majority (70–80%) of HIV-infected individuals belong to the group of typical progressors (**Figure 5**). They experience a six to eight years period of clinical latency (Buchbinder, Katz et al. 1994). However, despite the lack of symptoms, HIV infection is active as is indicated by the persistent replication

of virus and the progressive loss of peripheral CD4⁺ T cells (Embretson, Zupancic et al. 1993). Individuals with CD4⁺ T-cell counts >500 per µl of blood generally remain free of symptoms, whereas the appearance of constitutional symptoms is generally more frequent in individuals with CD4⁺ T-cell counts below 500 per µl. Progression to clinically apparent disease or AIDS-defining illness (CD4⁺ T-cell counts <200 per µl of blood) generally occurs within eight to ten years in typical progressors (Schnittman, Greenhouse et al. 1991).

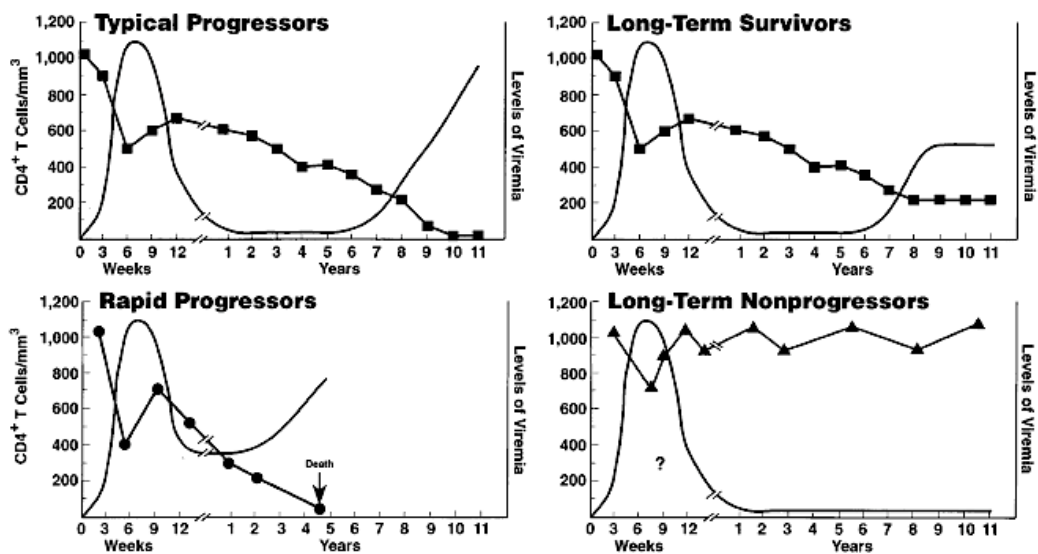


Figure 5. Course of HIV-1 Infection. In vivo the course of infection is characterized by the behaviour of the HIV viral load and the levels of CD4 positive cells. See text for figure details. **Figure adapted from (Pantaleo and Fauci 1996)**

Rapid Progressors

A significant percentage (10–15%) of HIV-infected individuals experience an unusually rapid progression to AIDS within two to three years after primary infection (Phair 1994). Rapid progressors may experience a prolonged acute viral syndrome; in addition, constitutional symptoms of variable severity may

persist after transition to the chronic phase of the infection (**Figure 5**). In rapid progressors the period of true clinical latency may be absent or very brief. Downregulation of the initial burst of viremia may not be very efficient in rapid progressors; even after the initial decrease, the levels of viremia may rise rapidly. Inefficient control of the initial burst of viremia and rapid rise in viremia within the first or second year after primary infection reflects a poor control of HIV infection by the immune system.

Long-Term Non-progressors

A small percentage (less than 5% on the basis of different cohorts) of HIV infected individuals do not experience progression of disease for an extended period of time (Buchbinder, Katz et al. 1994). Long-term non-progressors have CD4⁺ T-cell counts that are within the normal range and are stable over time (**Figure 5**); in addition, they generally have low levels of viremia and preservation of lymphoid tissue architecture and immune function. From a clinical standpoint, long-term nonprogressors are asymptomatic.

Long-Term Survivors

It remains unclear why in a small percentage of subjects who experience the progression of HIV disease within a period of time similar to typical progressors, both clinical and laboratory parameters, although abnormal, remain stable for an extended period of time (Zucconi, Jacobson et al. 1994).

Elite Controllers

It has been recently described a subset of HIV infected individuals who can achieve a long-term control of viremia and avoid immunodeficiency without the need for antiviral therapy (Deeks and Walker 2007). The data gathered from those persons with this phenotype indicate a strong relationship between virus control and the presence of certain host HLA class I alleles and CD8⁺ T cell responses generated through these alleles, as well as strong virus-specific CD4⁺ T cell responses.

2.2 Genetic variability of HIV-1

The continuous and erroneous replication of HIV-1 drives the rapid generation of mutant variants during the persisting infection. This characteristic leads to the formation of a related but genetically distinct virus population termed “viral quasi-species” (Domingo, Sabo et al. 1978; Goodenow, Huet et al. 1989; Meyerhans, Cheynier et al. 1989). This feature makes the virus to consist of a wide range of genotypic and phenotypic variants, most importantly mutants with resistance to antiviral drugs and mutants that are able to escape immune recognition by CD8⁺ cytotoxic T cells and antibodies (Richman 1994; Richman 1994; Havlir and Richman 1996).

2.2.1 HIV-1 classification

Based on the phylogenetic comparison of sequences from virus isolates, HIV-1 has been subdivided into three major sub-groups, named group M (main), group O (outlier) and group N (new) (Arien, Vanham et al. 2007).

Figure 6 shows the phylogeny of HIV-1 and its distant relationship to HIV-2 and to the Simian Immunodeficiency Virus (SIV) from chimpanzee. Based on phylogenetic analysis of a large number of HIV-1 sequences collected over the years and the fact that the first identified HIV group M infection case dates from 1959, it is most probable that the founder of the HIV-1 group M crossed from chimpanzee to humans at some point during the beginning of the 20th century (Korber, Muldoon et al. 2000).

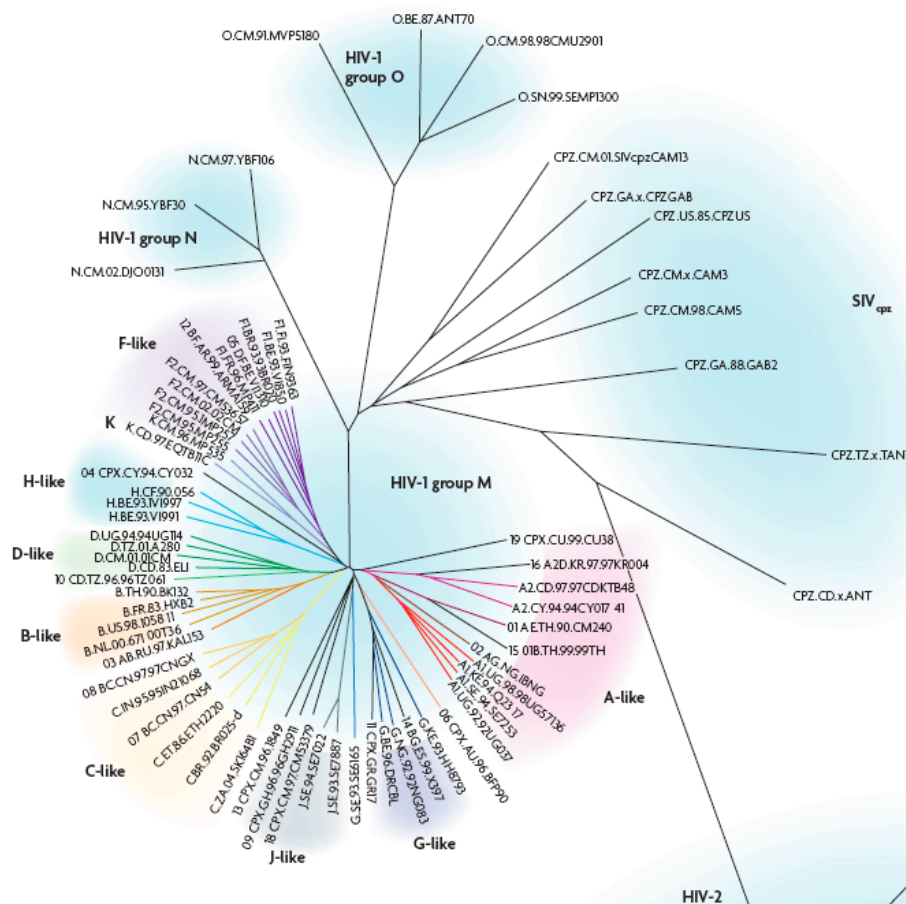


Figure 6. Phylogenetic tree showing the relationship between HIV-1, HIV-2 and SIVcpz. Figure taken from (Arien, Vanham et al. 2007)

Group M is the main cause of the HIV pandemic and has evolved into 9 distinct subtypes (A, B, C, D, F, G, H, J and K) (figure 6) (Kijak and

McCutchan 2005). Subtype C is responsible for more than 50% of world wide infections, followed by subtype B, subtype A and subtype D. The highest diversity of HIV-1 subtypes and recombinants is seen in the central African countries, which is likely to relate to the long time period since the start of the HIV epidemic in that particular region. This extensive genetic variation shown by HIV is mainly due to the error mechanisms involved in HIV replication.

2.2.2 Error mechanisms of HIV-1

Three main mechanisms contribute to the genetic variability of HIV: i) point mutations, ii) hypermutation and iii) recombination. Point mutations arise due to the RT lack of proofreading activity, resulting in an estimated probability of wrong base incorporation into the newly transcribed DNA of about 0.25 per genome per round of replication (Mansky and Temin 1995).

Hypermutation is a process tightly related to the function of the cellular proteins APOBEC3G and 3F (Harris and Liddament 2004). During reverse transcription, these proteins function as cytosine deaminases triggering massive deamination of deoxycytidine to deoxyuridine within the retroviral minus-strand cDNA (Harris, Bishop et al. 2003). As a result, and during synthesis of the plus-strand cDNA, an adenine base is incorporated, thus producing vast amounts of G to A mutations (Harris, Bishop et al. 2003). This process has been shown to generate up to 700 G to A mutations per genome per round of replication (Vartanian, Henry et al. 2002), representing an error catastrophe for the viral genome. HIV counteracts this effect through the viral

protein Vif that binds to APOBEC3 and 3F, and prevents the APOBEC proteins to be packaged inside the virions (Mariani, Chen et al. 2003).

Recombination plays a pivotal role in the generation of HIV variability. During HIV reverse transcription, and due to its low processivity, the RT can “drop” from one RNA strand to continue the synthesis of the minus-strand DNA chain at the other RNA strand (Coffin 1979). This cross-over between both RNA strands can occur at a high rate of up to 30 events per genome per round of replication (Levy, Aldrovandi et al. 2004). If multifinfection of a single cell occurs, recombination may lead to the generation of mosaic proviruses carrying pieces of genetic information derived from different parental RNA genomes.

2.2.3 HIV-1 multifinfection of single cells

HIV has the ability to infect a single cell more than once. Using fluorescence in situ hybridization (FISH) to quantify the provirus copy number per cell and PCR to test for sequence divergence, Jung et al. found a mean of 3 to 4 provirus in splenocytes from two infected patients (Jung, Maier et al. 2002). Multifinfection was also found to be common in SIVmac251 infected Rhesus macaques, in which after 29 weeks of infection more than 10% of the infected splenocytes harboured a mean of 2 provirus (Anke Schultz, PhD thesis, 2009).

The main consequence of multifinfection is the generation of recombinant forms of the virus. If at least two different HIV variants infect the same cell, this may lead to co-packaging of two distinct genomic RNA molecules into

the same virion. When this newly produced virus infects another host cell, the RT will copy both RNA strands to produce a single recombinant DNA provirus. This process can also lead to the production of a mosaic progeny, not only at the genomic level, but also at the protein level, a process named phenotypic mixing (Novick and Szilard 1951).

The precise mechanisms of HIV multifinfection are not yet fully understood. Single cells might be infected more than once by sequential infections with free viruses and infected cells, or via cellular dynamic structures involved in cell-to-cell viral transmission in which multiple virions might infect by a single contact of a target cell with an infected one (Dixit and Perelson 2004; Sourisseau, Sol-Foulon et al. 2007). It has been shown that HIV efficiently propagates between infected and uninfected CD4⁺ T cells and macrophages by the use of the so-called virological synapses and by interacting with cellular lipid rafts (Martin and Sattentau 2009). The virological synapse is a cellular structure appearing at the target-effector cell interface where Env, CD4 and co-receptor molecules are clustered. The directional cell-to-cell spread via the synapse accelerates the rate-limiting step of viral attachment (Sol-Foulon, Sourisseau et al. 2007), thus enhancing infection efficiency (Chen, Hubner et al. 2007). Lipid rafts are tightly packaged but dynamic micro domains in the cellular membrane. Its major component is cholesterol among other lipids (Simons and Ikonen 1997). Carter et al showed an involvement of lipid raft domains in HIV-1 entry in macrophages by co-localizing virus particles with a lipid raft marker at an early time post-infection and by isolating CD4 and CCR5 molecules associated with the lipid rafts

(Carter, Bernstone et al. 2009). Disrupting the lipid rafts by depletion of membrane cholesterol as well as inhibition of cholesterol synthesis showed a significant reduction in HIV entry and in surface expression of HIV receptors (Carter, Bernstone et al. 2009).

Two other cellular dynamic structures that are involved in cell-to-cell virus spread have been suggested to play a role in HIV mult infection. These are filopodial bridges (Sherer, Lehmann et al. 2007) and T-cell membrane nanotubes (Sowinski, Jolly et al. 2008). The filopodial bridges originate from non-infected cells and interact, through their tips, with infected cells. There, a strong association between the viral envelope glycoprotein in an infected cell with the receptor molecules in a target cell have been shown to stabilize the bridge, allowing for viruses to move along the outer surface of the filopodial bridge towards the target cell (Sherer, Lehmann et al. 2007). Membrane nanotubes are formed when T-cells make contact with each other, and are known to connect various cell types, including neuronal and immune cells. T-cell nanotubes are distinct from other cell types since a dynamic junction persists within the T-cell nanotubes allowing them to adopt variably shaped contours. HIV-1 transfers efficiently to uninfected T-cells through these nanotubes in a receptor-dependent manner (Sowinski, Jolly et al. 2008).

2.2.4 HIV-1 robustness in the face of variation

Despite its phenomenal genetic diversity at all levels, HIV demonstrates a remarkably robust phenotype. Robustness is the ability to function despite genetic perturbations. As discussed before, point mutations and

recombination events during reverse transcription of the viral genomic RNA contribute to this diversity, allowing HIV to evade selection pressures such as those exerted by antiviral drugs. Because mutations are usually deleterious, HIV has to keep a balance between replication errors and functionality. How this is achieved is poorly understood.

Two mechanisms might be playing a role in the robustness of HIV: i) the fitness interactions between mutations (termed epistasis) (Elena, Carrasco et al. 2006; Elena, Sole et al. 2010), and ii) the masking and hiding of low fitness genotypes by phenotypic mixing (Wilke and Novella 2003). This thesis work is focused on these two phenomena.

2.3 Epistasis

2.3.1 Definition of epistasis

In general, epistasis is defined as the interaction between genes. However, the use of the word to describe different statistical and biological concepts often leads to misunderstanding among authors in the literature (Cordell 2002). In his book Mendel's Principles of Heredity, biologist William Bateson first introduced the term "epistasis" to describe a phenomenon in which the effect of a genetic variant in one locus was altered or cloaked by a genetic variant at another locus (Bateson 1909). The result is that a phenotype of a certain genotype in one locus is only evident in those variants with a certain genotype at the second locus. **Table 1** shows a typical example of Bateson definition of epistasis. The effect of genotype at locus *A* is only present for the *B/B* variant; if genotype at locus *B* is *b/b* or *b/B* then the effect of at locus

A is not evident. The effect of genetic variation at locus *A* can be masked by locus *B*, therefore it is said that locus *B* is epistatic to locus *A*. In another words, if some gene or mutation combinations result in novel phenotypes, then those mutations must be interacting with each other within trails influencing the same phenotype.

GENOTYPE AT LOCUS <i>A</i>	GENOTYPE AT LOCUS <i>B</i>	
	<i>B/B</i>	<i>b/b</i> or <i>b/B</i>
<i>A/A</i>	1	0
<i>a/a</i> or <i>a/A</i>	0	0

Table 1. Example of the effect on the phenotype of different genotypes at two loci showing epistasis.

Years later, in 1918, Ronald Fisher used the term “epistacy” to describe the deviation from additivity in the effect of alleles at different loci with respect to their contribution to a phenotype (Fisher 1918). Even when this definition is not equivalent to Bateson’s original definition of epistasis, many population geneticists adopted the term “epistasis” to describe the same phenomena (Phillips 1998). According to Fisher, under the null hypothesis of no epistatic interaction, the contribution of combinations of mutations to a certain phenotype follows a linear distribution in which mutations are independent and contribute multiplicatively to the resulting effect. Any deviation from this linear model is sign of mutational interaction.

Recently, Patrick Phillips proposed three different categories in which the term epistasis might be applied: functional epistasis, compositional epistasis and statistical epistasis (Phillips 2008). Functional epistasis describes the

molecular interaction between proteins operating within the same pathways or complexing with one another. Compositional epistasis describes the traditional use of epistasis for the masking or blocking of one allele effect by an allele at another locus. Statistical epistasis is the concept established by Fisher and is the one most often used in the microbiology field since it yields the appropriate measures to describe evolutionary change and solves the problem of having large amounts of genetic combinations in a natural population (such as in bacteria and viruses), which may not manifest strictly on the phenotype but have an impact on fitness.

2.3.2 Types of epistatic interactions

Epistasis might act in different directions. Figure 7 shows a schematic representation of the type of mutational interactions and their effect on fitness measured on a multiplicative scale. If mutations interact so that their combined effect on fitness is greater than expected from their individual effects, then epistasis is said to be synergistic. By contrast, if mutations interact so that their combined effect is smaller than expected, then epistasis is called antagonistic. Depending on the nature of the mutations being deleterious or beneficial, the sign of epistasis can be positive or negative. When mutations are deleterious, synergistic interactions result in negative epistasis and antagonistic interactions result in positive epistasis. The contrary is true for beneficial mutations where synergistic interactions result in positive epistasis and antagonistic interactions result in negative epistasis (Michalakis and Roze 2004; Kouyos, Silander et al. 2007).

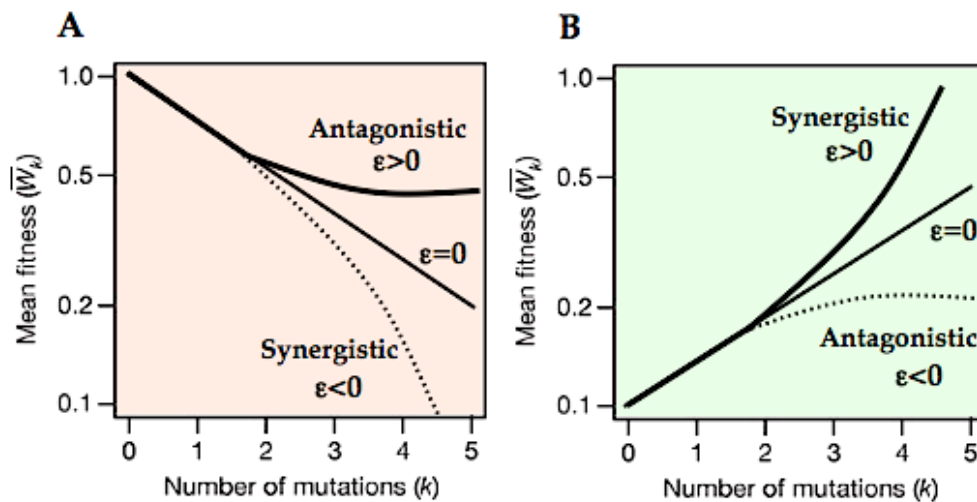


Figure 7. Type of epistatic interactions among mutations in a given genotype and their effect on fitness. Panel A shows the situation for deleterious mutations. Without epistasis ($\epsilon=0$), the accumulation of new mutations leads to a linear decrease in the mean fitness. Mutations can interact antagonistically making the effect on fitness smaller ($\epsilon>0$) or synergistically, making the effect greater ($\epsilon<0$). This leads to an increase or decrease of the expected fitness respectively. The opposite is true for beneficial mutations, but the sign of epistasis remains the same (Panel B).

2.3.3 Epistasis in the context of HIV

Epistatic effects have been observed in many fundamental biological processes like speciation (Gavrilets 2004), long-term selection in model organisms (Carlborg, Jacobsson et al. 2006), and in loci associated with human diseases (Badano, Leitch et al. 2006; Gregersen, Kranc et al. 2006; Cordell 2009). Epistatic interactions also have a central role in evolutionary topics such as the evolution of sexual reproduction (Otto and Gerstein 2006; de Visser and Elena 2007) and the structural evolution of genetic systems (de Visser, Hermisson et al. 2003; Ortlund, Bridgham et al. 2007).

With respect to viruses, interactions between mutations are also common. Epistasis among viral loci has been found in many diverse viruses like the DNA bacteriophage Phi-X174 (Burch and Chao 2004), the RNA

bacteriophage Phi-6 (Silander, Tenailon et al. 2007), the foot-and-mouth disease virus (Elena 1999), polio virus (Crotty, Cameron et al. 2001), vesicular stomatitis virus (Sanjuan, Moya et al. 2004), Chikungunya Virus (Tsetsarkin, McGee et al. 2009) and the human immunodeficiency virus (HIV) (Bonhoeffer, Chappey et al. 2004; van Opijnen, Boerlijst et al. 2006; Parera, Fernandez et al. 2007; Parera, Perez-Alvarez et al. 2009; da Silva, Coetzer et al. 2010). Although a wide range of mutational interactions (positive and negative) was observed, predominance for positive epistasis in viruses seems to be the trend. Epistasis may directly impact viral robustness and the efficiency of variant selection under therapy (Sanjuan, Moya et al. 2004; Elena, Carrasco et al. 2006; Kouyos, Silander et al. 2007; Rolland, Brander et al. 2007; Elena, Sole et al. 2010)

HIV is an ideal candidate to study epistatic interactions in viruses. First, the virus shows an extraordinary genetic diversity which is observed at all possible levels from between patient comparisons to even viral variants within multi-infected individual cells (Jung, Maier et al. 2002). This genetic diversity is accompanied by the capacity of HIV to rapidly adapt to changing environments. This is best exemplified by the rapid selection of escape mutants in response to antiviral drugs. Depending on the nature of the drug-HIV interaction, it may require just few weeks to fix the resistant mutants within the viral population *in vivo* (Havlir and Richman 1996). Second, HIV grows easily in cell culture and assays to determine viral fitness are well established. Third, there is abundant data on HIV sequences and

characteristics within patients that allow estimating the consequences of epistatic interactions within infected hosts.

Under the conditions of mutation-selection equilibrium, fitness interactions between mutations will affect the frequency of individual mutants within a virus population (Nowak 2000). A buffering effect of deleterious mutations is expected if epistasis would be positive. In this case, the abundance of deleterious mutants would be higher than expected and the viral population may respond faster to a new selection pressure supposing that the deleterious mutations would be beneficial under the new growth conditions. A clinically important example and test scenario for this is the selection of drug-resistant HIV variants after the use of antiretroviral treatment. By using amino acid sequence data of the reverse transcriptase and protease regions of HIV-1 isolates from infected individuals undergoing antiviral treatment and the corresponding fitness values measured *in vitro* in the absence of drugs, statistical evidence for the predominance of positive epistasis has been detected (Bonhoeffer, Chappey et al. 2004). However, a number of limitations of this study were raised. One major concern was the likely under-representation of low fit variants in the data set that could have led to false conclusions towards epistasis (Wang, Mittler et al. 2006). Such a biased genome representation seems inevitably linked to the experimental procedure used to generate the genotype to phenotype correlations. A preference for the major viral mutants and thus more fit variants is simply obtained by PCR-mediated amplification and the direct cloning of the respective HIV regions into HIV vectors for subsequent fitness

measurements. Thereby the clonal sequence representation is expected to be directly proportional to the respective fitness of the variant *in vivo*. Other limitations of the study were (i) the lack of fitness values in the presence of drugs so that epistatic effects and their consequences could be compared with and without medication and (ii) the lack of knowledge of the direct path of mutation accumulation including all intermediate mutants.

A straightforward and complementary approach to measure fitness interactions relies on the construction of HIV variants with all mutations along an evolutionary pathway, then measuring their individual and combined fitness effects, and comparing the results with predictions generated under the null hypothesis of non-epistatic interactions (Sanjuan, Moya et al. 2004). While this approach is experimentally feasible only for a limited number of variants and thus lacks completeness over all possible HIV mutation pathways, it is of highest resolution and captures all variants including those of very low fitness. The first part of this thesis work provides the results of the analysis of a specific mutation pathway that HIV follows within individuals after treatment with azidothymidine (AZT), a nucleoside-analog reverse transcriptase inhibitor.

2.4 Phenotypic Mixing

Phenotypic mixing might impact the evolution of a viral population (Bellew and Chang 2006; Elena, Carrasco et al. 2006). While mutation and recombination shape the HIV composition at the genomic level, multifinfection of single cells can lead to another important process: if two distinct virions

infect the same cell the resulting progeny may exhibit phenotypic mixing (Brenner 1957; Zavada, Bubenik et al. 1975). Upon transcription and translation, the genomic RNA of one parental virion may be packaged together with proteins derived from the genome of the other parent to form a new emerging virion (Figure 8). As a result, functional products packaged in the resulting virion might complement the lack of function of the original phenotype such as, for example, failure to integrate due to a defective HIV integrase (Gelderblom, Vatakis et al. 2008) or complementation of defective HIV Reverse Transcriptases and Proteases (Julias, Ferris et al. 2001). In addition, this whole process might contribute to viral robustness by help to rescue certain viruses from extinction by maintaining deleterious and/or low fitness mutants in the population (Wilke and Novella 2003), exert immune escape and expand cellular tropism (Zavada 1982; Canivet, Hoffman et al. 1990; Spector, Wade et al. 1990; Landau, Page et al. 1991; Markowitz, Mohri et al. 2005).

Since its first detection in bacteriophages (Novick and Szilard 1951), phenotypic mixing has been described for Polio Virus (Ledinko and Hirst 1961), Sindbis Virus (Burge and Pfefferkorn 1966), Food-and-Mouth Disease Virus (FMDV) (Wilke and Novella 2003), and also for HIV (Lusso, di Marzo Veronese et al. 1990; Lusso, Lori et al. 1990; Rayner, Cordova et al. 1997).

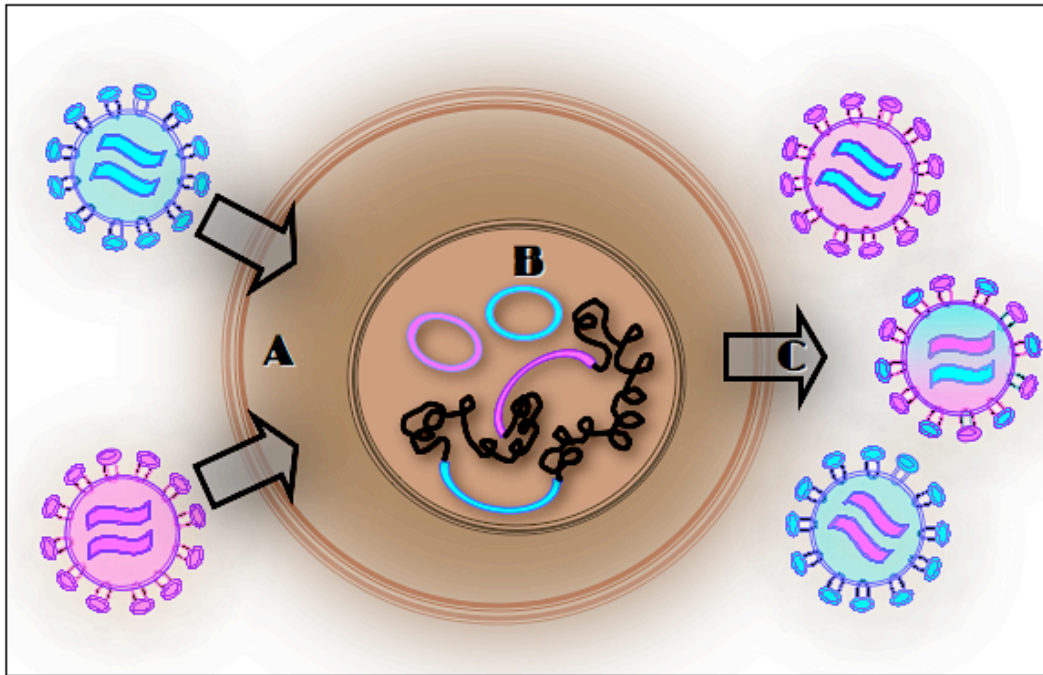


Figure 8. Schematic representation of the phenotypic mixing effect. A, if two different viruses infects the same cell, both parental RNA genomes get reversed transcribed into DNA and integrates into host cell chromosome. B, the proviruses begin to transcribe their DNA by the use of the host cell transcription machinery. Some forms of the viral DNA may remain as unintegrated circular forms. These do not contribute significantly to virus transcription. C, finally the viral RNA is translated within the cytoplasm where full-length viral RNA and structural proteins are randomly assembled into new emerging virions. This random assembly results in the production of mosaic viruses that can carry RNA and proteins derived from different parental proviruses.

For HIV and SIV, *in vivo* data show that multifinfection of single cells is common (Jung, Maier et al. 2002). This suggests that, besides recombination between different proviruses, phenotypic mixing of viral products might be common *in vivo* as well. Indeed, *in silico* simulations suggested that hiding of genetic material by phenotypic masking, that is when phenotypic traits derived from one provirus hide the genetic material of another provirus, might occur approximately 25% of the time (Bellew and Chang 2006). Modeling treatment with two different antiviral drugs showed that, as the treatment advance, an initial homogeneous population of virions (where the genotype

matched phenotype) was substituted by heterogeneous (phenotypically mixed) virions, which became dominant in the population throughout treatment (Bellew and Chang 2006).

To understand how phenotypic mixing might help (and to what extent) to shape a virus population in an infected individual, it is important to unfold how this process can affect infectivity and replication. Research studies on HIV RTase and RNase H indicate that limiting polymerase activity by mixing wild type and mutant RTase affects DNA synthesis (Julias, Ferris et al. 2001). Monitoring reverse transcription of phenotypically mixed virions by using real-time PCR showed that in HIV there is an excess of RTase and RNase H activity, suggesting a robustness strategy where an excess of enzyme activity compensates for the loss of function due to incorporation of mutant polymerase in the virions (Julias, Ferris et al. 2001). Incorporation of mutant glycoproteins resistant to entry inhibitors or to antibody neutralization might result in escape mutants. In addition, phenotypic mixing can result in multidrug resistance and altered cellular tropism, which in turn may influence disease progression (Markowitz, Mohri et al. 2005).

It is still not clear how different combinations of mutant RTase or surface glycoproteins may affect HIV infectivity and replication in the face of antiviral therapy. A straightforward approach to analyze such effects is the generation of phenotypically mixed variants carrying combinations of wild type and drug-resistant RTases or envelope proteins in a specified ratio and to measure their effects on single-round infections with and without the

addition of antiviral drug pressure. The second part of this thesis presents the results of such study by quantifying the fitness and infectivity of HIV variants that were phenotypically mixed. This provides estimates of the size of the phenotypic mixing effect as it would be expected *in vivo*.

2.5 Objectives

The fitness interactions between mutations, referred to as epistasis, can strongly impact evolution. For RNA viruses and retroviruses with their high mutation rates, epistasis may be particularly important to overcome fitness losses due to the accumulation of deleterious mutations and thus could influence the frequency of mutants in a viral population. The relative abundance of deleterious mutants may allow for a faster response to a new selective pressure supposing that the deleterious mutations would be beneficial under the new growth conditions. A clinically important example and test scenario for this is the selection of drug-resistant HIV variants after the use of antiretroviral treatment.

By masking the deleterious effects of mutations, phenotypic mixing could impact the dynamics of the viral quasispecies in an infected individual. Phenotypic mixing might contribute to i) the maintenance of low fitness variants, ii) immune escape, and iii) the cellular tropism of variants in a viral population.

In this work three central questions concerning these issues of the HIV dynamics in infected cells were addressed:

- 1) What is the fitness of individual HIV mutants with no or a low drug resistance phenotype along a specific mutational pathway? Does different host cell environments influence the fitness?
- 2) What is the nature of the epistatic effect on fitness of individual HIV drug-resistant variants? Are epistatic interactions powerful enough to change the expected frequency of HIV drug-resistant variants?
- 3) What is the magnitude of the phenotypic mixing effect on fitness of HIV variants? To what extent does phenotypic mixing influences infectivity?

To address these questions, the fitness of individual drug-resistant mutants was studied in the context of a classical mutational pathway, (the so-called 41-215 cluster), that HIV follows upon treatment with the reverse transcriptase inhibitor azidothymidine (AZT). Fitness measurements were performed in single round infection assays covering physiological drug concentrations *ex vivo* in different types of cells. The direction and magnitude of the epistatic effects were calculated based on the two-locus-two-allele model and the frequency of variants with and without epistasis was assessed by applying a steady-state model of HIV quasispecies dynamics.

The impact of phenotypic mixing on HIV infectivity and fitness was studied by constructing a set of virions containing up to 1:4-ratio combinations of

different wild type and resistant HIV glycoproteins and reverse transcriptases. To determine the effect of phenotypic mixing on envelope function and infectivity, viruses carrying mixes of wild type and entry inhibitor Enfuvirtide (T20) were constructed and tested. To determine the effect on the replication capacities (fitness), viruses carrying mixes of wild type and AZT-resistant RTases were tested. Finally, viruses containing mixes of both AZT-resistant RTases and T20-resistant glycoproteins were used to investigate the effect of phenotypic mixing on a simplified scenario that mimics the situation of a combination therapy.

Altogether, this thesis presents new insights on fitness behavior, epistatic and phenotypic mixing effects of HIV drug-resistant mutants and provides high-resolution data that can be incorporated into a complete mathematical model of HIV dynamics in patients.

3. Materials and Methods

3.1 Chemical reagents

Agarose	Applichem, Darmstadt
Ampicillin (Binotal™)	Ratiopharm, Ulm
CaCl ₂	Merck, Darmstadt
Glacial Acetic Acid	Merck, Darmstadt
Chloroform	Merck, Darmstadt
DMEM	Gibco® Invitrogen, Karlsruhe
DMSO	Applichem, Darmstadt
Ethanol	Roth, Karlsruhe
EDTA	Merck, Darmstadt
EtBr	Sigma-Aldrich, München
FCS	Invitrogen, Karlsruhe
HEPES	Gibco, Invitrogen, Karlsruhe
HCl	Merck, Darmstadt
Iso-Propyl alcohol	BMLS-Dar Es Salaam
IL-2 (Proleukin®)	Chiron Behring, Marburg
Isopropanol	Merck, Darmstadt
KCl	Merck, Darmstadt
LB-Agar	BD, Sparks, USA
LB-Medium	BD, Sparks, USA
L-glutamine	Gibco, Invitrogen, Karlsruhe
Methanol	Merck, Darmstadt
MgCl ₂	Merck, Darmstadt
NaCl	Applichem, Darmstadt

NaOH	Merck, Darmstadt
PBS	Sigma, Deisenhofen
Penicillin/Streptomycin	Biochrom AG, Berlin
Phenol	Merck, Darmstadt
PHA	Difko, Detroit, MI. USA
RPMI 1640	Lonza, Velviers, Belgien
RbCl	Merck, Darmstadt
Saccharose	Roth, Karlsruhe
SDS	Applichem, Darmstadt
TRIS	ICN Biomedicals Inc., Ohio, USA
Triton X-100	Applichem, Darmstadt
Tween20	Merck, Darmstadt

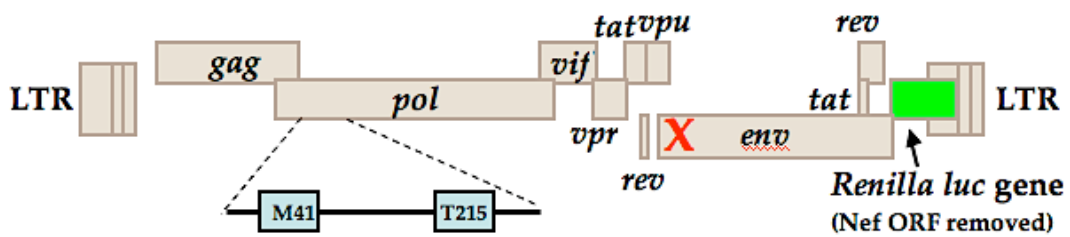
3.2 Experimental Design

3.2.1 Approach to quantify relative fitness of HIV-1 RT mutants

To measure the fitness of the HIV-1 RT mutants along the 41-215 AZT resistance pathway, the respective variants were generated by site-directed mutagenesis PCR (Ho, Hunt et al. 1989). The PCR products were cloned into the HIV-1 viral vector TN7-Stopp that carries the Renilla luciferase reporter gene instead of the HIV-1 Nef gene and lacks a functional HIV-1 Env gene (Figure 9A) (Neumann, Hagmann et al. 2005). The HIV pseudotypes were produced by co-transfection of the TN7-Stopp plasmid in 293T cells together with an HIV-1 Env expression plasmid. The resulting virus stocks were used to infect PBMC and TZM-bl as target cells without the addition of AZT and under physiological concentrations of the drug (Figure 9B). The

fitness values of the wild type and mutants were quantified by measuring the relative luciferase activity as their replication capacity in a single-cycle infection assay. To obtain the final relative fitness values of all variants, the mean fitness of the mutants were normalized to the mean fitness of the wild type without drug (See section 3.11 statistical analysis).

A



B

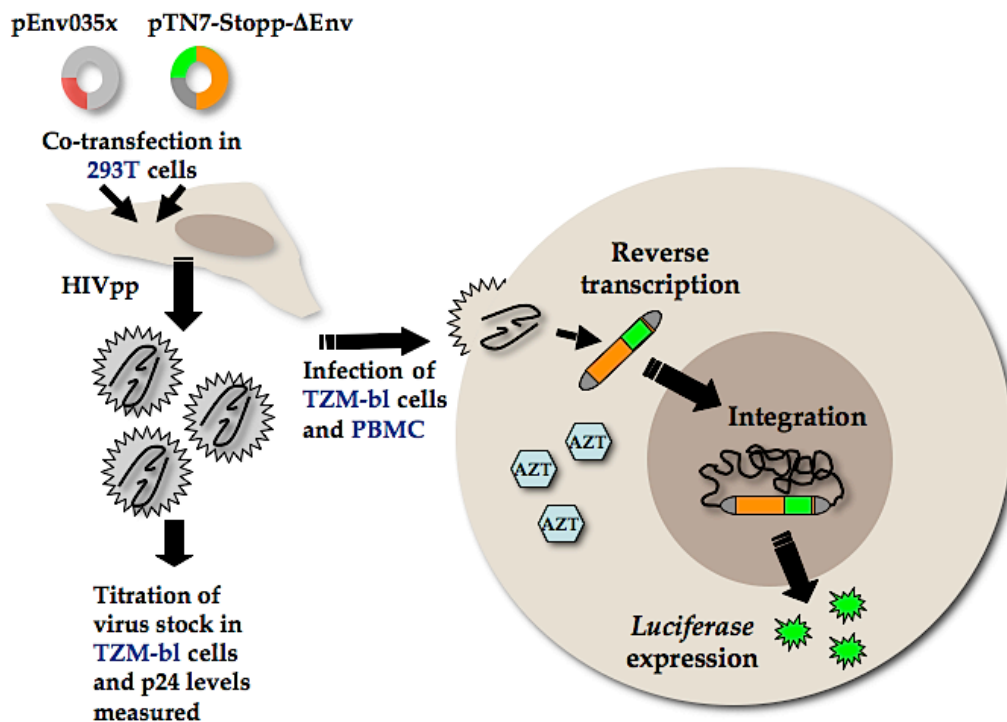


Figure 9. Experimental approach followed for the HIV-1 pseudotype production, infection and fitness measurements. A) Schematic representation of the TN7-Stopp HIV-based expression plasmids. Light blue boxes indicate the mutations introduced in the RT gene. The red X indicates the site in the Env gene where the insertional mutations are placed. B) Representation of the protocol for pseudotype production, titration and infection experiments (see text for details).

3.2.2 Approach to quantify phenotypic mixing effects on fitness

For the purpose of assessing the impact of phenotypic mixing on HIV infectivity and fitness, a set of three different experiments was designed (Figure 10). First, 22 single-round pseudotype viruses carrying specific mixes of wild type, M41L and M41L-T215Y AZT-resistant RTases were constructed to quantify the effect of phenotypic mixing on fitness without AZT and with the addition of drug (Figure 10, number 1).

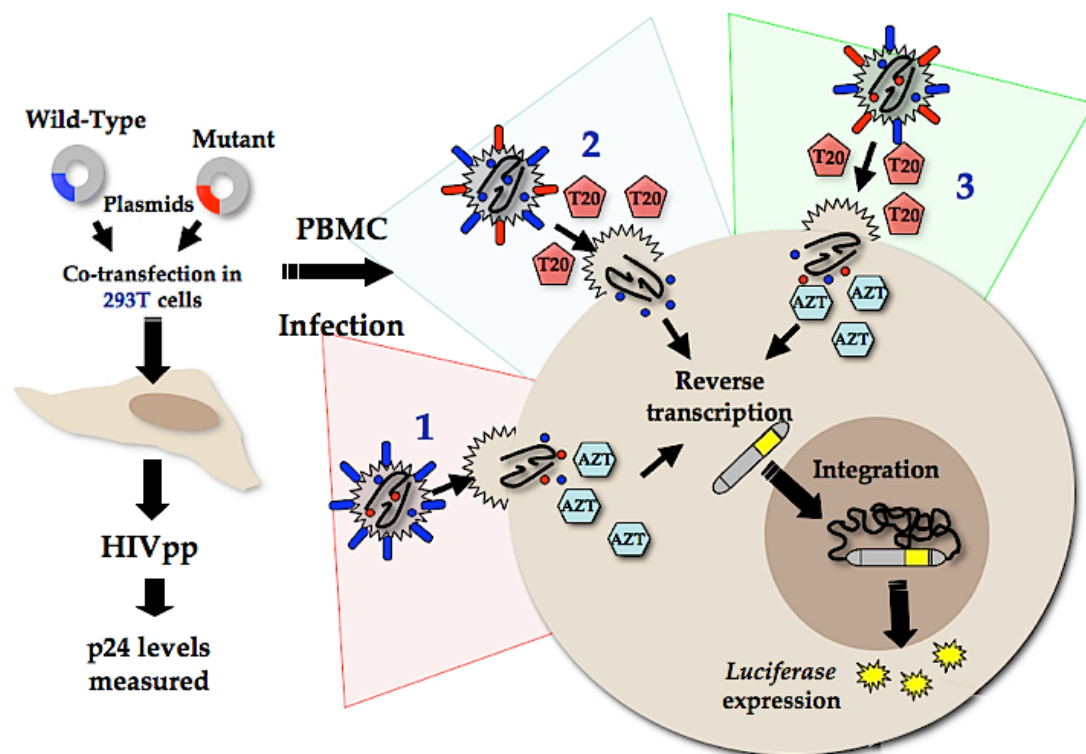


Figure 10. Schematic representation of the three approaches followed to study phenotypic mixing effects on infectivity and fitness (see text for details).

Second, a set of 5 single-round pseudotype viruses carrying mixes of wild type and the entry inhibitor Enfuvirtide (T20)-resistant envelopes were used to quantify the effect of phenotypic mixing on envelope function and infectivity (Figure 10, number 2). Finally viruses constructed with mixes of both AZT-resistant RTases and T20-resistant glycoproteins were used to

investigate the effect of phenotypic mixing on a simplified scenario that mimics the situation of a combination therapy (Figure 10, number 3). The production of phenotypically mixed pseudotypes and quantification of their effects was performed by following the general procedure described in section 3.2.1.

3.3 Plasmids

The source and the characteristics of the plasmids used in this work are described in Table 2.

Table 2. Plasmids used in this thesis work.

PLASMID	DESCRIPTION	SOURCE
pTN7-Stopp	HIV-1 NL4-3 based viral vector carrying the luciferase gene in the position of the nef gene	Dr. M T. Dittmar, Heidelberg
pEnv035x	Plasmid expressing a HIV CCR5-tropism envelope	Prof. C. Jassoy, Leipzig
pEnv035xMut	Plasmid expressing a HIV CCR5-tropism envelope carrying a mutation which confers resistance to the entry inhibitor T20	Prof. C. Jassoy, Leipzig
pGEM-T	Cloning vector carrying the SP6 and T7 promoters and T-overhangs for cloning of PCR products	Promega
pGEM-41L	Cloning vector carrying the M41L mutation of the HIV RTase	(1)
pGEM-215N	Cloning vector carrying the 215N mutation of the HIV RTase	(1)
pGEM-215S	Cloning vector carrying the 215S mutation of the HIV RTase	(1)
pGEM-215Y	Cloning vector carrying the 215Y mutation of the HIV RTase	(1)
pGEM-41L-215N	Cloning vector carrying the 41L and 215N mutation of the HIV RTase	(1)
pGEM-41L-215S	Cloning vector carrying the 41L and 215S mutation of the HIV RTase	(1)
pGEM-41L-215Y	Cloning vector carrying the 41L and 215Y mutation of the HIV RTase	(1)

Table 2. Continuation.

PLASMID	DESCRIPTION	SOURCE
pTN7-41L	pTN7-Stopp carrying the M41L mutation of the HIV RTase	(1)
pTN7-215N	pTN7-Stopp carrying the 215N mutation of the HIV RTase	(1)
pTN7-215S	pTN7-Stopp carrying the 215S mutation of the HIV RTase	(1)
pTN7-215Y	pTN7-Stopp carrying the 215Y mutation of the HIV RTase	(1)
pTN7-41L-215N	pTN7-Stopp carrying the 41L and 215N mutation of the HIV RTase	(1)
pTN7-41L-215S	pTN7-Stopp carrying the 41L and 215S mutation of the HIV RTase	(1)
pTN7-41L-215Y	pTN7-Stopp carrying the 41L and 215Y mutation of the HIV RTase	(1)

(1) Generated during this thesis work in the Institute for Virology, Homburg.

3.4 Cells and bacteria

3.4.1 Cell lines

293T cell line. 293T is a cell line derived from human embryonic kidney cells transformed by the adenovirus E1A gene. The cells stably express the large T-antigen of SV40 and are optimized for efficient transfection and production of lentiviral vectors. Therefore, these cells were chosen for the production of virus stocks used in this work.

TZM-bl cell line. TZM-bl is an indicator cell line previously designated JC53-bl clone 13. The TZM-bl cell line is a HeLa cell clone engineered to stably express CD4, CXCR4 and CCR5. These cells enable simple and quantitative analysis of HIV replication by an integrated copy of the long terminal repeat linked to a luciferase reporter gene. Expression of the indicator luciferase gene is under the control of the Tat protein that is expressed after HIV infection and viral DNA integration into the cell chromosome. These cells were used for titration of virus stocks and infection experiments.

DMSO	10% (v/v)
Penicillin	100 U/ml
Streptomycin	100 µg/ml
Gentomycin	0.25% (v/v)

DMEM medium

DMEM w/o L-Glutamin

Heat-inactivated FCS	10 % (v/v)
L-Glutamine	2 mM
Penicillin	100 U/ml
Streptomycin	100 µg/ml

RPM1 medium

RPMI 1640

Heat-inactivated FCS	10 % (v/v)
L-Glutamine	2 mM
Hepes buffer	10 mM
Penicillin	100 U/ml
Streptomycin	100 µg/ml

Foetal Calf Serum was heat-inactivated for 10 min at 40°C. For transfection and infection experiments, medium was prepared without the addition of antibiotics.

Trypane Blue solution (prepared with double distilled water)

Trypane blue 0.36 % (w/v)

NaCl 0.9 % (w/v)

Trypane Blue solution was sterile filtrated with a syringe micro-filter

3.5.2 Suspension cells

PBMC were cultured in RPMI medium. Cells were controlled for viability, spun down, washed with PBS solution and split in a 1:10 ratio with new medium every 2-3 days.

3.5.3 Adherent cells

293T cells and TZM-bl cells were cultured with DMEM medium. Cells were controlled for viability, washed with PBS, detached from the culture flask surface by a short incubation with Trypsin/EDTA and split in a 1:10 ratio with new medium every 2-3 days.

3.5.4 Cell counting

Cells were counted after Trypane blue staining in a microscope cell counting chamber (Neubauer chamber or haemocytometer). Trypane blue exclusively stains dead cells. The cell counting chamber has 4 quadrants, with each quadrant having a grid of 16 squares. 10 µl of cell samples was diluted into 90 µl Trypane blue, mixed well and added below the coverslide. For each sample all 4 quadrants were counted. The cell concentration is calculated

from the mean number of cells/quadrant multiplied by 10000 and the dilution factor.

3.5.5 Freezing and thawing cells

3.5.5.1 Freezing cells

In order to maintain the library of cells used in the laboratory, cells were aliquoted and cryopreserved in liquid nitrogen.

Protocol

- Cells were counted and spun down at 1400 rpm for 6 min.
- Supernatant was discarded and cells were washed once with PBS and spun down at 1400 rpm for 6 min.
- Supernatant was discarded and cells were resuspended in ice cold freezing media (10^7 cells/ml of freezing media).
- Cells were transferred to a freezing tube with the date, cell amount and cell type and frozen in a styropor (BASF) rack directly at -70°C .
- After 24 hours, the tubes were transferred to the liquid nitrogen tank for further storage.

3.5.5.2 Thawing cells

Vials of frozen cells were quickly thawed in hand and transferred into 10ml of a 37°C pre-warmed medium. Cells were spun down for 10 min at 900 rpm and the supernatant discarded. Cell pellets were washed two times with PBS, between centrifugations of 6 min at 1400 rpm, and transferred into the appropriate culture flask in RPMI or DMEM medium for subsequent culture.

3.5.6 Mycoplasma test

Before freezing, all cells were assayed for mycoplasma contamination by sampling of the cell cultures and performing a PCR-based test with primers specific for several strains of mycoplasma (VenorGeM, Minerva Biolabs). Mycoplasma contamination in cell cultures influences the metabolism of cells and interferes with cell growth and cell behaviour in immunological and biochemical assays. Therefore it was recommended to test periodically the cells for mycoplasma by PCR. The VenorGeM PCR kit contains mycoplasma-specific primers recognizing *Acholeplasma laidlawii*, *Mycoplasma synoviae*, *Mycoplasma hyorhinis*, *Mycoplasma arginini*, *Mycoplasma orale*, *Mycoplasma fermentans*, *Mycoplasma hominis* and *Mycoplasma salivarium*. The product of this PCR is 264-275bp long (dependent on the species). The PCR will also produce a product of 191 bp, an internal control. The cells have to be cultured without antibiotics for 4-5 days prior to testing, since they might inhibit the growth of mycoplasma to below the detection limit. The supernatant of adherent cells can be directly used for the PCR, but the supernatant of suspension cells had to be cleaned up first with Qiamp DNA blood Mini Kit (Qiagen).

Protocol:

PCR-Mix:

10x Reaction buffer	5µl
Primer/Nucleotide Mix	5µl
Internal control DNA	2µl

Sample	2µl
Taq Polymerase (5 U/µl)	0.2µl
H2O	up to 50µl

Thermocycling conditions:

1 cycle	94°C, 2 min
35 cycles	94°C, 30 sec.
1 cycle	55°C, 30 sec.
1 cycle	72°C, 30 sec.
Cool down to 4°C	

For the visualization of the results, a 1.5% agarose gel (5 mm thick, 5 mm comb) was prepared and samples run at 100-120V. 10 µl of loading buffer was added to the samples. Individual concentrations of buffer are specified in the manual of the Qiagen kit.

Procedure:

- Adherent cells:

-100 µl of cell culture supernatant in an 1,5ml reaction tube, incubate for 5 min at 100°C, centrifuge down for 5 sec at 13000 U/min. Supernatant can be used now for PCR.

- Suspension cells:

- 200 µl of cell culture supernatant was incubated for 5 min at 100°C.

- 200 µl buffer AL + 20 µl Protease was added and the mix vortexed for 15 sec, incubated at 56°C and spun down for 10 min.

- 200 µl of ethanol was added and the mix vortexed for 15 sec. After another centrifugation step, the supernatant was added to a spin column in a collection tube and centrifuged for 1 min at 6000 rpm.
- The spin column was put into a new collection tube and 500 µl buffer AW1 was added. The tube was centrifuged for 1 min at 6000 rpm.
- The spin column was put in a new collection tube and 500 µl buffer AW2 was added. The tube was centrifuged for 3 min at 20000 rpm.
- The spin column was put in a new collection tube and 200 µl buffer AE was added. After 1 min incubation at room temperature, the tubes were centrifuged for 1 min at 600rpm. The tube was centrifuged for 1 min at 6000 rpm. After this step, the collected supernatant could be used for the PCR.

3.6 Isolation of PBMC from “Buffy coats”

The PBMC were obtained from buffy coats. Infection of Peripheral Blood Mononuclear Cells (PBMC) from healthy blood donors with the HIV-1 pseudotypes was a major part of this work. A Buffy coat is the resulting fraction of anticoagulated blood after density gradient centrifugation, containing concentrated leucocytes. The Buffy coats were obtained from the blood bank of the Winterbergklinik, Saarbrücken. Blood donors were HIV-1, HIV-2, HBV and HCV negative.

Protocol:

- For each Buffy-coat 4 x 15 ml PBS and 4 x 15 ml Ficoll (Sigma, Deisenhofen) were prepared in 50 ml falcon tubes.
- Each PBS falcon was filled up with 20 ml of blood and mixed by inversion.

- The PBS/blood mixture was carefully added to the Ficoll-containing tubes and centrifuged 1 hour at 1800 rpm
- 10 ml of the supernatant phase was removed and the leucocytes ring collected using a 10 ml pipette avoiding the uptake of Ficoll.
- The collected ring was put into 50ml falcons with PBS and centrifuged for 6 min at 1600 rpm.
- The supernatant was carefully discarded and each pellet resuspended in 5 ml of H₂O for erythrocyte burst.
- Falcons were directly filled with PBS and repeatedly centrifuged for 6 min at 1600 rpm until the cell pellets lost the characteristic red color.
- Cells were resuspended in 50 ml of PBS and centrifuged for 10 min at 900 rpm
- The supernatant was decanted and the PBMC were then re-suspended in 30-50 ml of pre-warmed (37°C) RPMI medium and cultured at 37°C and 4.5% CO₂ until PBMC were further used for experiments or treated for cryopreservation.

3.7 Generation of wild type and drug resistant mutants

3.7.1 Site-directed PCR mutagenesis:

PCR site-directed mutagenesis was used to introduce the desired nucleotide changes at codons 41 and 215 of the reverse transcriptase gene of the HIV-1 NL4-3 molecular clone as template. This technique involves two PCR reactions using overlapping primers (Figure 11 and Table 4 for primer details), as follows: in the first PCR step (PCR 1a), a 1062 base pair fragment containing the desired region of the HIV-1 RT was amplified using a

5' primer carrying a unique restriction site for the BclI restriction enzyme (New England Biolabs) and the 3' overlapping primer carrying the desired RT mutation (Figure 11). In parallel, another PCR (PCR 1b) used the 3' primer carrying the restriction site for the AgeI restriction enzyme (New England Biolabs) and the 5' overlapping primer carrying the other desired RT mutation. The resulting fragments were isolated from an agarose gel and used as templates in the second PCR (PCR 2) with only the 5' BclI and the 3' AgeI primers giving rise to the final template.

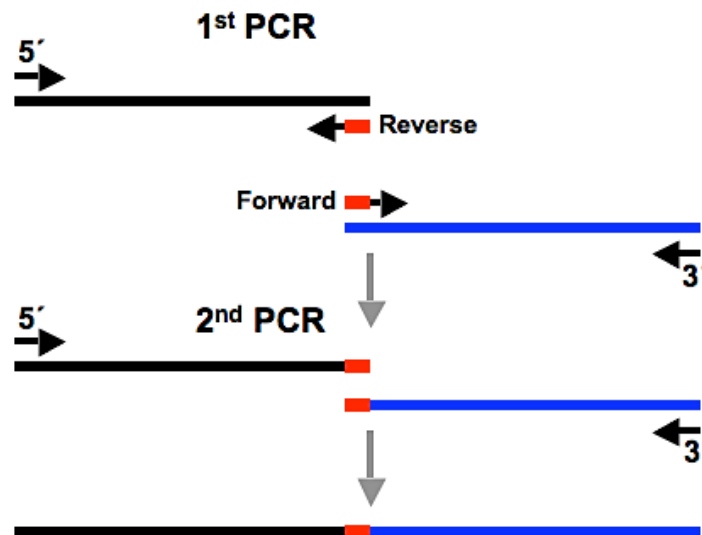


Figure 11. Representation of the site-directed PCR strategy. See text for details.

Table 4. Sequences of the primers used in this work.

Substitution	Template	Primer Name	Sequence (1)
-	NL4-3	3'AgeI	accggtt cttttagaatctcctgtt
-	NL4-3	BclI 5'	tgatcag aatactcatagaaatctcag
M41L	NL4-3	41L-f	gaaattgtacagaattgaaaaggaaggaaaaattc
	NL4-3	41L-r	gaaattttccttctttccaattctgtacaaattc
T215N	NL4-3	215N-f	gtgggatttaacacaccagac
	NL4-3	215N-r	atctggtatgtaaatccccac
T215S	NL4-3	215S-f	gtgggattttccacaccagac
	NL4-3	215S-r	atctgatatgaaaaatccccac
T215Y	NL4-3	215Y-f	gtgggattttacacaccagac
	NL4-3	215-r	atctgatatgaaaaatccccac

(1): Underlined and bold: restriction sites; underlined: codons with the introduced mutations

Protocol (for each mutant):

- First PCR (PCR 1a and PCR 1b)

Mix:

Buffer 10x	5 µl
dNTPs (25 mM)	1 µl
5' Primer (15 pmol)	0.5 µl
3' Primer (15 pmol)	0.5 µl
Taq-polymerase (5 U/µl, Roche)	0.5 µl
Template (1 pmol)	1 µl
H ₂ O	up to 50 µl

Thermocycling steps:

94°C for 2 min

30x cycles 94°C 30 sec

58°C 30 sec

68°C 45 sec

Final elongation step: 68°C for 7 min

- Second PCR (PCR 2)

Mix

Buffer 10x	5 µl
dNTPs (25 mM)	1 µl
5' Primer (15 pmol)	0.5 µl
3' Primer (15 pmol)	0.5 µl
Taq-polymerase (5 U/µl, Roche)	0.5 µl

Fragment PCR 1a (0.5 pmol)	2 µl
Fragment PCR 2b (0.5 pmol)	2 µl
H ₂ O	up to 50 µl

Thermocycling steps:

94°C for 2 min

30x cycles 94°C 30 sec

50°C 30 sec

72°C 60 sec

Final elongation step: 68°C for 7 min.

Samples were run on an agarose gel, isolated (Section 3.7.2) and commercially sequenced by dideoxy-sequencing (GATC Biotech, AG, Konstanz, Germany). The restriction sites introduced in the primers were used for the subsequent cloning of the mutated fragments.

3.7.2 Isolation of PCR fragments from agarose gels

Agarose gel electrophoresis allows the separation of charged molecules (such as DNA at neutral pH) in an electric field. The migration along the gel is dependent on net charge, size and shape of the nucleic acids and the gel matrix.

Protocol:

Buffers

- 50X TAE Buffer

Tris/HCL (pH 7.8) 2 M

Na-acetate	0.25 M
EDTA	0.5 M

Procedure

For identification of the PCR products and subsequent cloned vectors, a standard electrophoresis gel of 1% agarose inside a gel chamber with 1X TAE Buffer was used. DNA was stained by ethidium bromide (EtBr) at a final concentration of 0.7 µg/ml in 1X TAE Buffer. To visualize the running samples and increase their density, for loading the gel, samples were mixed with 1:5 volume of blue marker. A DNA Ladder of 1000 bp/1 Kb (GeneOn, Ludwigshafen) was used as a molecular weight standard, normally at the first and last lanes of the gel. Electrophoresis was carried out at 8 V/cm in 1 X TAE buffer and visualization of DNA-EtBr complexes was done under UV light. The fragments of gel with the corresponding PCR products were then cut out with a scalpel and the DNA purified with the use of a gel extraction kit from Qiagen (QIAquick Spin Gel Extraction Kit).

3.7.3 Cloning:

The cloning procedure followed two main steps:

- First, the products from PCR 2 were ligated into the pGEM-T vector (Promega) via TA cloning. The bacterial strain E. coli ER2925 (New England Biolabs) was transformed with the plasmids and selected on ampicillin agar plates. Plasmid DNA was extracted using the alkaline method. Samples were run on an agarose gel, isolated and sequenced by dideoxy-sequencing (GATC Biotech, AG, Konstanz, Germany).

- Second, pGEM-T plasmids containing the desired RT mutants were digested with the restriction enzymes AgeI and BclI (New England Biolabs) and the respective fragments were cloned into the pTN7-Stopp HIV-1 expression plasmid using the same restriction sites.

3.7.3.1 Ligation of PCR fragments into pGEM-T (Promega)

A peculiar property of Taq DNA polymerase is that, when DNA fragments are generated by PCR, the enzyme introduces one or two extra dATP deoxynucleotides onto the 3'-end of blunt double-stranded DNA in a template-independent manner. pGEM-T is a linearized vector with single 3'-terminal thymidine at both ends. These T-overhangs improve the efficiency of ligation of PCR products by preventing recircularization of the vector and providing compatible overhangs.

Protocol:

Product:

- pGEM-T Vector System

pGEM-T Vector	1.2 µg (50 ng/µl)
Control insert DNA	12 µl (4 ng/µl)
T4 DNA Ligase (4 U/µl)	100 units
2 X Rapid Ligation Buffer	200 µl

- Mix (each sample)

2 X Ligation buffer	5 µl
pGEM-T vector	1 µl
PCR product	3 µl

T4 DNA Ligase	1 μ l
H ₂ O	up to 10 μ l

Procedure:

The ligation of PCR products with pGEM-T was performed as indicated in the pGEM-T and pGEM-T Easy Vector Systems Technical Manual (Promega, #TM042, www.promega.com/tbs/tm042/tm042.pdf). The ligation reactions were mixed by pipetting and incubated overnight at 4⁰C.

3.7.3.2 Transformation of E. coli ER2925 (New England Biolabs)

Transformation of pGEM-T plasmids carrying the ligated PCR products was performed following the Rubidium Chloride (RbCl) method, which is very efficient due to the alkali-ions inside the buffer increasing the uptake of DNA by the bacteria.

Protocol:

Buffers

- Transformation Buffer 1

RbCl	0.1 M
MnCl ₂	0.05 M
CaCl ₂	0.01 M
CH ₃ COOH	0.03 M (pH 7.5 with NaOH)
Glycerin	15 %(v/v)
H ₂ O sterilized and filtered	

- Transformation Buffer 2

MOPS (pH 6.8)	0.01 M
RbCl	0.01 M
CaCl ₂	0.075 M
Glycerin	15 %(v/v)
H ₂ O sterilized and filtered	

Procedure:

To generate competent bacteria, 100 µl of bacteria was precultured in 20 ml LB medium at 37⁰C overnight. 8 ml of the precultured was scaled to 200 ml with LB medium and incubated for 1-2 hours at 37⁰C on a shaker platform. After measuring an OD₅₅₀ of 0.3, the cells were incubated on ice for 15 min and centrifuged 5 min at 2000 rpm. The bacterial pellet was resuspended in 16 ml of the transformation buffer 1, incubated on ice for 15 min and centrifuged again. The cells were inoculated in 4 ml of the transformation buffer 2 and 50 µl aliquots were placed and stored in eppendorf tubes.

Each bacteria aliquot was mixed with 10-50 ng of the desired DNA plasmids and incubated in ice for 30 min. Then, the mix was incubated for 90 sec at 42⁰C (heat shock), allowing the plasmid DNA to enter through the bacterial membrane pores. Immediately after the heat shock, the cells were incubated on ice for another 5-10 min and the mix incubated for 1-2 hours in 1 ml LB-medium. This last incubation step allows the bacteria to express the resistant gene inserted into the plasmid. The bacteria were plated on a 10 cm dish with LB-agar containing antibiotics and incubated at 37⁰C overnight. Only those bacteria that were efficiently transformed with the plasmid grew

colonies. The pGEM-T-containing bacteria were additionally identified by blue/white screening by inactivating the α -peptide coding region of the β -galactosidase enzyme that these plasmids carry. Selected colonies were picked from the plates and inoculated in 5 ml of LB medium for overnight growing.

3.7.3.3 Plasmid isolation with the alkaline method

To obtain the plasmid DNA, it has to be separated from the bacterial genomic DNA. By increasing pH and adding suitable reagents, the cells are lysed and the DNA and proteins denaturized. Once this process is neutralized, the plasmids reconstitute easily due to their small sizes, regaining their circular form and remaining in the solution. Genomic DNA, proteins and other bacterial products are lost from the resulting solution.

Protocol:

Buffers:

- STET Buffer

Saccharose	8 %(w/v)
Tris-HCL	50 mM (pH 8.0)
EDTA	50 mM
Triton X-100	0.1 % (v/v)

- Solution 1

NaOH	0.2 N
SDS	1 %(w/v)

- Solution 2

K-acetate	0.3 M (pH 4.8)
LiCl	9.0 M

Procedure:

The 5 ml overnight culture was centrifuged 5 min at 5000 rpm and the cell pellets were resuspended in 150 µl of the STET buffer. By adding 250 µl of the Solution 1 to the mix and 5min incubation at room temperature the cells are lysed. The neutralization is achieved by adding 350 µl of Solution 2 and 30 min incubation on ice. By centrifugation of the resulting solution, the bacterial genomic DNA and proteins are separated from the plasmid DNA that in turn was precipitated by the addition of 95 % ethanol. The plasmid DNA was washed in 70 % ethanol, dried and resolved in 20 µl of RNaseA-containing water.

3.7.3.4 Sub-cloning into the HIV vector pTN7-Stopp

The pGEM-T plasmids containing the desired RT mutants were digested with the restriction enzymes AgeI and BclI (New England Biolabs) and the respective fragments were cloned into the pTN7-Stopp HIV-1 expression plasmid using the same restriction sites. Digestion by these two enzymes produces two fragments: one of 1060 bp carrying the insert with the desired mutations, and another of 3000 bp (for pGEM-T) and 12000 bp (for pTN7-Stopp) carrying the linearized plasmid vectors.

Protocol:

Enzymes

A list of the restriction enzymes used in this work is listed in Table 5.

Table 5. Properties of the restriction enzymes used in this study.

ENZYME	SEQUENCE	CUT SITE	PROPERTIES
Age I	ACCGGT	A/CCGGT TGGCC/A	Optimal at 37 ⁰ C, suitable for extended digestion. No star activity
BclI	TGATCA	T/GATCA ACTAG/T	Optimal at 50 ⁰ C, suitable for extended digestion. No star activity.

Enzyme Buffer:

K-acetate	50 mM
Tris-acetate	20 mM
Mg-acetate	10 mM
Dithiothreitol	1 mM
pH	7.9

Mix:

Enzyme buffer	1.5 µl
BSA	0.2 µl
AgeI	0.5 µl
BclI	0.5 µl
Plasmid DNA	5µl (0.5 ng/µl)
H2O	up to 20 µl

Procedure:

- The mixes of pGEM-T (carrying the insert with the mutations) and pTN7-Stopp plasmids were first incubated for 2 hours at 37⁰C to allow

digestion by the Agel enzyme. After this first incubation, the temperature was raised to 50⁰C to allow an optimal enzymatic activity of BclI.

- The digested samples were run on an agarose gel and the desired fragments (insert and vector) isolated as described in section 3.7.2. The inserts were then ligated to the vector in a 3:1 ratio following a similar approach as described in section 3.7.3.1.
- Ligation products (the reconstituted pTN7-Stopp plasmid with the corresponding inserts) were then transformed in E.coli ER2925 as described in Section 3.7.3.2 and plasmids isolated as described in Section 3.7.3.3.
- The pTN7-Stopp plasmids were sequenced by dideoxy-sequencing (GATC Biotech, AG, Konstanz, Germany).

For production of large amounts of plasmid DNA, the whole procedure was up-scaled by using the QIAGEN Plasmid Maxi Kit (Qiagen).

3.7.4 Production of HIV-1 pseudotype stocks

For pseudo-typed virus generation, wild type or mutated pTN7-Stopp plasmids were co-transfected with the pEnv035x (a specific plasmid expressing a CCR5-tropic HIV-1 envelope gene) into the 293T cell line. Briefly, 293T cells (10⁶ cells) were transfected with 4 µg of each plasmid DNA using Lipofectamine-2000 (Invitrogen). 48 hours after transfection, virus-containing supernatants were harvested and filtered with 0.45 µm

cellulose-acetate filters (Schleicher & Schuell). Virus stocks were titrated, assayed for p24 levels and stored in 1 ml aliquots at - 80°C until use.

3.7.4.1 Transfection of plasmids and collection of virus stocks

Mix (for each sample)

Solution 1

pTN7-Stopp	3 µg
pEnv035x	3 µg
Optimem (Invitrogen)	up to 50µl

Solution 2

Lipofectamine-2000	2 µl
Optimem (Invitrogen)	up to 50 µl

Procedure:

- 293T cell cultures from 50 ml culture flasks were washed. Cells were counted and plated in 10 cm culture dishes at a density of 10^6 cells/dish with 10 ml of fresh DMEM medium.
- Solution 1 and Solution 2 were incubated separately for 5 min at room temperature (one tube of Solution 1 was left without plasmids and used as a transfection control).
- Both solutions were combined, gently mixed and incubated for 20 min at room temperature to allow plasmid-lipofectamine complexes to form.
- The 100 µl mixture was then added to each plate one drop at the time in a clock-wise manner.

- The transfected dishes were cultured for 48 hours at 37°C in a CO₂ culture chamber.
- Supernatant of transfected cells was carefully removed with a 10ml sterile syringe and filtered with 0.45 µm filters into 15 ml falcon tubes. 1ml aliquots of each supernatant were transferred to 1.5 ml cryotubes and stored at -80°C.
- The remaining cell monolayer of each dish was washed twice with 2-3 ml PBS and assayed for Renilla luciferase expression inside the cells (See Section 2.9)

3.7.4.2 Titration of HIV-1 pseudoviruses with TZM-bl cells

TCID₅₀/ml:

The titer, or TCID₅₀/ml, of an HIV stock indicates the number of infective doses per ml, not the number of virus particles per se. While the total amount of virus in a stock can be measured by a p24 ELISA, the titration assay quantitates infection competent viruses. For titrations, virus stocks were serially diluted in a 96-well plate with the indicator cell line TZM-bl in triplicate for each dilution. The TCID₅₀/ml of each stock is calculated using the dilution point at which 50 % of the cultures are infected.

MOI:

The multiplicity of infection, or MOI, refers to the amount of infective doses used relative to the number of target cells being infected. The MOI is adjusted according to experimental conditions. For example, if the chosen MOI is 0.01 and a total of 5x10⁶ target cells are used, 5x10⁴ cells will initially be infected. Then, if the titer of the virus stock is 1x10⁶ per ml, or 1x10³ per

µl, one would need 50 µl to infect the 5×10^6 cells at a final MOI of 0.01.

Titration of virus stocks was performed by the dilution method with the TZM-bl indicator cell line as target cells and by using the Britelite Luminescence Reporter Gene Assay System (PerkinElmer, #6016979) for quantification of luciferase expression. Prior to the titration procedure, one vial of lyophilized Britelite Substrate Solution was reconstituted with 250 ml of Britelite Buffer Solution. After the substrate was dissolved, the solution was distributed into 15 ml conical polypropylene tubes and stored at -80°C .

Procedure (for two virus stocks)

Day 1

- 100 µl of DMEM medium was pipetted in all wells of a 96-well flat-bottom culture plate.
- 25 µl of virus stock 1 was transferred to each well of the column 1, from wells A to D of the 96-well plate.
- 25 µl of virus stock 2 was transferred to each well of column 1, from wells E to H of the 96-well plate.
- 5-fold serial dilutions were made by mixing and transferring 25 µl of each well from column 1 to column 11. 25 µl from column 11 was discarded and column 12 was left untreated as control.
- 1×10^4 TZM-bl cells in 100 µl medium containing 15 µg DEAE dextran/ml (30 µl per 10 ml = 33 µl per 11 ml) was added to each well and the plate was incubated for 48 hours at 37°C in a 5 % CO_2 incubator.

Day 3

- 100 μ l of culture medium was removed from each well and 100 μ l of the Britelite reagent solution was added to each well.
- After 2 min incubation at room temperature, the contents of each well were mixed several times and 150 μ l were transferred to a 96-well white plate for luminescence measurement.
- Each plate was read in an automated luminometer (PerkinElmer) at an exposure of 1 sec/well, maximum 10 min after addition of the Britelite reagent.
- The raw luciferase values were used to calculate the TCID₅₀/ml according to the method of Reed and Muench using an excel-macro data sheet (provided by Dr. Steffi Link at the Fraunhofer-Institut IBMT, St. Ingbert, Saarland).

3.7.4.3 p24 quantification

Virus stocks were tested for the amount of p24 levels in the transfected supernatant. Even when the amount of p24 in the supernatant cannot indicate the viability of a virus, it gives an idea of the amount of viral particles present in the supernatant. Therefore, the p24 values can also be used to normalize infections. The amount of p24 in the virus stocks was quantified using a standard p24-antigen ELISA diagnostic kit (PerkinElmer). The kit provides reagents for immune complex disruption of antigen/antibody complexes in samples using a combination of low pH and heat. The samples are neutralized and transferred to a microplate. The captured antigen is complexed with biotinylated polyclonal antibody to HIV-1 p24, followed by a streptavidin-HRP (horseradish peroxidase) conjugate. The resulting complex

is detected by incubation with ortho-phenylenediamine-HCl, which produces a yellow color that is directly proportional to the amount of HIV-1 p24 captured. The absorbance of each microplate well was determined by using a microplate reader calibrated against the absorbance of an HIV-1 standard curve.

(PerkinElmer:

http://las.perkinelmer.com/content/Manuals/MAN_HIV1p24ELISA.pdf)

3.8 Antiviral drugs

3.8.1 Zidovudine (AZT, Sigma).

Zidovudine or azidothymidine (AZT) is a thymidine analog reverse transcriptase inhibitor (NRTI). NRTIs are deoxynucleoside triphosphate analogs, but lack a free 3'-hydroxyl group. When taken up by cells, AZT is phosphorylated by thymidine kinases to the active AZT-triphosphate. Once AZT is incorporated into the nascent viral DNA, in a reaction catalyzed by HIV-1 reverse transcriptase (RT), further RT-dependent chain elongation is stopped due to the 3'azido-group (Sluis-Cremer, Arion et al. 2000). AZT was the first approved antiviral drug for treatment of HIV infection.

3.8.2 Enfuvirtide (T20, Roche)

Enfuvirtide (T20) is a synthetic 36-amino-acid oligopeptide fusion inhibitor belonging to the broader group of antiretroviral agents known as entry inhibitors. After binding of virus particles to the CD4 receptor on T lymphocytes and monocytes, molecular rearrangements in the transmembrane subunit of the HIV-1 envelope glycoprotein (gp41) result in

fusion of the virus and cell membranes. These rearrangements involve the association of two helically coiled heptad repeats (HR-1 and HR-2) located in the ectodomain of the trimeric gp41 complex in the gp41 ectodomain. T20 is derived from HR-2 and corresponds to amino acids 127 to 162 of gp41 (Wild, Shugars et al. 1994). Binding of T20 to the trimeric HR-1 complex prevents the association of HR-1 with HR-2, thereby inhibiting fusion and blocking virus entry.

3.8.3 Range of drug concentrations

For the infection experiments, azidothymidine (AZT, Sigma) was used at final concentrations of 0, 0.03, 0.3, 0.1, 0.5, 1, 2, 2.5, 5 and 10 μM for the infection experiments. These cover the physiological concentrations of anti-retroviral therapy (Slusher, Kuwahara et al. 1992; Fletcher, Kawle et al. 2000). The HIV-1 entry-inhibitor Enfuvirtide (T20) was used at final concentrations of 0.08, 0.1, 0.5, 0.8, 2.5 and 10 $\mu\text{g/ml}$ (Neumann, Hagmann et al. 2005).

3.9 Pseudotype infections and determination of relative fitness

Target cells for infection experiments were peripheral blood mononuclear cells (PBMC) from healthy blood donors and TZM-bl cells. Cells were cultured overnight and the next day plated in triplicate or quadruple on 96-well V-bottom plates (Greiner) at a density of 10^5 cells/well. Cells were left untreated (0 μM AZT or 0 $\mu\text{g/ml}$ T20 for the phenotypic mixing experiments) or pre-incubated for 2 hours before infections with drugs at the final concentrations mentioned in section 2.8.3. PBMC from healthy donors were stimulated overnight with Phytohaemagglutinin (PHA, Difco) at a

concentration of 2.5 µg/ml prior to the drug incubation. Infections were performed for each drug treatment by adding wild type and mutant virus at an MOI of 0.5 in 100 µl of medium to untreated or treated cells for each well. Forty-eight hours after infection, cells were washed and assayed for luciferase activity with the Renilla Luciferase Assay System Kit (Promega) (see Section 2.10). The measured luciferase activities from infections were normalized to the transfection efficiencies of 293T cells during HIV pseudotype preparation and/or to the p24 levels of the corresponding viral stocks. The final relative fitness values for all HIV AZT-resistant variants were obtained by relating them to the fitness of the wild type (see 2.11 Statistical analysis). This approach was also followed in the phenotypic mixing experiments.

3.10 Renilla Luciferase Assay

Renilla luciferase is a monomeric 36 kDa protein, which catalyzes the oxidation of coelenterate-luciferin (coelenterazine) to produce light emissions. Post-translational modification is not required for its activity; therefore the enzyme can function as a genetic reporter immediately following translation. The Renilla Luciferase Assay System from Promega (#E2820, #TM055, www.promega.com) is designed to provide a fast and sensitive method of detecting the luciferase from sea pansy (*Renilla reniformis*). It enables measurement of Renilla luciferase activity using either the wild type or new synthetic Renilla luciferase as a primary reporter to study replication and transcriptional regulation, or to normalize experimental variations such as differences in transfection efficiencies.

Product:

Assay Substrate (100X)	1000 µl
Assay Buffer	100 ml
Assay Lysis Buffer (5X)	30 ml

Storage at -20°C

Procedure:

Before cell handling for luciferase measurements, one volume of the 100X Assay Substrate was added to 100 volumes of the Assay Buffer to produce the 1X Substrate Buffer Solution. Since this buffer is prepared fresh, the volume changed depending on the number of measurements performed that particular day.

i) Transfections

- After removing the culture medium, cells were treated briefly with PBS and the PBS discarded.
- 1 ml of the Assay Lysis Buffer (1X, with distilled water) was added to each culture dish. After 5 min incubation, homogeneous lysates were prepared by manually scraping the cells from the culture dishes and transferring them to 1.5 ml eppendorf tubes (Greiner).
- A 96-well white plate was prepared by adding 50 µl of the 1X Substrate Buffer Solution to each well depending on the number of measurements to perform.
- The lysates were cleared from cellular debris by a 30 sec centrifugation at

4⁰C and 50 µl of each lysate was transferred to a 96-well white plate.

- After gently mixing the contents in the wells and incubating the plate for 5 min, the plate was placed in the automated luminometer and the light units measured at an exposure of 5 sec/well.

ii) Infections:

- 48 hours after infections, the 96-well V-Shape plates were centrifuged for 5min at 1400 rpm. The cells remain at the bottom of the V-Shape well.

- The culture medium from each well was carefully taken out, and 60 µl of the Assay Lysis Buffer (1X, with distilled water) was added to each well.

- Each plate was incubated 10 min. During this period, a 96-well white plate was prepared by adding 50 µl of the 1X Substrate Buffer Solution to each well.

- After the 10 min incubation, the contents of each well in the 96-well V-Shape plates were mixed and 50 µl of the lysates were transferred to the 96-well white plates.

- After gently mixing the contents in the wells and incubating the plate for 5 min, the plate was placed in the automated luminometer and the relative light units per second (RLU/s) measured at an exposure of 5 sec/well.

3.11 Fitness estimations and statistical analysis

The method of estimating the mean fitness value for every HIV pseudotype infection was performed as follows:

- (i) The mean value of a given number of independent measurements of RLU/s was estimated for each pseudotype (*RLUpseudotype*).

- (ii) The mean background value, i.e. control (*RLUcontrol*) was used to correct the original value from the background by subtracting it, $RLUcorrected = RLU pseudotype - (3 \times RLUcontrol)$.
- (iii) To normalize the corrected replication capacity, we used the transfection efficiency parameter, *teff*, thus getting absolute fitness estimate $f_{abs} = RLUcorrected / teff$.
- (iv) Finally, the absolute fitness estimates were normalized with respect to the absolute fitness value of the wild type genome without drug (f_0): $f = f_{abs} / f_0$, giving the final relative fitness values.

The above estimates of the mutant fitness by using the sample means were supplemented by evaluating their sample variances using the formulas for variances of the products and ratios of independent random variables (Armitage 2002). The donor cell data were used to estimate the mean fitness and variance values for each mutant using standard formulas for the mean and variance of the sum of independent random variables.

To evaluate the epistasis values two different approaches were used. One is based upon a direct calculation of the mean and variance values using the epistasis formula (see Section 4, Results) and the rules for dealing with the functions of random variables (Armitage 2002). The second one implements a parametric bootstrap method to make inference about the mean and its associated standard error. To this end a normal distribution with the corresponding estimated sample mean and variance was used to draw the fitness values of wt, single- and double mutant

genomes with the size of the generated sample of 1000. The 95% confidence intervals were calculated using the bootstrap estimates of the standard deviation (SD) as $\text{mean} \pm 1.96 * \text{SD}$ (See Section 7 Appendix)

The statistical analysis, epistasis calculations and the steady-state model presented in this thesis work was performed in collaboration with Prof. Gennady Bocharov and Anna Ignatovich from the Institute of Numerical Mathematics, Russian Academy of Sciences, Moscow, Russian Federation.

4. Results

4.1 The fitness ranking of individual mutants drives patterns of epistatic interactions in HIV-1

4.1.1 Selection of a HIV-1 mutation pathway for analysis of epistatic interactions.

In order to measure the relative fitness of specific HIV variants, analyze epistatic effects and their dependence on environmental factors such as host cells and antiviral drugs, a specific mutational pathway that HIV-1 follows *in vivo* during treatment with zidovudine (AZT) was chosen (Figure 12).

AZT is the prototypic reverse transcriptase (RT) inhibitor first used in infected patients and is a common component of current anti-retroviral formulations. Once inside the cells, AZT is phosphorylated by thymidine kinases to the active AZT-triphosphate. Upon incorporation into the growing HIV DNA strand, the RT-dependent chain elongation is stopped due to the 3'azido-group (Sluis-Cremer, Arion et al. 2000). Treatment of HIV-infected individuals with AZT leads to the selection of AZT-resistant HIV-mutants with defined amino acid changes in the RT. The HIV-1 resistance pathway chosen is characterized by the key AZT-resistant mutations at positions 41 and 215 of the RT (Lacey and Larder 1994; Beerenwinkel, Daumer et al. 2005).

Even when the mechanisms of resistance are not completely clear, biochemical studies have suggested a mechanism of AZT resistance

involving terminal AZT removal from the blocked primer strand in an ATP-dependent pyrophosphorolysis reaction (Boyer, Sarafianos et al. 2001; Boyer, Sarafianos et al. 2002). This reaction might be enhanced by the T215Y mutation by promoting ATP binding (Boyer, Sarafianos et al. 2001). Contacts with the 215 side chain could be made via parallel aromatic ring stacking of the adenine base of ATP, forming a number of van der Waals contacts as has been suggested previously (Boyer, Sarafianos et al. 2001; Boyer, Sarafianos et al. 2002) (Boyer et al, 2001). Structural mechanisms whereby the M41L mutation could lead to increased ATP binding are less clear. The 41 residue is located some distance from the 215 residue and is somewhat buried, making direct interaction with ATP unlikely (Chamberlain, Ren et al. 2002). The M41L mutation introduces a branched side chain that potentially might disrupt this buried region. It thus seems more likely that a conformational rearrangement occurs either within the catalytic complex or on binding of ATP rather than that there are two distinct ATP binding positions, each of which is strengthened by the mutations at either residue 41 or residue 215. The former model would be consistent with the strong effect of the combination of the M41L and T215Y mutations on AZT resistance.

A schematic representation of the pathway is shown in Figure 12. The highly AZT-resistant double mutant M41L-T215Y appears *in vivo* after around 255 weeks of treatment and requires a number of intermediate mutants of which only the M41L and T215Y mutants are commonly observed (Beerenwinkel, Daumer et al. 2005). However, at least one of the other possible

intermediates, T215S, T215N, M41L-T215S and M41L-T215N must have been transiently generated (Figure 12, in grey).

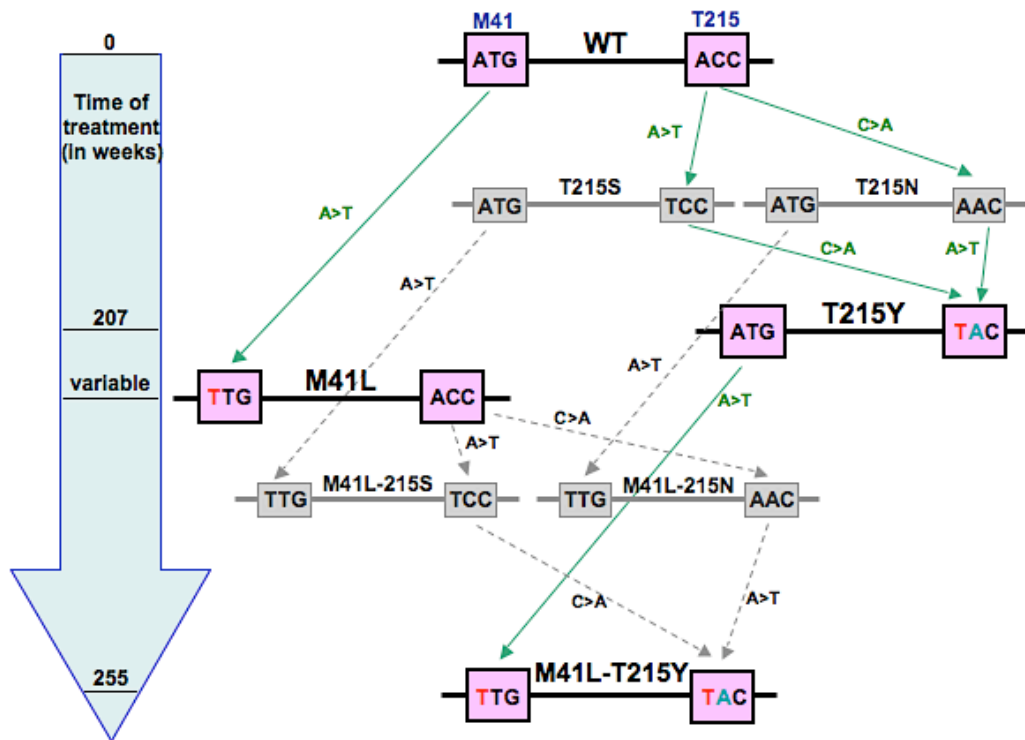


Figure 12. Mutation pathway of the HIV-1 reverse transcriptase under AZT therapy *in vivo*. The scheme shows one common *in vivo* developmental pathway of AZT-resistant HIV-1 mutants at amino acid positions 41 and 215 in the reverse transcriptase. Amino acids are given in the one letter code. In the block arrow, estimated waiting times of mutant appearance are marked. The values are according to estimations from Beerenwinkel, et al. (Beerenwinkel, Daumer et al. 2005) The flowchart arrows highlight the respective nucleotide changes. Mutants commonly found *in vivo* are in bold type while mutants in grey are not observed *in vivo* or are rare.

4.1.2 Generation of AZT-resistant mutants of HIV-1, fitness determination and epistasis calculations.

All seven HIV-1 RT mutants from the AZT-resistance pathway (Figure 12) were generated by site-directed PCR and cloned into an HIV-1 NL4-3-based vector that is deficient in the expression of a functional envelope (Env)

protein and contains the *Renilla* luciferase gene in the position of *nef* (Neumann, Hagmann et al. 2005). Respective HIV-1 Env-pseudotyped viruses that can only undergo a single round of infection in susceptible target cells were subsequently produced from 293T cells after co-transfection with RT mutants and an HIV-1 *env* expression plasmid. The relative fitness of the mutant viruses was assessed under a range of physiologically relevant AZT concentrations by infecting the TZM-bl cell-line or primary peripheral blood lymphocytes (PBMCs) from two healthy donors (here referred to as Donors 1 and 2) and measuring the relative luciferase activities of the variants compared to that of the wild-type (Materials and Methods). The epistatic interaction E of the mutations was then calculated according to the epistasis definition in a two-locus-two-allele model. In the context of this work, the term locus refers to a mutant site in the HIV genome that confers drug resistance. The two alleles represent drug sensitivity (wild type) or drug resistance (mutant) depending on the mutations at each locus. With two loci and two alleles coding for drug sensitivity, there are four types of viruses which are fully sensitive, partially resistant and fully resistant. Under this conditions, epistasis (E) is calculated with the formula:

$$E = W_{00} \cdot W_{11} - W_{01} \cdot W_{10} \text{ [Equation 1]},$$

where W_{00} is the fitness of fully sensitive virus (the wild type), W_{11} the fitness of the double mutant and W_{01} , W_{10} are the fitness of both single mutants, respectively.

A visual approach to estimate positive or negative epistasis is by plotting the fitness measured experimentally against the expected fitness calculated based on the assumption of no epistatic interactions (van Opijnen, Boerlijst et al. 2006; Kouyos, Silander et al. 2007). This is done by multiplying the fitness of the single mutants and graphically comparing the resulting fitness with the fitness of the double mutants.

4.1.3 The fitness ranking of AZT-resistant HIV-1 RT mutants corresponds to their frequency distribution in AZT-treated patients.

The distribution of fitness relative to that of the wild type for all single and two-point HIV-1 RT mutants infecting TZM-bl cells or PBMC in the presence of 0 to 10 μM AZT is shown in Figure 13 and the respective values are given in Table A1 in the Appendix. With the TZM-bl cell line and the PBMC of these two blood donors as target cells, the wild-type virus has a varying fitness advantage over the AZT-resistant variants in the absence of drug. Increasing drug concentrations render particularly the mutants M41L, T215Y and M41L/T215Y more fit than the wild type. These dominant RT mutants have been analyzed previously and the determined relative fitness values are concordant with previous findings (Harrigan, Bloor et al. 1998; Wang, Mittler et al. 2006). Similarly concordant are the inhibitory concentration 50 (IC_{50}) values for AZT that have been determined for these mutants (Richman, Shih et al. 1991; Arts, Quinones-Mateu et al. 1998; Harrigan, Bloor et al. 1998; Maeda, Venzon et al. 1998; Petropoulos, Parkin et al. 2000) and which can be derived from these fitness measurements as a function of drug concentrations. The newly analyzed intermediate mutants T215S, T215N,

M41L-T215S and M41L-T215N of the AZT-resistance pathway exhibit low fitness values under all drug concentrations with the 215S mutants being slightly fitter than the 215N. Thus, taken together, the ranking order of the fitness values for all RT mutants in the presence of AZT correspond well with the frequency distribution of the respective mutants found in patients under AZT treatment i.e. T215Y > M41L > T215S > T215N (Stanford Drug Resistance Database, <http://hivdb.stanford.edu>).

The fine structure of the fitness distribution of the RT mutants in TZM-bl and PBMC revealed interesting features. First, the relative fitness of the AZT-resistant mutants is influenced by the host-cell environment. For example, the mutants T215Y and M41L-T215Y exhibit a higher relative fitness without drug in PBMC of donor 2 than in PBMC of donor 1 or TZM-bl cells. Furthermore, with the exception of the M41L-T215S, the non-dominant RT mutants are fitter in TZM-bl cells under all AZT concentrations than in PBMC. Second, the fitness of the wild type in the presence of AZT is usually higher in PBMC than in TZM-bl cells. This amounts to an about 10-fold and 30-fold difference under 2 μ M and 5 μ M AZT respectively. Under 10 μ M AZT, the replication of the wild type was practically not detectable in all cell-types. Third, the fitness differences between the wild type and the RT mutants are not constant. For example, with 5 μ M AZT, the highly resistant mutant M41L/T215Y exhibits a 160-fold higher fitness than the wild type in TZM-bl cells but is only around 6-fold or 20-fold fitter in PBMC of donor 1 and 2, respectively. Thus, the fitness behavior of the wild type and the RT mutants as a function of AZT concentrations is cell type dependent. This correlates

well with the observation that HIV replication and adaptation strongly depends on the host-cell environment (Arts and Wainberg 1994; Arts, Marois et al. 1996; van Opijnen, de Ronde et al. 2007).

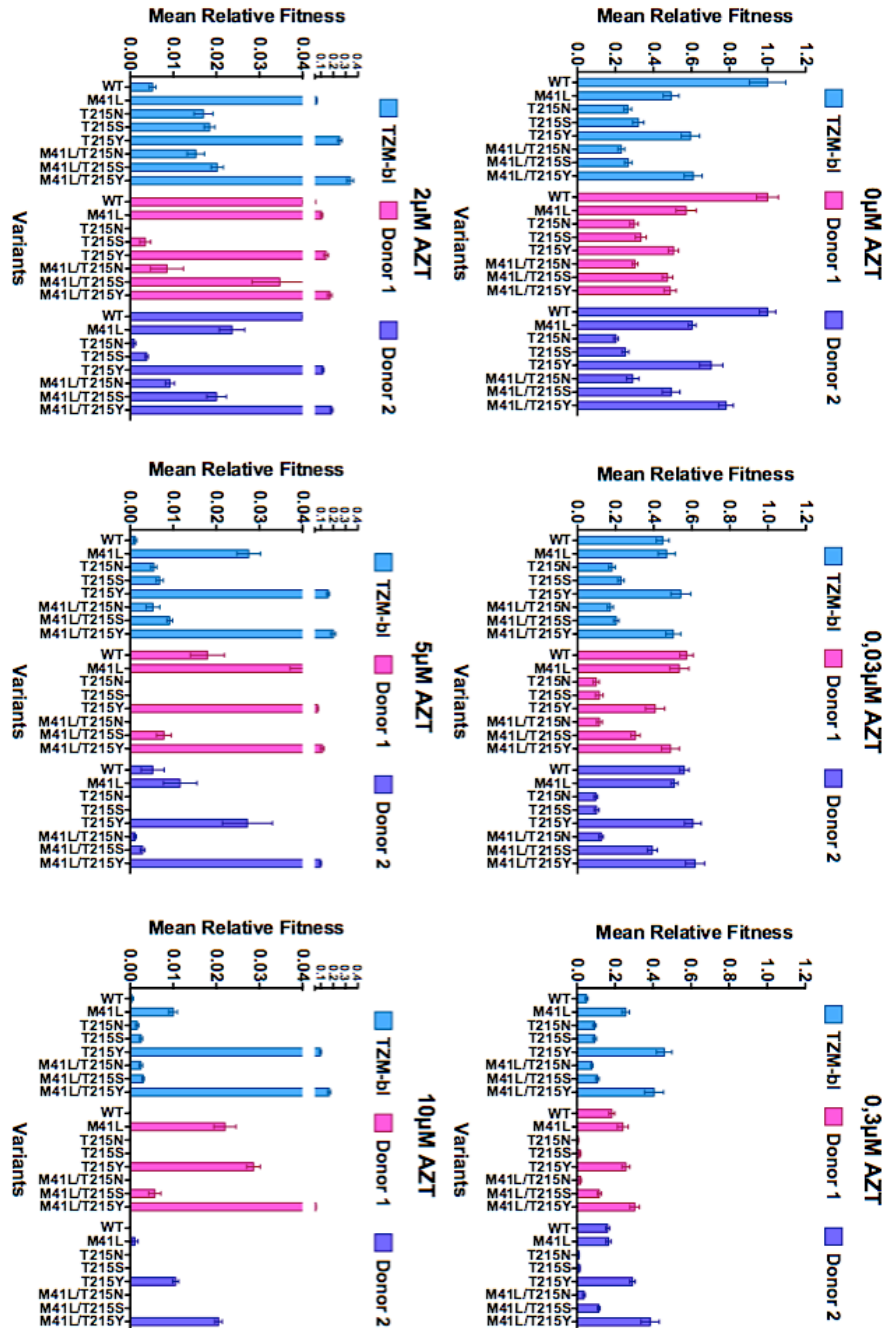


Figure 13. Relative fitness values of HIV-1 reverse transcriptase mutants along an AZT-resistance pathway.
Mean fitness distribution for wild type (WT) and mutants in the TZM-b1 cell line (light blue) and PBMC from Donor 1 (pink) and Donor 2 (dark blue) as a function of AZT concentration. The values are the mean of three or four independent infections. Error bars are standard error of the mean.

4.1.4 The HIV-1 AZT-resistance pathway is characterized by strong and varying epistasis between the RT mutations at amino acids 41 and 215.

In order to analyze possible interactions between the mutations of the key amino acids along the AZT-resistance pathway, epistasis (E) was calculated from the determined fitness values according to equation 1. Without drug pressure, E is always strongly positive for the TZM-bl cells and both PBMC Donors (Table A2 in Appendix) however the relative values for the three double mutants differ in the target cells. To better visualize the epistatic interactions between all RT mutations, the experimental fitness values of the double mutants (i.e. the observed fitness) were plotted against the products of the fitness of the one-point mutants (i.e. the expected fitness under the assumption of no epistatic interactions) (Figure 14A). Positive epistasis means that the fitness of the double mutants is higher than expected (the diagonal line corresponds to no epistatic effects). To test whether the overall finding of epistatic interactions is statistically robust, we performed bootstrapping to generate randomized data sets (N=1000) and applied the same analysis. In all cases the mean epistasis values were significantly greater than zero (Table A2 in Appendix).

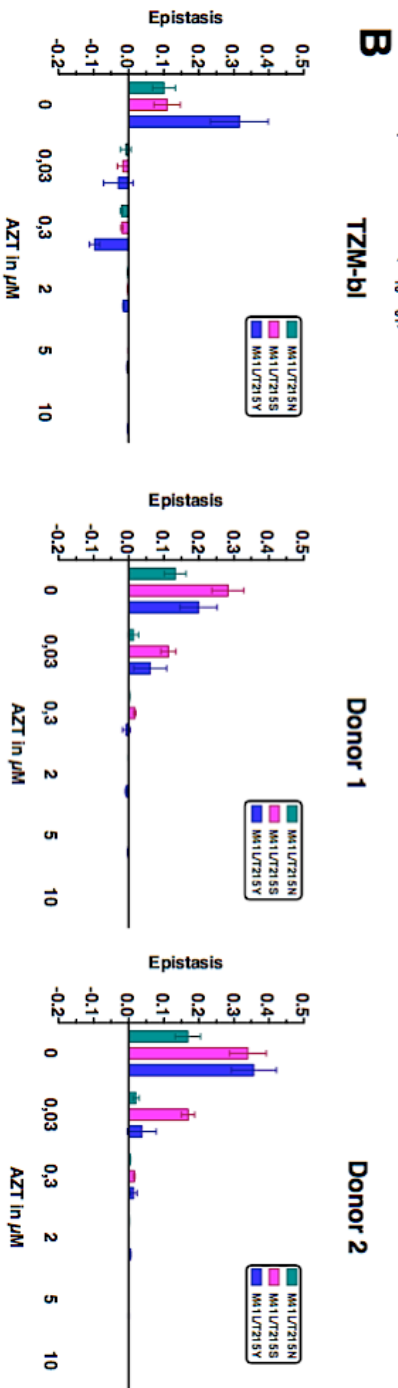
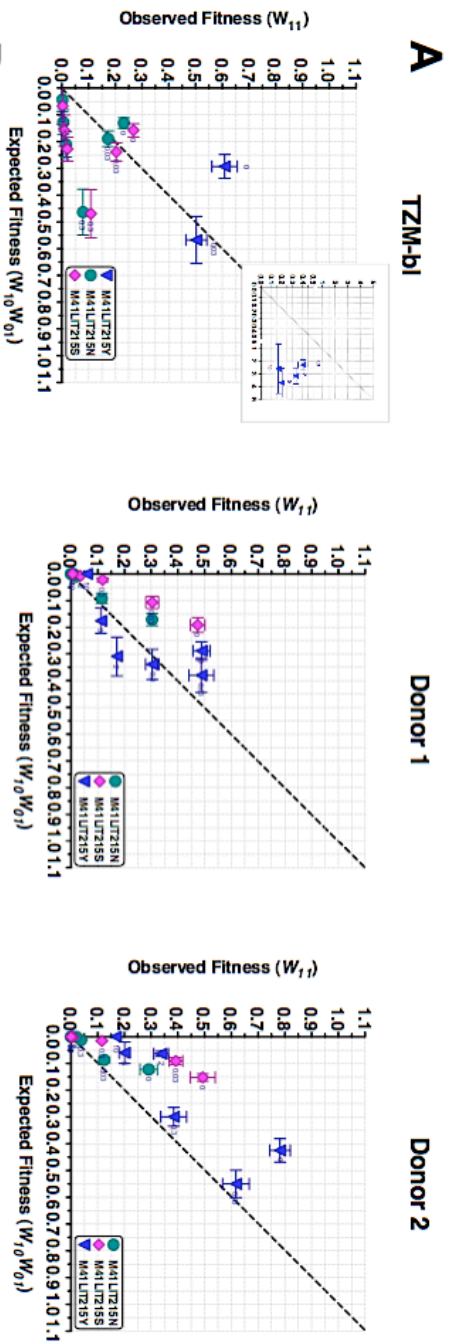


Figure 14. Epistasis in AZT-resistant HIV-1 reverse transcriptase mutants. (A) The observed relative fitness of double mutants W_{11} along an AZT resistance pathway under different AZT concentrations is plotted against the product of the relative fitness of the single mutants $W_{10} \times W_{01}$. The latter reflect the expected fitness if there is no epistasis. Values are calculated for the fitness in T2M-b1 cells and PBMC from two healthy donors (named Donors 1 and 2). The diagonal line corresponds to absence of epistasis while the areas of positive and negative epistasis are above and below respectively. Error bars indicate standard error of the mean. (B) Positive epistasis declines in strength with increasing AZT concentrations. Epistasis values for the three HIV-1 double mutants along the AZT resistance pathway are plotted against AZT concentrations. Error bars indicate standard error of the mean.

4.1.5. The epistatic interactions between the mutations changed upon increasing drug pressure and differed between the target cells used.

An increase in AZT concentrations resulted in a decrease of epistasis. The three different double mutants showed a varying relative decrease in the different target cells. With TZM-bl cells, the sign of epistasis changed to negative already from the lowest AZT concentration whereas with the PBMC of donors 1 and 2, epistasis was mainly (donor 1) or always (donor 2) positive (Figure 14B). The change in the sign of epistasis in the TZM-bl cells is mainly due to the fitness ranking of the wild type, which is relatively low, and the 1-point mutants, which are relatively high in these cells as compared to PBMC (Figure A1). Together these observations show that the type of fitness interaction may change along with the environmental conditions under which it is analyzed. In the absence of drug, the fitness loss due to the acquisition of resistance mutations is compensated by a strong antagonistic interaction (positive epistasis) in all cases. However when AZT is present, the fitness interaction is still antagonistic (now negative epistasis) in TZM-bl cells but becomes mainly synergistic (now positive epistasis) in PBMC. Thus the fitness gain is less than expected for TZM-bl cells but mainly higher than expected for PBMC.

4.1.6 Epistasis affects the relative abundance of drug-resistant HIV-1 mutants.

The fitness interactions between the mutations along a drug-resistance pathway are expected to have an impact on the relative mutant frequencies in a viral population. This in turn may be of great clinical importance for the

selection of drug-resistance under antiviral treatment because a higher or lower steady state level of a resistant mutant may lead to a faster or slower outgrowth. Having determined all fitness values for all mutants along the AZT-resistance pathway, a quantitative estimate of the effect of epistasis on the relative abundance of the double mutants was performed. For this, the expected fitness values under the assumption of no epistasis were calculated from the experimentally determined fitness values and used to analyze the respective steady state frequencies assuming a mutation-selection equilibrium as defined by the general model of HIV quasispecies dynamics (Nowak 2000). Under this condition, the relative abundance of the wild-type virus and the 1-point and 2-point mutants can be estimated by computing the eigenvectors of the following eigenvalue problem [Equation 2]:

$$\begin{bmatrix} (1-\mu_1)(1-\mu_2)W_{00} & (1-\mu_1)\mu_2W_{01} & \mu_1(1-\mu_2)W_{10} & \mu_1\mu_2W_{11} \\ (1-\mu_1)\mu_2W_{00} & (1-\mu_1)(1-\mu_2)W_{01} & \mu_1\mu_2W_{10} & \mu_1(1-\mu_2)W_{11} \\ \mu_1(1-\mu_2)W_{00} & \mu_1\mu_2W_{01} & (1-\mu_1)(1-\mu_2)W_{10} & (1-\mu_1)\mu_2W_{11} \\ \mu_1\mu_2W_{00} & \mu_1(1-\mu_2)W_{01} & (1-\mu_1)\mu_2W_{10} & (1-\mu_1)(1-\mu_2)W_{11} \end{bmatrix} \times \begin{bmatrix} y_{00} \\ y_{01} \\ y_{10} \\ y_{11} \end{bmatrix} = \lambda \begin{bmatrix} y_{00} \\ y_{01} \\ y_{10} \\ y_{11} \end{bmatrix}$$

Here, y_{00} and y_{11} denote the equilibrium abundance of the wild-type virus and the 2-point mutant, respectively, whereas y_{01} and y_{10} denote the equilibrium abundance of the 1-point mutants. The parameters μ_1 and μ_2 characterize the mutation rate for the first position and for the second position respectively. Under the simplifying assumption that the mutation rate μ is not affected by the mutations itself, the relative frequencies of the 2-point mutants can be readily calculated using our fitness data (Table A1) and MATLAB routines (www.mathworks.com). The results are shown in Figure 15 and Table A3.

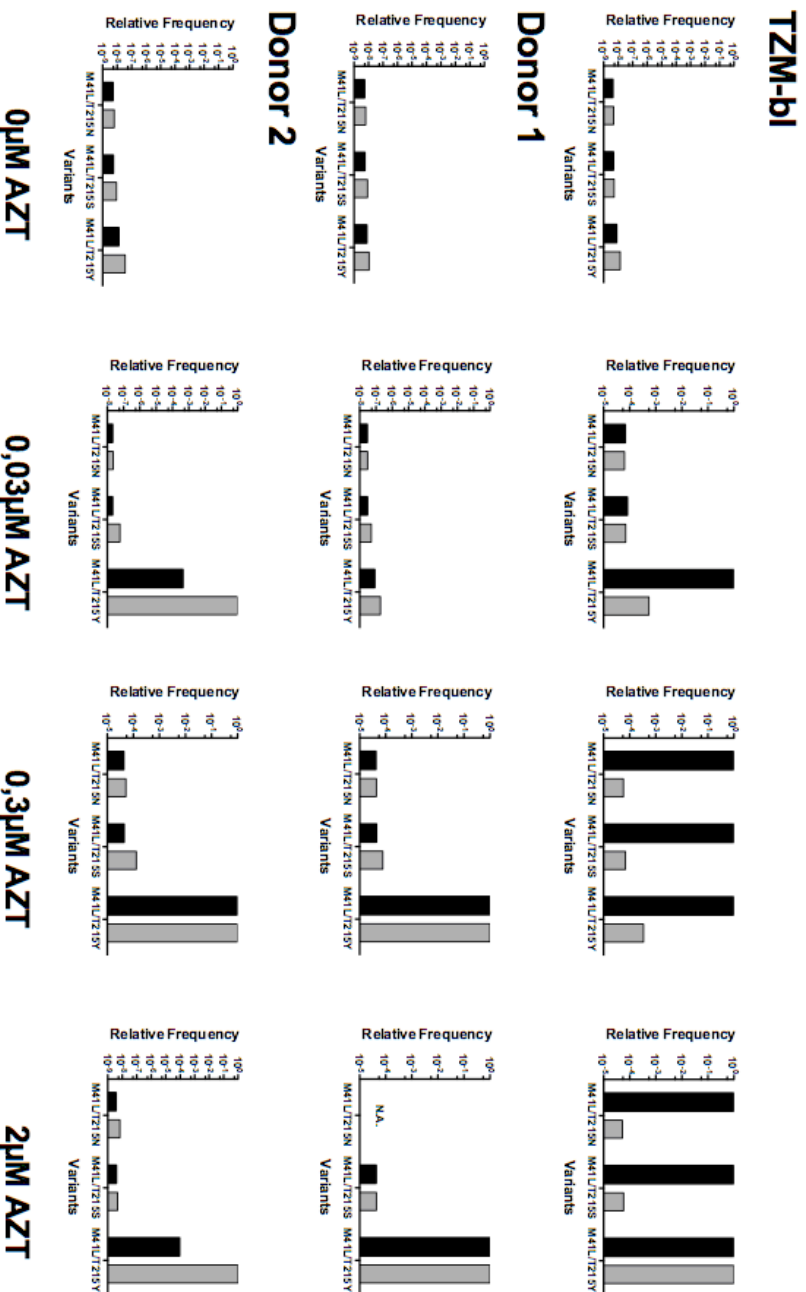


Figure 15. Effect of epistasis on the relative frequencies of drug-resistant HIV-1 mutants within the viral population. The plot shows the estimated relative frequencies of the double mutants along the AZT resistance pathway under different AZT concentrations for TZM-b1 cells and both PBMC donors without epistasis (black bars) and with epistasis (grey bars). Without drug pressure, epistasis has a small effect on the mutant frequencies. With the addition of drug, epistasis has a varying effect on the mutant frequencies that is dependent on the fitness ranking of the wild type, 1-point mutants and 2-point mutants. Calculations were performed according to an established model specified in equation 2 (see text for details). Fitness values were taken from Table A3.

Depending on the AZT concentration, the presence of epistasis has a marginal or a significant effect on the relative frequency distribution of the 2-point mutants within the virus population. Importantly, high epistasis values do not directly predict a large effect on that distribution. For example, without AZT when epistasis is highest, the relative mutant frequencies are around 10^{-8} to 10^{-9} and epistasis affect that frequencies up to 3-fold (Figure 15 and Table A3). In the presence of AZT when epistasis values were significantly smaller, frequency effects of up to around 10,000-fold are observed. Taking the M41L/T215Y mutant in the presence of 0.03 μ M AZT as an example, epistasis increased the relative frequency around 10,000-fold according to the measurements in PBMC of donor 2 (Table A3c), diminished it around 10,000-fold according to the measurements in TZM-bl (Table A3a) or left it relatively unchanged (PBMC donor 1, Table A3b). Furthermore, the frequency effects were not linear. Taking again the M41L/T215Y mutant, epistasis increased the relative frequency around 10,000-fold at 0.03 μ M AZT and 2 μ M AZT, however had nearly no effect at 0.3 μ M AZT. This complex behavior is due to the fact that the epistasis effect on mutant frequencies strongly depends on the distribution of the relative fitness values for wild type, intermediate mutants and the 2-point mutant, i.e their ranking.

If the intermediate one-point mutants (at least one of them) have larger fitness value than the two-point mutant would have in the absence of epistasis then the effect would be strong. Otherwise the two-point mutant will be dominating with and without epistasis. Let us consider two examples: Under 0.3 μ M AZT in PBMC of donor 2, the fitness values for wild type, M41L,

T215Y and M41L-T251Y are 0.162, 0.166, 0.293 and 0.385, respectively (Table A1c). Thus, one would expect that the M41L-T251Y mutant will be dominating because of its highest fitness and its relative frequency is expected to be close to 1 (in fact 0.999; Table A3c). Assuming no epistatic interaction, the relative fitness for the same variants are 0.162, 0.166, 0.293 and 0.300, respectively. Again the M41L-T251Y mutant remains to be dominating because it has the highest fitness and its relative frequency is close to 1 (0.998). In the case of 2 μ M AZT, the fitness values with epistasis are 0.0426, 0.0236, 0.116 and 0.187, respectively. The M41L-T251Y mutant will be dominating with a relative frequency close to 1 (in fact 0.999). Assuming no epistasis, the relative fitness is 0.0426, 0.0236, 0.116 and 0.0642, respectively. Now the 1-point T251Y mutant will be dominating because it has the highest fitness and its relative frequency is expected to be close to 1. In this case the relative frequency of the two point mutant M41L-T251Y is only 0.0000897. Thus the epistatic effect is large although the epistasis value is small (Figure 14B).

4.2 Phenotypic mixing modulates the infectivity and fitness of HIV drug-resistant variants.

4.2.1 Selection of variants for the analysis of phenotypic mixing effects

To address whether HIV variants phenotypically mixed with wild type and AZT-resistant RT may impact fitness of phenotypically variants, mutations M41L, T215Y and the double mutant M41L-T215Y from the AZT-resistant pathway were chosen. 22 different pseudotypes that carry up to 1:4 ratios of

wild type and drug-resistant RT were produced. Another set of 5 different pseudotypes contained a mix of wild type and Enfuvirtide (T20)-resistant envelope proteins, and a set of 4 pseudotypes were produced with a mix of wild type and mutant RT and envelope proteins. (See Materials and Methods).

4.2.2 The fitness change of virions carrying mixed RTases is gradual and in-between the pure phenotypes

The comparative distribution of fitness for all phenotypically mixed variants infecting PBMC in the presence of 0 to 10 μ M AZT is shown in Figure 16. Fitness values are related to the fitness of the virion carrying all copies of wild type RT (here referred as «100% wild type»). Overall, the fitness of the phenotypically mixed pseudotypes was in between the pure virions (i.e. the virions carrying 100% of the wild type or 100% of the mutant RT), and the decline in the fitness without drug (or the increase with drug) was rather gradual as the % of mutant RT inside the virions increased (Figure 16).

Without the addition of drug, the wild type has a fitness advantage over all the phenotypically mixed variants. Interestingly, with already 25% of the M41L RT, the fitness was reduced to only a 50% of the pure wild type. (Figure 16, upper left). This initial decrease in fitness was not changed as the amount of M41L RTases inside the virion increased. It was previously estimated that each HIV-1 virion contains about 50 RT molecules (Coffin 1979). Thus the inclusion of around of around 25% or 10 to 12 molecules of the RT carrying the M41L mutation is sufficient to lower the fitness similar to

the variant carrying all copies of the M41L RT. Mixing copies of wild-type and the T215Y or the M41L-T215Y mutant RTases showed a decrease in fitness which was proportional to the increase of the number of mutant RT inside the virion (Figure 16, second and third group). The decrease in fitness shown by these intermediates was not significant until 50 to 75% copies of these mutant RT were present inside the virions, contrasting with the fitness behavior observed in the wild type - M41L mixes (see Discussion). The fitness of pseudotypes mixed solely with the M41L, T215Y and the M41L-T215Y resistant RT did not significantly differ from the fitness of the pure phenotypes as shown by the standard errors of the mean (Figure 16, upper left).

Upon addition of AZT, the phenotypically mixed variants exhibit higher relative fitness than the one carrying all copies of the wild type RT. With the exception of the mix wild type plus the M41L, which under 1 and 2 μ M AZT decreased the fitness of the intermediate pseudotypes, all virions carrying at least 25% of mutant RTases showed a higher relative fitness than the wild type under the whole range of AZT concentrations (Figure 16). This fitness difference was larger as the concentrations of the drug increased and again gradual between the extremes. Similar to what is shown in the previous fitness analysis, only virions carrying 75 to 100% of the highly resistant T215Y and M41L-T215Y RTases replicate efficiently under high concentrations of drug.

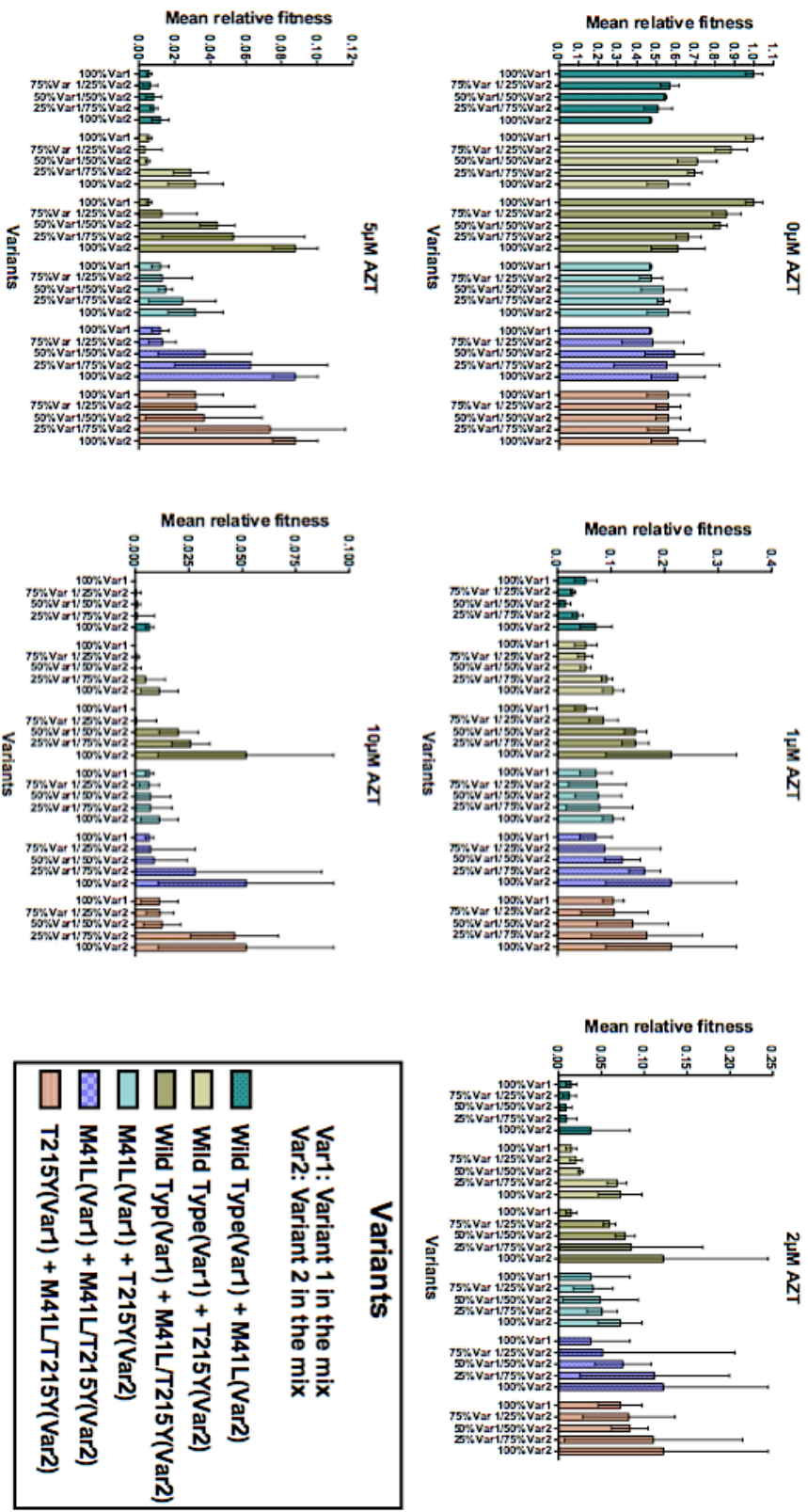


Figure 16. Relative fitness of the phenotypically mixed RTase HIV-1 variants. Bar-plot with the mean relative fitness of wild type and phenotypically mixed variants in PBMC from Donor 3 as a function of drug concentration. Values are the mean of three independent experiments. The inset describes the nomenclature depicted in the x-axes. Error bars are standard errors of the mean. Note the change in scale between traits.

4.2.3 Incorporation of Enfuvirtide (T20)-resistant envelope proteins do not affect trimer function but alter the infectivity of phenotypically mixed virions.

HIV envelope proteins arrange in trimers on the virion surface (Liu, Bartesaghi et al. 2008). Envelope binding to the CD4 receptor results in a major reorganization of the Env trimer, causing an outward rotation and displacement of each gp120 monomer. This is followed by a rearrangement of the gp41 region along the central axis of the trimer, leading to a closer contact between the viral and target cell membranes (Liu, Bartesaghi et al. 2008). Enfuvirtide (T20) binds to the gp41 and prevents viral entry by blocking the conformational change needed for fusion. If binding of Enfuvirtide to a single gp41 molecule in the trimer would be sufficient to block its function, heterotrimers consisting of a mix of sensitive and T20-resistant (T20^{Res}) monomers should be blocked at approximately the same IC₅₀ as homotrimers (C. Jassoy, unpublished data).

In order to analyze the effect of phenotypic mixing on HIV infectivity and trimer function, a set of five pseudotypes was produced. These included virions carrying a ratio of up to 1:4 mixes of wild type and T20^{Res} envelopes (i.e. virions carrying 100% of the wild type envelope in its surface, 75% of wild type plus 25% T20^{Res}, 50% of both and 25% wild type plus 75% of T20^{Res}). Figure 17 shows the relative infectivity of all variants in PBMC from two different donors (Donors 4 and 5) without T20 and under increasing concentrations of the drug. T20 decreased the infectivity of the fully sensitive pseudotype (i.e. the 100% wild type virus) in a dose-dependent manner. The

IC₅₀ for T20 in these cells was between 0.08 and 1 µg/ml of T20 for the fully sensitive variant (100% wild type) (Figure 17A, upper left), whereas in cells from Donor 4, the T20 IC₅₀ for the pseudotypes carrying 50% of resistant envelopes was 0.4 µg/ml of T20. This is in the range of the T20 IC₅₀ for HIV-1 isolates using CCR5 as coreceptor *in vivo* (Derdeyn, Decker et al. 2000). Interestingly, the low infectivity (around 10%) exhibited by the fully resistant pseudotype (the 100% T20^{Res}) without drug remained mostly constant until concentrations of 2 µg/ml of T20. Under concentrations of 10 µg/ml of the drug, the 100% wild type pseudotype was completely blocked and the infectivity of the 100%-T20^{Res} was reduced by 50% (Figure 17B). The infectivity of the intermediate variants was, as with the phenotypically mixed RTases, in between the pure pseudotypes.

The gradual decline in relative infectivity, and the observation that pseudovirions containing different ratios of both sensitive and resistant glycoproteins were only slightly less sensitive to enfuvirtide than the fully resistant pseudovirions (as shown by the change in the IC₅₀), suggests that heterotrimers formed with wild type and T20-resistant glycoproteins are not completely blocked by enfuvirtide. This is in agreement with similar data obtained by Prof. Christian Jassoy, Leipzig (personal communication). However, these observations may be insufficient to make further assumptions on trimer function. For instance, it is yet not clear how many trimers HIV carries in its viral membrane, and how many are needed to successfully infect a cell. The literature is inconclusive in this respect. Recently, mathematical models on the stoichiometry of HIV entry suggested

Figure 17. Phenotypic mixing of glycoproteins alter the infectivity HIV variants in a dose-dependent manner. Bar-plot of the relative infectivity (as the % of infected cells) in PBMC from two donors for the five phenotypically mixed HIV pseudotypes and under increasing concentrations of T20. The graph is divided in four panels for better visualization of the data. A) Infectivity under the range of 0 to 0.4µg/ml T20. B) Infectivity under 2 and 10 µg/ml T20. Error bars are standard errors of the mean.

4.2.4 AZT and T20 in combination altered the fitness distribution of phenotypically mixed double-resistance variants

In order to analyze the effect of phenotypic mixing on fitness under the combination of two antiviral drugs, pseudotypes carrying wild type and the AZT-resistant T215Y RTases were produced together with mixes of wild-type and T20-resistant envelopes (T20^{Res}). Infections were performed in PBMC from two donors (Donors 6 and 7) without drug and under concentrations of both drugs combined.

Figure 18 shows the mean relative fitness distribution for all variants infecting PBMC under 0 to 10µM AZT in combination with T20 at the same concentrations. Overall, the phenotypically mixed variants exhibit a slightly higher replication capacity in cells from Donor 6 than in cells from Donor 7. Without the addition of drugs, the variant carrying both wild type RTases and envelopes has the fitness advantage over the intermediate ones, which as seen in sections 4.2.2 and 4.2.3, show a fitness decrease that is in between the pure pseudotypes. Interestingly, the intermediate variants carrying either resistant RT or resistant envelopes in combination with the wild type (WT RT-T20^{Res} ENV or T215Y RT-WT ENV) showed a similar relative fitness, indicating that the inclusion of the wild type into the virion compensates equally to the fitness loss introduced by the mutants (Figure 18A).

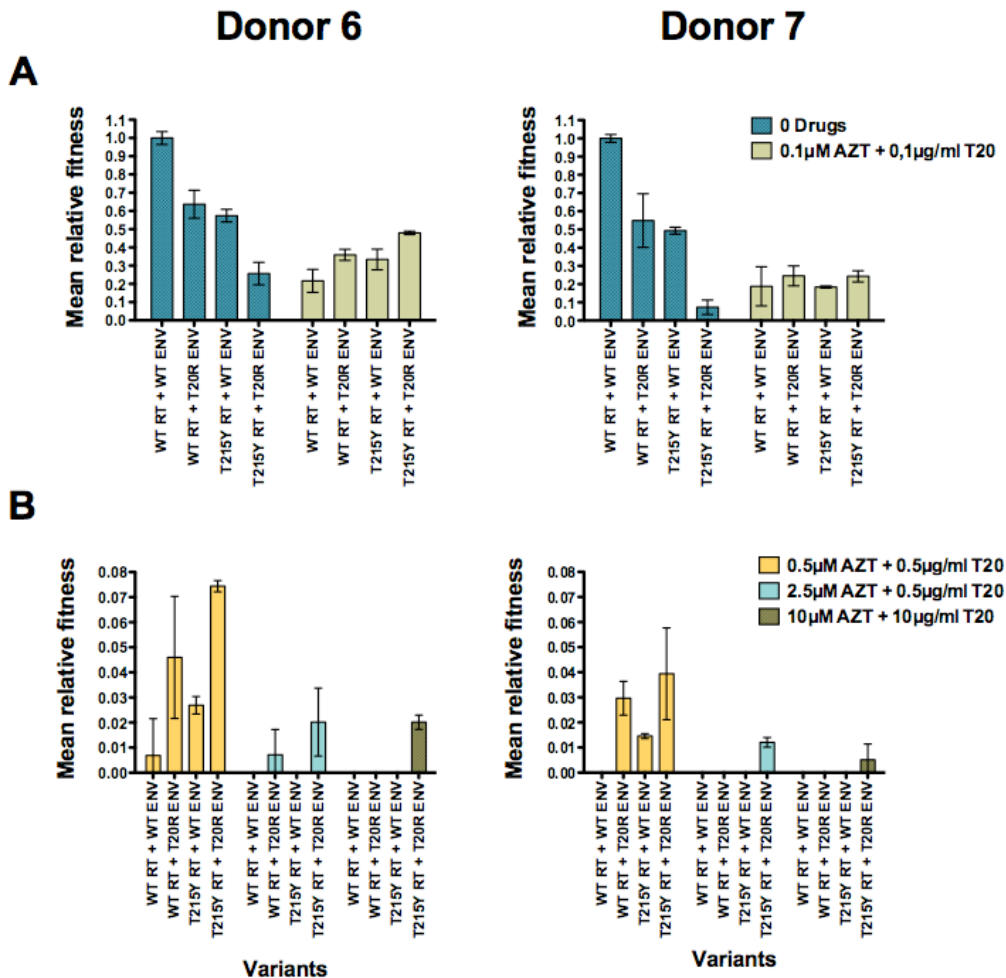


Figure 18. Relative fitness of variants carrying a combination of drug resistant RTases and Envelope proteins. Bar-plot of the relative fitness in PBMC from two donors for the phenotypically mixed HIV pseudotypes and under increasing concentrations of AZT and T20. The graph is divided into four panels for better visualization of the data. A) Fitness under 0 and 0.1 μM AZT plus 0.1 μg/ml T20. B) Fitness under 0.5, 2.5 and 10 μM AZT plus 10 μg/ml T20. Error bars are standard errors of the mean.

AZT and T20 in combination altered the fitness distribution of the phenotypically mixed pseudotypes. Increasing concentrations of the drugs render the T215Y RT-T20^{Res} ENV more fit. Under 10 μM AZT in combination with 10 μg/ml T20 it is the only variant still replicating (Figure 18B). Of interest was the observation that in both donors, virions carrying the T20^{Res}

ENV exhibited higher relative fitness independent of the RT phenotype that it carried. Under 0.5 μM AZT and 0.5 $\mu\text{g/ml}$ T20, the difference in fitness favoring the WT RT-T20^{Res} ENV over the T215Y RT-WT ENV phenotype was 50% (Figure 18B). It appears that, with the addition of drugs, the counterweight effect provided by the respective mutant phenotype (as observed without drug pressure) does no longer help to compensate for the fitness loss and the pseudotypes carrying the T20^{Res} envelope have the fitness advantage irrespective of the RT phenotype, probably due to their ability to enter the cell more efficiently.

5. Discussion

5.1 On the impact of epistatic interactions in HIV

Epistasis is a fundamental component of the genetic architecture of biological entities and has been suggested to play a main role in the evolutionary dynamics of virus populations (Michalakis and Roze 2004; Sanjuan, Moya et al. 2004; Bellew and Chang 2006; Elena, Carrasco et al. 2006). Epistatic interactions were found to be present in many diverse DNA and RNA viruses (Crotty, Cameron et al. 2001; You and Yin 2002; Burch and Chao 2004; Sanjuan, Moya et al. 2004; Silander, Tenailon et al. 2007; Tsetsarkin, McGee et al. 2009), and a wide range of mutational interactions (positive and negative) was observed. Epistatic interactions may directly impact viral robustness and the efficiency of variant selection under therapy (Sanjuan, Moya et al. 2004; Elena, Carrasco et al. 2006; Kouyos, Silander et al. 2007; Rolland, Brander et al. 2007; Elena, Sole et al. 2010).

Due to its genetic diversity, established *in vitro* assays, *in silico* models and the availability of large amounts of *in vivo data* from infected patients, HIV is an ideal candidate to study fitness interactions. In this thesis work, the fitness of all HIV-1 mutants along the classical 215-41 AZT-resistance pathway was quantified under physiological concentrations of the drug *ex vivo*, and the values of the fitness interactions between the mutations were calculated and used to estimate the impact of epistasis on the relative mutant frequencies within the viral population. Overall, the pattern of epistasis was complex and dependent on the drug concentrations and the host cells used. Without AZT, epistasis was consistently positive within the TZM-bl cell line and the PBMC

of both of the blood donors tested, and resulted in an estimated 1.5 to 2.8-fold increase in the ratio of the highly resistant 2-point mutant M41L-T251Y to wild type (Figure 15). The presence of environmental pressure (in the form of physiological concentrations of AZT) leads to a concentration-dependent decrease in the strength of the epistatic interactions (Figure 14). The sign and the size of epistasis differ between the host cells used and the numerical values did not predict the epistatic effect on the mutant frequency. This complex behavior is explained by the fitness ranking of all mutants in the presence of AZT and the uneven fitness distribution of the 1-point mutants between the target cells.

The observed positive epistasis under drug-free conditions has a buffering effect on the mutant distribution and caused an increase of the relative frequency of the highly AZT-resistant 2-point mutant M41L-T251Y over the expected frequency if epistasis would be absent. However this relative frequency increase from about 1×10^{-8} to about 3.6×10^{-8} (Table A3) within the virus population is only marginal considering an estimated effective population size of HIV *in vivo* of around 10^3 to 10^4 (Althaus and Bonhoeffer 2005). In the presence of AZT, the sign of epistasis varies with the drug concentrations and the host cells used. As a consequence, epistasis increases or decreases the relative 2-point mutant frequencies or leaves it relatively unchanged. For example, under $0.03 \mu\text{M}$ AZT and TZM-bl as host cells, epistasis decreases the relative frequency of M41L-T215Y from 1 to 5.5×10^{-4} , whereas with PBMC from Donor 2, epistasis increases the relative frequency from 4.5×10^{-4} to almost 1 (Figure 15). Although these estimated

relative frequencies under drug pressure are now in the range of the effective population size of HIV *in vivo* (a condition where epistatic effects are expected to be relevant), the variable and complex pattern of fitness interactions and their dependence on specific environmental conditions, suggests that there are no consistent experimental criteria to derive general statements on the importance of the epistatic effects for the mutant frequency at the population level.

Epistasis was suggested to possibly contribute to viral robustness, the ability of a virus to maintain stable functioning despite genetic and environmental perturbations (Sanjuan, Forment et al. 2006; Elena, Sole et al. 2010). In general, single mutations in a viral genome are naturally deleterious, reducing the fitness of the virus. If the deleterious effects of the mutations are strong enough, those variants might be lost rapidly and the population forced to cluster in reduced and narrow peaks of the adaptive fitness landscape (Elena, Carrasco et al. 2006). The observed predominance of positive epistasis among viral genomes suggests a buffering effect as subsequent mutations occur, such that the mutant spectrum is enlarged (Montville, Froissart et al. 2005; Kouyos, Otto et al. 2006; Sanjuan, Forment et al. 2006). This in turn may become beneficial for the virus population in the context of a strong selection pressure like antiviral treatment. However, as shown in this thesis work, for the mutants along the AZT resistance pathway, the buffering effect without AZT is so low that positive epistasis is unlikely to be a major contributing factor to the robustness of HIV i.e. to allow low fitness mutants to survive in an HIV population *in vivo*, and thus, making the adaptive fitness

landscape flatter. Therefore, other mechanisms than epistasis may be considered as of prime importance within infected individuals to contribute to HIV robustness. First, the HIV provirus can persist for months independent of the replicative capacity of the respective mutant (Chun, Finzi et al. 1995). Second, multi-infection of single cells *in vivo* is common and thus phenotypic mixing can contribute to mutant survival (Jung, Maier et al. 2002; Gelderblom, Vatakis et al. 2008). The recent suggestion that HIV is evolving towards a more robust population due to the selection of a lower fitness landscape is compatible with such a scenario (Arien, Vanham et al. 2007; Rolland, Brander et al. 2007).

The development of drug resistance in HIV infection remains one of the most challenging difficulties in antiviral treatment. The dynamics of resistant mutants depends on a number of virus replication parameters such as the fitness values, the number of available target cells and mutation/recombination rates. Although the interplay between these factors has been studied using mathematical models, their results suffer from not being based on exact values for all parameters. Fitness is a major determinant in the selection process of drug-resistant mutants that is amenable to experimental quantification. In this respect, the fitness estimates for a complete spectrum of AZT-resistant mutants as a function of the drug concentrations obtained in this thesis work established a solid quantitative basis for further data-driven *in silico* studies.

In summary, this part of the study provides with high-resolution fitness values along an important HIV drug-resistance mutation pathway and quantifies the impact of epistasis on mutant frequencies. The pattern of epistatic interactions between the specific mutations was complex and dependent on environmental factors such as the presence and absence of drugs and the host cells used. While some interactions compensate fitness losses, the effect on the relative mutant frequencies was small so that epistasis as a buffering mechanism for fitness losses might be rather inefficient. The effect of epistasis on the mutant frequencies strongly depended on the change in the fitness ranking of individual variants upon incorporation of selective pressure and in the host cell environment. Taken together, the data presented in this work caution from over-interpreting qualitative data on epistasis for evolutionary dynamics of viruses without knowledge of the fitness ranking of the complete mutant spectrum.

5.2 On the impact of phenotypic mixing in HIV

One of the major consequences of single-cell multifinfection in HIV is the generation of mixed viruses carrying viral features derived from different proviruses, a process called phenotypic mixing (Novick and Szilard 1951). Phenotypic mixing of viral products has been studied in many viruses (Lusso, di Marzo Veronese et al. 1990; Lusso, Lori et al. 1990; Rayner, Cordova et al. 1997; Wilke and Novella 2003). By altering the characteristics of a viral population (i.e. changes in cellular tropism, infectivity and fitness), this

phenomenon might have a direct impact on vaccine effectiveness and antiviral therapy.

For HIV, *in vivo* data show a proviral copy number of around 2 to 4 in single-infected cells (Jung, Maier et al. 2002). This suggests that, besides recombination between different proviruses, phenotypic mixing of viral products might be common. In this thesis work, a thorough analysis of the fitness and infectivity of different phenotypically mixed HIV variants is presented. Fitness and infectivity of HIV-1 pseudotypes carrying an up to 1:4 ratio of mixes of wild type and drug-resistant RTases and envelopes was experimentally quantified by infecting PBMC from different donors and under physiological concentrations of antiviral drugs *ex vivo*. The up to 1:4 ratio of mixing chosen for the experiments is in agreement with the estimated proviral copy number in infected cells, thus they capture a condition which is in the range of what could be expected *in vivo*. Overall, the fitness and infectivity of the phenotypically mixed variants decreased gradually between the extreme phenotypes in a ratio-dependent manner (Figure 16). Increasing drug concentrations rendered the extreme phenotypes more fit.

An interesting exception was the observation that, without drug, the addition of 25% of the M41L mutant RTase inside the virions was sufficient to decrease by half the fitness of the original wild type phenotype (Figure 16). This initial decline in fitness was maintained among all in-between phenotypes carrying this mutant RTase and contrasted with the fitness behavior of the phenotypically variants carrying mixes of wild type and T215Y

or M41L-T215Y mutant RTases. This particular observation might be due to the combination of two main factors: i) the physical properties of the M41L mutation and ii) the RT copy number inside the virions. Structural studies suggest that an RT carrying the T215Y mutation alter the interactions between the RT and the template-primer resulting in a higher processivity than RT carrying the M41L residue, which is somewhat buried in the RT structure (Tantillo, Ding et al. 1994). Thus, viruses carrying a mix of wild type and T215Y RT might replicate more efficiently than viruses carrying only copies of the M41L RT. This is in agreement with a study by Julias et al. showing that, in virions phenotypically mixed with wild type RT and a catalytically inactive RT, a substantial decrease in replication took place when the virions contained around 50% catalytically active polymerase (Julias, Ferris et al. 2001), a similar behaviour as observed here with the M41L mutated RT. Second, it has been estimated that HIV carries around 50 molecules of the RT inside a single virion (Stromberg, Hurley et al. 1974; Stromberg and Wilson 1974; Coffin 1979; Haseltine, Coffin et al. 1979). The reason for such high copy number is that the HIV-1 RT is a weak processive polymerase frequently dissociating from its primer-template. Even when a large number of RTase molecules may be required to complete viral DNA synthesis, it is not known if several RT molecules inside the reverse transcription complex compete for their recruitment to the template-primer. If that would be the case, it could be assumed that a competition between wild type and M41L RT for the template primer, plus the structural properties of the M41L RT, may be the reason of the fitness behavior observed in these phenotypically mixed variants. However this experiment has to be repeated.

Another situation was simulated in which a glycoprotein that is sensitive to the fusion inhibitor enfuvirtide (T20) (i.e. wild type envelope) and a T20-resistant derivative were phenotypically expressed in an up to 1:4 ratio and used to infect PBMC under different concentration of T20. With the exception of the variant carrying all copies of the T20-resistant envelope, T20 gradually decreased the infectivity in a dose-dependent manner. In the range of the T20 IC_{50} for HIV-1 isolates using CCR5 as coreceptor *in vivo* (Derdeyn, Decker et al. 2000), the IC_{50} for the fully sensitive pseudotype (i.e. the 100% wild type virus) in these cells was between 0.08 and 1 $\mu\text{g/ml}$ of T20 for the fully sensitive variant (100% wild type) and 0.4 $\mu\text{g/ml}$ of T20 for the pseudotypes carrying 50% of resistant envelopes. The pseudovirions that contained both sensitive and resistant glycoproteins were only slightly less sensitive to enfuvirtide than the resistant pseudovirions under 2 $\mu\text{g/ml}$ of T20. Interestingly, the low infectivity (around 10%) exhibited by the fully resistant pseudotype (the 100% T20_{Res}) without drug remained mostly constant until concentrations of 2 $\mu\text{g/ml}$ of T20. Under concentrations of 10 $\mu\text{g/ml}$ of the drug, the 100% wild type pseudotype was completely blocked and the infectivity of the 100%-T20_{Res} was reduced by 50%. The infectivity of the intermediate variants was, as with the phenotypically mixed RT, in between the pure pseudotypes.

The gradual decline in relative infectivity, (from the wild type through the in-between variants), and the observation that pseudovirions containing different ratios of both sensitive and resistant glycoproteins were only slightly

less sensitive to enfuvirtide than the fully resistant, suggests that heterotrimers formed with wild type and T20-resistant glycoproteins are not completely blocked by enfuvirtide. This is in agreement with similar data obtained by Prof. Christian Jassoy (personal communication). However, these observations may be insufficient to make further assumptions on trimer function. For instance, it is yet not clear how many trimers HIV carries in its viral membrane, and how many are needed to successfully infect a cell. The literature is inconclusive in this point.

Infection of phenotypically mixed variants that are dual-resistant to AZT and T20 in combination, revealed some interesting features. First, without the addition of drugs, the intermediate variants carrying either resistant RTases or resistant envelopes in combination with the wild type showed a comparative mean relative fitness. This initially suggests that, in a drug-free environment, the inclusion of the wild type phenotype into the virion compensates equally to the fitness losses introduced by the mutant phenotypes. Second, upon addition of AZT and T20 in combination, the phenotypically mixed virions carrying the T20^{Res} ENV exhibit higher relative fitness independent of the RT that it carried. Under 0.5 μ M AZT and 0.5 μ g/ml T20, the difference in fitness favoring the WT RT-T20^{Res} ENV over the T215Y RT-WT ENV phenotype was around 50%. Under the combination of AZT and T20, both resistance features (the ability to efficiently enter the cells and to reverse transcribe the genome) must contribute to the overall fitness. However, It appears that it is the virus ability to enter the cell by means of a resistant envelope rather than the RT that allows HIV to replicate more

efficiently under these conditions. To some extent, this observation may support the notion that, by means of phenotypic mixing, an otherwise detrimental feature (genotypic or phenotypic) might be useful for the virus in the face of a changing environment (Wilke and Novella 2003; Bellew and Chang 2006; Gelderblom, Vatakis et al. 2008).

Despite the few exceptions highlighted above, the overall findings suggest that the incorporation of certain mutant products inside the virions does not change drastically the function of the resulting phenotype. This supports the notion that phenotypic mixing might contribute to the viral robustness *in vivo*. To further address this issue, the fitness and infectivity values generated from these experiments will be feed into a complete mathematical model of HIV evolution.

6. References

- Alkhatib, G., C. Combadiere, et al. (1996). "CCR5: a RANTES, MIP-1alpha, MIP-1beta receptor as a fusion cofactor for macrophage-tropic HIV-1." Science **272**(5270): 1955-8.
- Althaus, C. L. and S. Bonhoeffer (2005). "Stochastic interplay between mutation and recombination during the acquisition of drug resistance mutations in human immunodeficiency virus type 1." J Virol **79**(21): 13572-8.
- Arien, K. K., G. Vanham, et al. (2007). "Is HIV-1 evolving to a less virulent form in humans?" Nat Rev Microbiol **5**(2): 141-51.
- Armitage, P. B., G. Matthews J.N.S. (2002). Statistical Methods in Medical Research, Blackwell Science Ltd.
- Arts, E. J., J. P. Marois, et al. (1996). "Effects of 3'-deoxynucleoside 5'-triphosphate concentrations on chain termination by nucleoside analogs during human immunodeficiency virus type 1 reverse transcription of minus-strand strong-stop DNA." J Virol **70**(2): 712-20.
- Arts, E. J., M. E. Quinones-Mateu, et al. (1998). "Mechanisms of clinical resistance by HIV-I variants to zidovudine and the paradox of reverse transcriptase sensitivity." Drug Resist Updat **1**(1): 21-8.
- Arts, E. J. and M. A. Wainberg (1994). "Preferential incorporation of nucleoside analogs after template switching during human immunodeficiency virus reverse transcription." Antimicrob Agents Chemother **38**(5): 1008-16.
- Badano, J. L., C. C. Leitch, et al. (2006). "Dissection of epistasis in oligogenic Bardet-Biedl syndrome." Nature **439**(7074): 326-30.
- Balvay, L., M. Lopez Lastra, et al. (2007). "Translational control of retroviruses." Nat Rev Microbiol **5**(2): 128-40.
- Barre-Sinoussi, F., J. C. Chermann, et al. (1983). "Isolation of a T-lymphotropic retrovirus from a patient at risk for acquired immune deficiency syndrome (AIDS)." Science **220**(4599): 868-71.
- Bateson, W. (1909). "Mendel's Principles of Heredity."

- Beerenwinkel, N., M. Daumer, et al. (2005). "Estimating HIV evolutionary pathways and the genetic barrier to drug resistance." J Infect Dis **191**(11): 1953-60.
- Bellew, R. K. and M. W. Chang (2006). "Modeling recombination's role in the evolution of HIV drug resistance." Artificial Life X: 3-7.
- Bonhoeffer, S., C. Chappey, et al. (2004). "Evidence for positive epistasis in HIV-1." Science **306**(5701): 1547-50.
- Boyer, P. L., S. G. Sarafianos, et al. (2001). "Selective excision of AZTMP by drug-resistant human immunodeficiency virus reverse transcriptase." J Virol **75**(10): 4832-42.
- Boyer, P. L., S. G. Sarafianos, et al. (2002). "Nucleoside analog resistance caused by insertions in the fingers of human immunodeficiency virus type 1 reverse transcriptase involves ATP-mediated excision." J Virol **76**(18): 9143-51.
- Brenner, S. (1957). "Genetic control and phenotypic mixing of the adsorption cofactor requirement in bacteriophages T2 and T4." Virology **3**(3): 560-74.
- Buchbinder, S. P., M. H. Katz, et al. (1994). "Long-term HIV-1 infection without immunologic progression." Aids **8**(8): 1123-8.
- Burch, C. L. and L. Chao (2004). "Epistasis and its relationship to canalization in the RNA virus phi 6." Genetics **167**(2): 559-67.
- Burge, B. W. and E. R. Pfefferkorn (1966). "Phenotypic mixing between group A arboviruses." Nature **210**(5043): 1397-9.
- Callahan, M. A., M. A. Handley, et al. (1998). "Functional interaction of human immunodeficiency virus type 1 Vpu and Gag with a novel member of the tetratricopeptide repeat protein family." J Virol **72**(10): 8461.
- Canivet, M., A. D. Hoffman, et al. (1990). "Replication of HIV-1 in a wide variety of animal cells following phenotypic mixing with murine retroviruses." Virology **178**(2): 543-51.
- Cao, Y., L. Qin, et al. (1995). "Virologic and immunologic characterization of long-term survivors of human immunodeficiency virus type 1 infection." N Engl J Med **332**(4): 201-8.
- Carlborg, O., L. Jacobsson, et al. (2006). "Epistasis and the release of genetic variation during long-term selection." Nat Genet **38**(4): 418-20.

- Carter, G. C., L. Bernstone, et al. (2009). "HIV entry in macrophages is dependent on intact lipid rafts." Virology **386**(1): 192-202.
- Chamberlain, P. P., J. Ren, et al. (2002). "Crystal structures of Zidovudine- or Lamivudine-resistant human immunodeficiency virus type 1 reverse transcriptases containing mutations at codons 41, 184, and 215." J Virol **76**(19): 10015-9.
- Chen, P., W. Hubner, et al. (2007). "Predominant mode of human immunodeficiency virus transfer between T cells is mediated by sustained Env-dependent neutralization-resistant virological synapses." J Virol **81**(22): 12582-95.
- Chun, T. W., D. Finzi, et al. (1995). "In vivo fate of HIV-1-infected T cells: quantitative analysis of the transition to stable latency." Nat Med **1**(12): 1284-90.
- Clark, S. J., M. S. Saag, et al. (1991). "High titers of cytopathic virus in plasma of patients with symptomatic primary HIV-1 infection." N Engl J Med **324**(14): 954-60.
- Coffin, J., A. Haase, et al. (1986). "What to call the AIDS virus?" Nature **321**(6065): 10.
- Coffin, J. M. (1979). "Structure, replication, and recombination of retrovirus genomes: some unifying hypotheses." J Gen Virol **42**(1): 1-26.
- Cordell, H. J. (2002). "Epistasis: what it means, what it doesn't mean, and statistical methods to detect it in humans." Hum Mol Genet **11**(20): 2463-8.
- Cordell, H. J. (2009). "Detecting gene-gene interactions that underlie human diseases." Nat Rev Genet **10**(6): 392-404.
- Cornell, M., K. Technau, et al. (2009). "Monitoring the South African National Antiretroviral Treatment Programme, 2003-2007: the IeDEA Southern Africa collaboration." S Afr Med J **99**(9): 653-60.
- Crotty, S., C. E. Cameron, et al. (2001). "RNA virus error catastrophe: direct molecular test by using ribavirin." Proc Natl Acad Sci U S A **98**(12): 6895-900.
- da Silva, J., M. Coetzer, et al. (2010). "Fitness epistasis and constraints on adaptation in a human immunodeficiency virus type 1 protein region." Genetics **185**(1): 293-303.

- Daecke, J., O. T. Fackler, et al. (2005). "Involvement of clathrin-mediated endocytosis in human immunodeficiency virus type 1 entry." J Virol **79**(3): 1581-94.
- de Visser, J. A. and S. F. Elena (2007). "The evolution of sex: empirical insights into the roles of epistasis and drift." Nat Rev Genet **8**(2): 139-49.
- de Visser, J. A., J. Hermisson, et al. (2003). "Perspective: Evolution and detection of genetic robustness." Evolution **57**(9): 1959-72.
- Deeks, S. G. and B. D. Walker (2007). "Human immunodeficiency virus controllers: mechanisms of durable virus control in the absence of antiretroviral therapy." Immunity **27**(3): 406-16.
- Derdeyn, C. A., J. M. Decker, et al. (2000). "Sensitivity of human immunodeficiency virus type 1 to the fusion inhibitor T-20 is modulated by coreceptor specificity defined by the V3 loop of gp120." J Virol **74**(18): 8358-67.
- Dixit, N. M. and A. S. Perelson (2004). "Multiplicity of human immunodeficiency virus infections in lymphoid tissue." J Virol **78**(16): 8942-5.
- Domingo, E., D. Sabo, et al. (1978). "Nucleotide sequence heterogeneity of an RNA phage population." Cell **13**(4): 735-44.
- Doms, R. W. and J. P. Moore (2000). "HIV-1 membrane fusion: targets of opportunity." J Cell Biol **151**(2): F9-14.
- Elena, S. F. (1999). "Little evidence for synergism among deleterious mutations in a nonsegmented RNA virus." J Mol Evol **49**(5): 703-7.
- Elena, S. F., P. Carrasco, et al. (2006). "Mechanisms of genetic robustness in RNA viruses." EMBO Rep **7**(2): 168-73.
- Elena, S. F., R. V. Sole, et al. (2010). "Simple genomes, complex interactions: epistasis in RNA virus." Chaos **20**(2): 026106.
- Embretson, J., M. Zupancic, et al. (1993). "Massive covert infection of helper T lymphocytes and macrophages by HIV during the incubation period of AIDS." Nature **362**(6418): 359-62.
- Feng, Y., C. C. Broder, et al. (1996). "HIV-1 entry cofactor: functional cDNA cloning of a seven-transmembrane, G protein-coupled receptor." Science **272**(5263): 872-7.

- Fisher, R. (1918). "The correlation between relatives on the supposition of Medelian inheritance." Trans. Roy. Soc. Edinb. **52**: 339-433.
- Fletcher, C. V., S. P. Kawle, et al. (2000). "Zidovudine triphosphate and lamivudine triphosphate concentration-response relationships in HIV-infected persons." AIDS **14**(14): 2137-44.
- Frankel, A. D. and J. A. Young (1998). "HIV-1: fifteen proteins and an RNA." Annu Rev Biochem **67**: 1-25.
- Ganser-Pornillos, B. K., M. Yeager, et al. (2008). "The structural biology of HIV assembly." Curr Opin Struct Biol **18**(2): 203-17.
- Gavrilets (2004). "Fitness Landscapes and the Origin of Species."
- Gelderblom, H. C., D. N. Vatakis, et al. (2008). "Viral complementation allows HIV-1 replication without integration." Retrovirology **5**: 60.
- Goodenow, M., T. Huet, et al. (1989). "HIV-1 isolates are rapidly evolving quasispecies: evidence for viral mixtures and preferred nucleotide substitutions." J Acquir Immune Defic Syndr **2**(4): 344-52.
- Gottlieb, M. S., R. Schroff, et al. (1981). "Pneumocystis carinii pneumonia and mucosal candidiasis in previously healthy homosexual men: evidence of a new acquired cellular immunodeficiency." N Engl J Med **305**(24): 1425-31.
- Gregersen, J. W., K. R. Kranc, et al. (2006). "Functional epistasis on a common MHC haplotype associated with multiple sclerosis." Nature **443**(7111): 574-7.
- Harrigan, P. R., S. Bloor, et al. (1998). "Relative replicative fitness of zidovudine-resistant human immunodeficiency virus type 1 isolates in vitro." J Virol **72**(5): 3773-8.
- Harris, R. S., K. N. Bishop, et al. (2003). "DNA deamination mediates innate immunity to retroviral infection." Cell **113**(6): 803-9.
- Harris, R. S. and M. T. Liddament (2004). "Retroviral restriction by APOBEC proteins." Nat Rev Immunol **4**(11): 868-77.
- Haseltine, W. A., J. M. Coffin, et al. (1979). "Structure of products of the Moloney murine leukemia virus endogenous DNA polymerase reaction." J Virol **30**(1): 375-83.
- Havlir, D. V. and D. D. Richman (1996). "Viral dynamics of HIV: implications for drug development and therapeutic strategies." Ann Intern Med **124**(11): 984-94.

- Ho, S. N., H. D. Hunt, et al. (1989). "Site-directed mutagenesis by overlap extension using the polymerase chain reaction." Gene 77(1): 51-9.
- Hsu, K., J. Seharaseyon, et al. (2004). "Mutual functional destruction of HIV-1 Vpu and host TASK-1 channel." Mol Cell 14(2): 259-67.
- Julias, J. G., A. L. Ferris, et al. (2001). "Replication of phenotypically mixed human immunodeficiency virus type 1 virions containing catalytically active and catalytically inactive reverse transcriptase." J Virol 75(14): 6537-46.
- Jung, A., R. Maier, et al. (2002). "Multiply infected spleen cells in HIV patients." Nature 418(6894): 144.
- Kijak, G. H. and F. E. McCutchan (2005). "HIV diversity, molecular epidemiology, and the role of recombination." Curr Infect Dis Rep 7(6): 480-8.
- Kliger, Y., S. G. Peisajovich, et al. (2000). "Membrane-induced conformational change during the activation of HIV-1 gp41." J Mol Biol 301(4): 905-14.
- Korber, B., M. Muldoon, et al. (2000). "Timing the ancestor of the HIV-1 pandemic strains." Science 288(5472): 1789-96.
- Kouyos, R. D., S. P. Otto, et al. (2006). "Effect of varying epistasis on the evolution of recombination." Genetics 173(2): 589-97.
- Kouyos, R. D., O. K. Silander, et al. (2007). "Epistasis between deleterious mutations and the evolution of recombination." Trends Ecol Evol 22(6): 308-15.
- Kramer, B., A. Pelchen-Matthews, et al. (2005). "HIV interaction with endosomes in macrophages and dendritic cells." Blood Cells Mol Dis 35(2): 136-42.
- Kwong, P. D., R. Wyatt, et al. (1998). "Structure of an HIV gp120 envelope glycoprotein in complex with the CD4 receptor and a neutralizing human antibody." Nature 393(6686): 648-59.
- Lacey, S. F. and B. A. Larder (1994). "Mutagenic study of codons 74 and 215 of the human immunodeficiency virus type 1 reverse transcriptase, which are significant in nucleoside analog resistance." J Virol 68(5): 3421-4.
- Landau, N. R., K. A. Page, et al. (1991). "Pseudotyping with human T-cell leukemia virus type I broadens the human immunodeficiency virus host range." J Virol 65(1): 162-9.

- Ledinko, N. and G. K. Hirst (1961). "Mixed infection of HeLa cells with polioviruses types 1 and 2." Virology **14**: 207-19.
- Levy, D. N., G. M. Aldrovandi, et al. (2004). "Dynamics of HIV-1 recombination in its natural target cells." Proc Natl Acad Sci U S A **101**(12): 4204-9.
- Liu, J., A. Bartesaghi, et al. (2008). "Molecular architecture of native HIV-1 gp120 trimers." Nature **455**(7209): 109-13.
- Lusso, P., F. di Marzo Veronese, et al. (1990). "Expanded HIV-1 cellular tropism by phenotypic mixing with murine endogenous retroviruses." Science **247**(4944): 848-52.
- Lusso, P., F. Lori, et al. (1990). "CD4-independent infection by human immunodeficiency virus type 1 after phenotypic mixing with human T-cell leukemia viruses." J Virol **64**(12): 6341-4.
- Maeda, Y., D. J. Venzon, et al. (1998). "Altered drug sensitivity, fitness, and evolution of human immunodeficiency virus type 1 with pol gene mutations conferring multi-dideoxynucleoside resistance." J Infect Dis **177**(5): 1207-13.
- Magnus, C., P. Rusert, et al. (2009). "Estimating the stoichiometry of human immunodeficiency virus entry." J Virol **83**(3): 1523-31.
- Mansky, L. M. and H. M. Temin (1995). "Lower in vivo mutation rate of human immunodeficiency virus type 1 than that predicted from the fidelity of purified reverse transcriptase." J Virol **69**(8): 5087-94.
- Mariani, R., D. Chen, et al. (2003). "Species-specific exclusion of APOBEC3G from HIV-1 virions by Vif." Cell **114**(1): 21-31.
- Markowitz, M., H. Mohri, et al. (2005). "Infection with multidrug resistant, dual-tropic HIV-1 and rapid progression to AIDS: a case report." Lancet **365**(9464): 1031-8.
- Martin, N. and Q. Sattentau (2009). "Cell-to-cell HIV-1 spread and its implications for immune evasion." Curr Opin HIV AIDS **4**(2): 143-9.
- McDougal, J. S., J. K. Nicholson, et al. (1986). "Binding of the human retrovirus HTLV-III/LAV/ARV/HIV to the CD4 (T4) molecule: conformation dependence, epitope mapping, antibody inhibition, and potential for idiotypic mimicry." J Immunol **137**(9): 2937-44.

- Mehle, A., B. Strack, et al. (2004). "Vif overcomes the innate antiviral activity of APOBEC3G by promoting its degradation in the ubiquitin-proteasome pathway." *J Biol Chem* **279**(9): 7792-8.
- Meyerhans, A., R. Cheynier, et al. (1989). "Temporal fluctuations in HIV quasispecies in vivo are not reflected by sequential HIV isolations." *Cell* **58**(5): 901-10.
- Michalakakis, Y. and D. Roze (2004). "Evolution. Epistasis in RNA viruses." *Science* **306**(5701): 1492-3.
- Montville, R., R. Froissart, et al. (2005). "Evolution of mutational robustness in an RNA virus." *PLoS Biol* **3**(11): e381.
- Neil, S. J., V. Sandrin, et al. (2007). "An interferon-alpha-induced tethering mechanism inhibits HIV-1 and Ebola virus particle release but is counteracted by the HIV-1 Vpu protein." *Cell Host Microbe* **2**(3): 193-203.
- Neumann, T., I. Hagmann, et al. (2005). "T20-insensitive HIV-1 from naive patients exhibits high viral fitness in a novel dual-color competition assay on primary cells." *Virology* **333**(2): 251-62.
- Nisole, S. and A. Saib (2004). "Early steps of retrovirus replicative cycle." *Retrovirology* **1**: 9.
- Norris, P. J. and E. S. Rosenberg (2002). "CD4(+) T helper cells and the role they play in viral control." *J Mol Med* **80**(7): 397-405.
- Novick, A. and L. Szilard (1951). "Virus strains of identical phenotype but different genotype." *Science* **113**(2924): 34-5.
- Nowak, A. M. M., R M (2000). *Virus Dynamics*, Oxford University Press Inc.
- Ortlund, E. A., J. T. Bridgham, et al. (2007). "Crystal structure of an ancient protein: evolution by conformational epistasis." *Science* **317**(5844): 1544-8.
- Otto, S. P. and A. C. Gerstein (2006). "Why have sex? The population genetics of sex and recombination." *Biochem Soc Trans* **34**(Pt 4): 519-22.
- Pantaleo, G. and A. S. Fauci (1996). "Immunopathogenesis of HIV infection." *Annu Rev Microbiol* **50**: 825-54.
- Parera, M., G. Fernandez, et al. (2007). "HIV-1 protease catalytic efficiency effects caused by random single amino acid substitutions." *Mol Biol Evol* **24**(2): 382-7.

- Parera, M., N. Perez-Alvarez, et al. (2009). "Epistasis among deleterious mutations in the HIV-1 protease." J Mol Biol **392**(2): 243-50.
- Peterlin, B. M. and D. Trono (2003). "Hide, shield and strike back: how HIV-infected cells avoid immune eradication." Nat Rev Immunol **3**(2): 97-107.
- Petropoulos, C. J., N. T. Parkin, et al. (2000). "A novel phenotypic drug susceptibility assay for human immunodeficiency virus type 1." Antimicrob Agents Chemother **44**(4): 920-8.
- Phair, J. P. (1994). "Keynote address: variations in the natural history of HIV infection." AIDS Res Hum Retroviruses **10**(8): 883-5.
- Phillips, P. C. (1998). "The language of gene interaction." Genetics **149**(3): 1167-71.
- Phillips, P. C. (2008). "Epistasis--the essential role of gene interactions in the structure and evolution of genetic systems." Nat Rev Genet **9**(11): 855-67.
- Rayner, M. M., B. Cordova, et al. (1997). "Population dynamics studies of wild-type and drug-resistant mutant HIV in mixed infections." Virology **236**(1): 85-94.
- Richman, D., C. K. Shih, et al. (1991). "Human immunodeficiency virus type 1 mutants resistant to nonnucleoside inhibitors of reverse transcriptase arise in tissue culture." Proc Natl Acad Sci U S A **88**(24): 11241-5.
- Richman, D. D. (1994). "Drug resistance in viruses." Trends Microbiol **2**(10): 401-7.
- Richman, D. D. (1994). "Resistance, drug failure, and disease progression." AIDS Res Hum Retroviruses **10**(8): 901-5.
- Rolland, M., C. Brander, et al. (2007). "HIV-1 over time: fitness loss or robustness gain?" Nat Rev Microbiol **5**(9): C1.
- Salami, A. K., J. A. Ogunmodele, et al. (2009). "Cryptococcal meningitis in a newly diagnosed AIDS patient: a case report." West Afr J Med **28**(5): 343-6.
- Saloura, V., P. D. Grivas, et al. (2009). "Intracerebral progression of Hodgkin lymphoma in a man with HIV." Postgrad Med **121**(6): 170-5.
- Salzwedel, K. and E. A. Berger (2000). "Cooperative subunit interactions within the oligomeric envelope glycoprotein of HIV-1: functional

- complementation of specific defects in gp120 and gp41." Proc Natl Acad Sci U S A **97**(23): 12794-9.
- Sanjuan, R., J. Forment, et al. (2006). "In silico predicted robustness of viroid RNA secondary structures. II. Interaction between mutation pairs." Mol Biol Evol **23**(11): 2123-30.
- Sanjuan, R., A. Moya, et al. (2004). "The contribution of epistasis to the architecture of fitness in an RNA virus." Proc Natl Acad Sci U S A **101**(43): 15376-9.
- Schindler, M., D. Rajan, et al. (2010). "Vpu serine 52 dependent counteraction of tetherin is required for HIV-1 replication in macrophages, but not in ex vivo human lymphoid tissue." Retrovirology **7**: 1.
- Schnittman, S. M., J. J. Greenhouse, et al. (1991). "Frequent detection of HIV-1-specific mRNAs in infected individuals suggests ongoing active viral expression in all stages of disease." AIDS Res Hum Retroviruses **7**(4): 361-7.
- Sherer, N. M., M. J. Lehmann, et al. (2007). "Retroviruses can establish filopodial bridges for efficient cell-to-cell transmission." Nat Cell Biol **9**(3): 310-5.
- Silander, O. K., O. Tenaillon, et al. (2007). "Understanding the evolutionary fate of finite populations: the dynamics of mutational effects." PLoS Biol **5**(4): e94.
- Simons, K. and E. Ikonen (1997). "Functional rafts in cell membranes." Nature **387**(6633): 569-72.
- Sluis-Cremer, N., D. Arion, et al. (2000). "Molecular mechanisms of HIV-1 resistance to nucleoside reverse transcriptase inhibitors (NRTIs)." Cell Mol Life Sci **57**(10): 1408-22.
- Slusher, J. T., S. K. Kuwahara, et al. (1992). "Intracellular zidovudine (ZDV) and ZDV phosphates as measured by a validated combined high-pressure liquid chromatography-radioimmunoassay procedure." Antimicrob Agents Chemother **36**(11): 2473-7.
- Sol-Foulon, N., M. Sourisseau, et al. (2007). "ZAP-70 kinase regulates HIV cell-to-cell spread and virological synapse formation." Embo J **26**(2): 516-26.

- Sougrat, R., A. Bartesaghi, et al. (2007). "Electron tomography of the contact between T cells and SIV/HIV-1: implications for viral entry." PLoS Pathog **3**(5): e63.
- Sourisseau, M., N. Sol-Foulon, et al. (2007). "Inefficient human immunodeficiency virus replication in mobile lymphocytes." J Virol **81**(2): 1000-12.
- Sowinski, S., C. Jolly, et al. (2008). "Membrane nanotubes physically connect T cells over long distances presenting a novel route for HIV-1 transmission." Nat Cell Biol **10**(2): 211-9.
- Spector, D. H., E. Wade, et al. (1990). "Human immunodeficiency virus pseudotypes with expanded cellular and species tropism." J Virol **64**(5): 2298-308.
- Stromberg, K., N. E. Hurley, et al. (1974). "Structural studies of avian myeloblastosis virus: comparison of polypeptides in virion and core component by dodecyl sulfate-polyacrylamide gel electrophoresis." J Virol **13**(2): 513-28.
- Stromberg, K. and S. H. Wilson (1974). "Structural studies of avian myeloblastosis virus. Selective release of ribonucleoprotein polypeptides from the core component and partial purification of the DNA polymerase." Biochim Biophys Acta **361**(1): 53-8.
- Tang, H., K. L. Kuhen, et al. (1999). "Lentivirus replication and regulation." Annu Rev Genet **33**: 133-70.
- Tantillo, C., J. Ding, et al. (1994). "Locations of anti-AIDS drug binding sites and resistance mutations in the three-dimensional structure of HIV-1 reverse transcriptase. Implications for mechanisms of drug inhibition and resistance." J Mol Biol **243**(3): 369-87.
- Tsetsarkin, K. A., C. E. McGee, et al. (2009). "Epistatic roles of E2 glycoprotein mutations in adaption of chikungunya virus to *Aedes albopictus* and *Ae. aegypti* mosquitoes." PLoS One **4**(8): e6835.
- Van Damme, N., D. Goff, et al. (2008). "The interferon-induced protein BST-2 restricts HIV-1 release and is downregulated from the cell surface by the viral Vpu protein." Cell Host Microbe **3**(4): 245-52.
- van Opijnen, T., M. C. Boerlijst, et al. (2006). "Effects of random mutations in the human immunodeficiency virus type 1 transcriptional promoter

- on viral fitness in different host cell environments." J Virol **80**(13): 6678-85.
- van Opijnen, T., A. de Ronde, et al. (2007). "Adaptation of HIV-1 depends on the host-cell environment." PLoS ONE **2**(3): e271.
- Vartanian, J. P., M. Henry, et al. (2002). "Sustained G-->A hypermutation during reverse transcription of an entire human immunodeficiency virus type 1 strain Vau group O genome." J Gen Virol **83**(Pt 4): 801-5.
- Wang, K., J. E. Mittler, et al. (2006). "Comment on "Evidence for positive epistasis in HIV-1"." Science **312**(5775): 848; author reply 848.
- Wild, C. T., D. C. Shugars, et al. (1994). "Peptides corresponding to a predictive alpha-helical domain of human immunodeficiency virus type 1 gp41 are potent inhibitors of virus infection." Proc Natl Acad Sci U S A **91**(21): 9770-4.
- Wildum, S., M. Schindler, et al. (2006). "Contribution of Vpu, Env, and Nef to CD4 down-modulation and resistance of human immunodeficiency virus type 1-infected T cells to superinfection." J Virol **80**(16): 8047-59.
- Wilke, C. O. and I. S. Novella (2003). "Phenotypic mixing and hiding may contribute to memory in viral quasispecies." BMC Microbiol **3**: 11.
- You, L. and J. Yin (2002). "Dependence of epistasis on environment and mutation severity as revealed by in silico mutagenesis of phage t7." Genetics **160**(4): 1273-81.
- Zavada, J. (1982). "The pseudotypic paradox." J Gen Virol **63** (Pt 1): 15-24.
- Zavada, J., J. Bubenik, et al. (1975). "Phenotypically mixed vesicular stomatitis virus particles produced in human tumor cell lines." Cold Spring Harb Symp Quant Biol **39** Pt 2: 907-12.
- Zucconi, S. L., L. P. Jacobson, et al. (1994). "Impact of immunosuppression on health care use by men in the Multicenter AIDS Cohort Study (MACS)." J Acquir Immune Defic Syndr **7**(6): 607-16.

7. Appendix

7.1 Table A1

Table A1a. Relative fitness values and statistics for the wild-type and AZT-resistant HIV-1 RTase mutants in the TZM-bl cell line

AZT (µM)	Statistics	Variants									
		WT	M41L	T215N	T215S	T215Y	M41L/T215N	M41L/T215S	M41L/T215Y		
0	Mean	0.49293	0.26555	0.32099	0.59467	0.23177	0.26802	0.50889			
	Var	0.03634	0.0017272	0.003336	0.0092782	0.0012855	0.0014603	0.0089212			
	Std dev	0.19053	0.041559	0.057758	0.096324	0.035854	0.038214	0.094452			
0.03	Mean	0.095315	0.0414465	0.020795	0.028879	0.048162	0.017927	0.019107	0.047226		
	Var	0.44741	0.46827	0.18123	0.22827	0.54255	0.17291	0.20357	0.50312		
	Std dev	0.0044882	0.0079099	0.0011664	0.0011296	0.010668	0.001054	0.00081364	0.0061188		
0.3	Mean	0.065994	0.088938	0.034153	0.03361	0.10328	0.032465	0.028524	0.078223		
	Var	0.033497	0.044469	0.0170765	0.016905	0.05164	0.0162325	0.014262	0.0391115		
	Std dev	0.051425	0.25668	0.092919	0.094054	0.45925	0.07909	0.10834	0.40557		
2	Mean	0.0019759	0.0015176	0.0003145	0.00040375	0.0055834	0.00012109	0.00037954	0.01002		
	Var	0.014057	0.040219	0.017734	0.020093	0.081138	0.011004	0.019482	0.1001		
	Std dev	0.0070285	0.0201095	0.008987	0.0100465	0.040569	0.005502	0.009741	0.05005		
5	Mean	0.0051893	0.064249	0.017045	0.018443	0.25434	0.015259	0.020222	0.33798		
	Var	2.51E-06	0.00016126	1.92E-05	6.20E-06	0.0013022	1.61E-05	7.88E-06	0.0030183		
	Std dev	0.0015848	0.012899	0.0043764	0.00249	0.036086	0.0040139	0.002807	0.054939		
10	Mean	0.0007924	0.0063495	0.0021882	0.001245	0.018043	0.00200695	0.0014035	0.0274695		
	Var	0.001186	0.027546	0.0054781	0.0068521	0.15889	0.0052818	0.0091683	0.20133		
	Std dev	6.11E-07	2.95E-05	1.99E-06	2.77E-06	0.00050966	1.00E-05	1.76E-06	0.0016762		
5	Mean	0.00078162	0.0054343	0.0014115	0.0016658	0.022576	0.0031688	0.0013262	0.040942		
	Var	0.00039081	0.00271715	0.00070575	0.0008329	0.011288	0.0015844	0.0006631	0.020471		
	Std dev	0.00037756	0.0099972	0.0016468	0.0025467	0.097839	0.0024935	0.0030081	0.16804		
10	Mean	5.80E-07	4.01E-06	5.53E-07	5.28E-07	0.00028192	6.91E-07	3.20E-07	0.00057946		
	Var	0.0007618	0.0020014	0.00074341	0.00072515	0.016791	0.0008314	0.00056569	0.024072		
	Std dev	0.0003909	0.0010007	0.000371705	0.000362575	0.0083955	0.0004157	0.000282845	0.012036		

Table A1b. Relative fitness values and statistics for the wild-type and AZT-resistant HIV-1 RTase mutants in PBMC from Donor 1

AZT (μ M)	Statistics	Variants									
		WT	M41L	T215N	T215S	T215Y	M41L/T215N	M41L/T215S	M41L/T215Y		
0	Mean	1	0.57193	0.29873	0.33441	0.50579	0.30354	0.47412	0.48842		
	Var	0.013094	0.011296	0.0019313	0.003367	0.0028137	0.00090975	0.0029509	0.0040698		
	Std. dev	0.11443	0.10628	0.043947	0.058025	0.053044	0.030162	0.054322	0.063795		
0.03	Std. err	0.057215	0.05314	0.0219735	0.0290125	0.026522	0.015081	0.027161	0.0318975		
	Mean	0.57248	0.5343	0.097951	0.11452	0.40772	0.11551	0.30437	0.4876		
	Var	0.0049237	0.010118	0.0010892	0.0016226	0.010228	0.00093316	0.0023029	0.0086912		
0.3	Std. dev	0.070169	0.10059	0.033003	0.040281	0.10113	0.030548	0.047889	0.093226		
	Std. err	0.0350945	0.050295	0.0165015	0.0201405	0.050565	0.015274	0.0239945	0.046613		
	Mean	0.1836	0.24162	0.0072649	0.017038	0.25798	0.019572	0.11819	0.30422		
2	Var	0.00092875	0.0032814	1.59E-05	8.43E-05	0.0016894	7.82E-05	0.00045846	0.0025129		
	Std. dev	0.030475	0.057283	0.0039862	0.0091832	0.04109	0.0089438	0.021412	0.050128		
	Std. err	0.0152375	0.0286415	0.0019931	0.0045916	0.020545	0.0044219	0.010706	0.025064		
5	Mean	0.048489	0.10539	0	0.0034896	0.14252	0.0085322	0.034745	0.17162		
	Var	0.00029066	0.00034245	0.00012238	6.47E-06	0.0013833	5.92E-05	0.00016548	0.0013456		
	Std. dev	0.017049	0.018505	0.011063	0.0025442	0.037192	0.0076925	0.012664	0.036683		
10	Std. err	0.0085245	0.0092525	0.0053145	0.0012721	0.018596	0.00394625	0.006432	0.0183415		
	Mean	0.017957	0.042661	0	0	0.073836	0	0.0078361	0.11186		
	Var	6.25E-05	0.00012238	0.00015948	0.00015948	0.00015948	0	1.18E-05	0.00089363		
	Std. dev	0.007907	0.011063	0.012629	0.012629	0.012629	0.0034401	0.0034401	0.029894		
	Std. err	0.0039535	0.0053145	0.0063145	0.0063145	0.0063145	0.00172005	0.00172005	0.014947		
	Mean	0	0.022027	0	0	0.028658	0	0.0057119	0.059252		
	Var		2.65E-05			9.89E-06		7.96E-06	3.42E-05		
	Std. dev		0.0051437			0.003143		0.0028207	0.0058499		
	Std. err		0.00257185			0.0015715		0.00141035	0.00292495		

Table A1c. Relative fitness values and statistics for the wild-type and AZT-resistant HIV-1 RTase mutants in PBMC from Donor 2

AZT (μM)	Statistics	Variants							
		WT	MA1L	T215N	T215S	T215Y	MA1L/T215N	MA1L/T215S	MA1L/T215Y
0	Mean	0.60398	0.20344	0.25286	0.70386	0.29144	0.49304	0.78211	
	Var	0.0073411	0.00064431	0.0012505	0.014985	0.0042076	0.0086832	0.0059639	
	Std dev	0.08569	0.025383	0.035363	0.12241	0.064866	0.093184	0.077226	
0.03	Std err	0.04284	0.0199275	0.0126915	0.0176815	0.061205	0.032433	0.046592	
	Mean	0.56022	0.50883	0.095828	0.10023	0.60567	0.12426	0.39282	
	Var	0.0025148	0.00131	0.00040334	0.00069277	0.0077787	0.00056515	0.002639	
0.3	Std dev	0.050148	0.036194	0.020083	0.026321	0.088197	0.023773	0.051362	
	Std err	0.025074	0.018097	0.0100415	0.0131605	0.0440985	0.0118965	0.025681	
	Mean	0.16226	0.16627	0.011927	0.01554	0.29251	0.038069	0.11565	
2	Var	0.00041961	0.00075498	8.14E-06	1.91E-06	0.00089438	1.85E-04	0.00020138	
	Std dev	0.020485	0.027477	0.0028524	0.0013832	0.028906	0.013586	0.014191	
	Std err	0.0102425	0.0137385	0.0014262	0.0006916	0.014953	0.006793	0.0070955	
5	Mean	0.042648	0.023637	0.00092379	0.0038235	0.11608	0.020068	0.00923	
	Var	3.00E-05	3.45E-05	5.80E-07	5.17E-07	0.00024885	2.07E-05	4.53E-06	
	Std dev	0.0054749	0.0058777	0.00076155	0.00071894	0.015775	0.0045548	0.002129	
10	Std err	0.00273745	0.00293885	0.000380775	0.00035947	0.0078875	0.0022774	0.0010645	
	Mean	0.0052242	0.011629	0	0	0.02723	0.0011425	0.0029013	
	Var	2.85E-05	6.11E-05	0	0	0.00013455	3.09E-07	1.18E-06	
0	Std dev	0.0053342	0.0078171	0	0	0.011599	0.00055551	0.0010847	
	Std err	0.0026671	0.00390855	0	0	0.0057895	0.000277755	0.00054235	
	Mean	0.0010917	0	0	0	0.010589	0	0	
0	Var	2.10E-06	0	0	0	2.12E-06	0	0	
	Std dev	0.0014494	0	0	0	0.0014559	0	0	
	Std err	0.0007247	0	0	0	0.00072795	0	0	

Table A2a. Epistasis values and statistics for the AZT-resistant HIV-1 RTase double mutants in the TZM-bl cell line

		Variants					
		General formulas			Bootstrap analysis		
AZT (µM)	Statistics	M41U7215N	M41U7215S	M41U7215Y	M41U7215N	M41U7215S	M41U7215Y
0	Mean	0.10097	0.1098	0.31576	1.01E-01	1.08E-01	3.15E-01
	Var	4.20E-03	5.67E-03	2.75E-02	3.83E-03	5.95E-03	2.76E-02
	Std dev	0.06491	0.075269	0.16573	6.19E-02	7.71E-02	1.66E-01
0.03	Std err	0.032405	0.0376345	0.082865	1.96E-03	2.44E-03	5.26E-03
	Mean	-0.0075061	-0.01581	-0.028959	-7.84E-03	-1.62E-02	-3.34E-02
	Var	8.75E-04	1.02E-03	7.14E-03	9.59E-04	1.06E-03	7.72E-03
0.3	Std dev	0.029575	0.031958	0.0845	3.10E-02	3.26E-02	8.79E-02
	Std err	0.0147875	0.015979	0.04225	9.79E-04	1.03E-03	2.78E-03
	Mean	-0.019783	-0.01857	-0.097025	-0.019524	-0.018497	-9.59E-02
2	Var	3.68E-05	4.50E-05	8.47E-04	3.51E-05	4.47E-05	8.68E-04
	Std dev	0.0060643	0.0067053	0.029096	5.92E-03	6.69E-03	2.95E-02
	Std err	0.00303215	0.00335265	0.014548	1.87E-04	2.11E-04	9.32E-04
5	Mean	-0.0010159	-0.00108	-0.014587	-0.0010133	-0.0010799	-0.014619
	Var	1.30E-07	8.27E-08	1.64E-05	1.21E-07	8.72E-08	1.73E-05
	Std dev	0.00036064	0.00028759	0.0040488	3.47E-04	2.95E-04	4.16E-03
10	Std err	0.00018032	0.000143795	0.0020244	1.10E-05	9.34E-06	1.31E-04
	Mean	-1.45E-04	-1.78E-04	-0.004138	-1.45E-04	-1.75E-04	-4.17E-03
	Var	2.49E-09	3.63E-09	1.18E-06	2.60E-09	3.66E-09	1.17E-06
0.03	Std dev	4.99E-05	6.02E-05	0.0010842	5.10E-05	6.05E-05	1.08E-03
	Std err	2.49705E-05	0.00003012	0.0000421	1.61E-06	1.91E-06	3.42E-05
	Mean	-1.55E-05	-2.43E-05	-9.15E-04	-1.54E-05	-2.41E-05	-9.19E-04
0.3	Var	7.24E-11	8.61E-11	8.45E-08	7.76E-11	8.56E-11	8.53E-08
	Std dev	8.51E-06	9.28E-06	2.91E-04	8.81E-06	9.25E-06	2.92E-04
	Std err	4.25495E-06	4.6401E-06	0.000145305	2.79E-07	2.93E-07	9.24E-06

7.2 Table A2

Table A2b. Epistasis values and statistics for the AZT-resistant HIV-1 RTase double mutants in PBMC from Donor 1.

AZT (μ M)	Statistics	General formulas				Bootstrap analysis	
		M41L/T215N	M41L/T215S	M41L/T215Y	M41L/T215N	M41L/T215S	M41L/T215Y
0	Mean	0.13269	0.28286	0.19914	0.13412	0.28663	0.20088
	Var	3.79E-03	8.34E-03	1.11E-02	0.0036157	0.0097278	0.01481
	Std.dev	0.061561	0.091299	0.1053	0.060131	0.09863	0.10715
	Std.err	0.0307805	0.0456495	0.05285	0.0019015	0.0031189	0.0033894
0.03	Mean	0.01379	0.11306	0.0613	0.013079	0.11456	0.05985
	Var	7.95E-04	1.83E-03	8.77E-03	0.00082894	0.0018623	0.009005
	Std.dev	0.028198	0.042831	0.093632	0.028791	0.043154	0.094895
	Std.err	0.014099	0.0214155	0.046816	0.00091046	0.0013647	0.0030008
0.3	Mean	0.0018382	0.017584	-0.0064763	0.0018504	0.017555	-0.0054002
	Var	4.22E-06	3.50E-05	4.96E-04	4.14E-05	3.33E-05	0.00049241
	Std.dev	0.0020538	0.0059167	0.02226	0.0020348	0.0057677	0.02219
	Std.err	0.0010269	0.00295835	0.01113	6.43E-05	0.00018239	0.00070172
2	Mean	Not Applicable	4.60E-05	-0.0066982	NA	5.01E-05	-0.0066068
	Var	(NA)	2.56E-07	3.49E-05		2.61E-07	3.64E-05
	Std.dev		0.00050573	0.0059083		0.00051072	0.0060318
	Std.err		0.000252865	0.00295415		1.62E-05	0.00019074
5	Mean	NA	NA	-0.0011412	NA	NA	-0.0011527
	Var			2.10E-06		1.99E-06	
	Std.dev			0.0014503		0.0014113	
	Std.err			0.00072515		4.46E-05	
10	Mean	NA	NA	NA	NA	NA	NA
	Var						
	Std.dev						
	Std.err						

Table A2c. Epistasis values and statistics for the AZT-resistant HIV-1 RTase double mutants in PBMC from Donor 2.

		General formulas					Bootstrapped analysis				
		Variants									
AZT (µM)		M41L/T215N	M41L/T215S	M41L/T215Y	M41L/T215N	M41L/T215S	M41L/T215S	M41L/T215Y			
0	Mean	0.16856	0.34031	0.35699	1.65E-01	3.37E-01	3.60E-01				
	Var	5.16E-03	1.11E-02	1.68E-02	5.00E-03	1.04E-02	1.75E-02				
	Std.dev	0.07186	0.10531	0.12952	7.07E-02	1.02E-01	1.32E-01				
	Std.err	0.03593	0.052655	0.06476	2.24E-03	3.23E-03	4.18E-03				
0.03	Mean	0.020853	0.16906	0.037667	2.10E-02	1.68E-01	4.23E-02				
	Var	3.35E-04	1.42E-03	6.80E-03	3.43E-04	1.46E-03	6.48E-03				
	Std.dev	0.018292	0.03763	0.081238	1.85E-02	3.82E-02	8.05E-02				
	Std.err	0.009146	0.018915	0.040619	5.86E-04	1.21E-03	2.55E-03				
0.3	Mean	0.0041938	0.016181	0.013825	0.0043255	0.016194	1.48E-02				
	Var	5.88E-06	1.12E-05	3.98E-04	5.93E-06	1.17E-05	4.35E-04				
	Std.dev	0.0024255	0.0033519	0.019954	2.43E-03	3.42E-03	2.09E-02				
	Std.err	0.00121275	0.00167595	0.009977	7.70E-05	1.08E-04	6.60E-04				
2	Mean	0.00083403	0.00030326	0.005245	0.00084001	0.00030908	0.0052025				
	Var	5.08E-08	1.17E-08	2.42E-06	4.99E-08	1.19E-08	2.53E-06				
	Std.dev	0.00022539	0.00010837	0.001555	2.23E-04	1.09E-04	1.59E-03				
	Std.err	0.000112695	0.000054185	0.0007775	7.06E-06	3.46E-06	5.03E-05				
5	Mean	NA	NA	0.00019382	NA	NA	2.08E-04				
	Var			3.60E-07			3.74E-07				
	Std.dev			0.00060003			6.12E-04				
	Std.err			0.000300015			1.93E-05				
10	Mean	NA	NA	NA	NA	NA	NA				
	Var										
	Std.dev										
	Std.err										

7.3 Table A3

Table A3a. Relative frequency values for the 2-point AZT-resistant HIV-1 RTase mutants in the TZM-bl cell line for Positive Epistasis (bold) and Negative Epistasis (italic).

AZT (μM)	M41UT215N Epistasis (No epistasis)	M41UT215S Epistasis (No epistasis)	M41UT215Y Epistasis (No epistasis)
0	$4.9 \cdot 10^{-2}$ <i>($4.3 \cdot 10^{-2}$)</i>	$5.3 \cdot 10^{-2}$ <i>($4.7 \cdot 10^{-2}$)</i>	$1.4 \cdot 10^{-2}$ <i>($7.8 \cdot 10^{-3}$)</i>
0.03	$6.34 \cdot 10^{-5}$ <i>($6.72 \cdot 10^{-5}$)</i>	$7.07 \cdot 10^{-5}$ <i>($8.16 \cdot 10^{-5}$)</i>	$5.5 \cdot 10^{-4}$ <i>($9.99 \cdot 10^{-3}$)</i>
0.3	$5.78 \cdot 10^{-5}$ <i>($9.999 \cdot 10^{-3}$)</i>	$6.92 \cdot 10^{-5}$ <i>($9.999 \cdot 10^{-3}$)</i>	$3.42 \cdot 10^{-4}$ <i>($9.999 \cdot 10^{-3}$)</i>
2	$5.25 \cdot 10^{-5}$ <i>($9.999 \cdot 10^{-3}$)</i>	$5.84 \cdot 10^{-5}$ <i>($9.999 \cdot 10^{-3}$)</i>	$9.998 \cdot 10^{-1}$ <i>($9.999 \cdot 10^{-3}$)</i>
5	$4.95 \cdot 10^{-5}$ <i>($9.999 \cdot 10^{-3}$)</i>	$6.0 \cdot 10^{-5}$ <i>($9.999 \cdot 10^{-3}$)</i>	$9.998 \cdot 10^{-1}$ <i>($9.999 \cdot 10^{-3}$)</i>
10	$5.33 \cdot 10^{-5}$ <i>($9.999 \cdot 10^{-3}$)</i>	$5.72 \cdot 10^{-5}$ <i>($9.999 \cdot 10^{-3}$)</i>	$9.999 \cdot 10^{-1}$ <i>($9.9992 \cdot 10^{-3}$)</i>

Table A3b. Relative frequency values for 2-point AZT-resistant HIV-1 RTase mutants in PBMC from Donor 1 for Positive Epistasis (bold) and Negative Epistasis (italic)

AZT (μM)	M41L/T215N Epistasis (No epistasis)	M41L/T215S Epistasis (No epistasis)	M41L/T215Y Epistasis (No epistasis)
0	<i>6.4*10⁻⁹</i> <i>(5.3*10⁻⁹)</i>	<i>8.6*10⁻⁹</i> <i>(5.6*10⁻⁹)</i>	<i>1.1*10⁻⁸</i> <i>(7.6*10⁻⁹)</i>
0.03	<i>3.1*10⁻⁸</i> <i>(2.9*10⁻⁸)</i>	<i>5.2*10⁻⁸</i> <i>(3.0*10⁻⁸)</i>	<i>1.9*10⁻⁷</i> <i>(8.4*10⁻⁸)</i>
0.3	<i>4.4*10⁻⁵</i> <i>(4.2*10⁻⁵)</i>	<i>7.8*10⁻⁵</i> <i>(4.4*10⁻⁵)</i>	<i>9.995*10⁻¹</i> <i>(9.997*10⁻¹)</i>
2	Not Applicable (NA)	<i>4.4*10⁻⁵</i> <i>(4.3*10⁻⁵)</i>	<i>9.997*10⁻¹</i> <i>(9.999*10⁻¹)</i>
5	NA	NA	<i>9.998*10⁻¹</i> <i>(9.999*10⁻¹)</i>
10	NA	NA	NA

Table A3c. Relative frequency values for 2-point AZT-resistant HIV-1 RTase mutants in PBMC from Donor 2 for with and without Epistasis.

AZT (μM)	MA1UT215N EPISTASIS (NO EPISTASIS)	MA1UT215S EPISTASIS (NO EPISTASIS)	MA1UT215Y EPISTASIS (NO EPISTASIS)
0	$6.3 \cdot 10^{-9}$	$9.0 \cdot 10^{-9}$	$3.6 \cdot 10^{-8}$
	($5.1 \cdot 10^{-9}$)	($5.4 \cdot 10^{-9}$)	($1.3 \cdot 10^{-8}$)
0.03	$2.3 \cdot 10^{-8}$	$6.0 \cdot 10^{-8}$	0.998
	($2.1 \cdot 10^{-8}$)	($2.1 \cdot 10^{-8}$)	($4.4 \cdot 10^{-4}$)
0.3	$5.2 \cdot 10^{-5}$	$1.3 \cdot 10^{-4}$	0.999
	($4.3 \cdot 10^{-5}$)	($4.4 \cdot 10^{-5}$)	(0.998)
2	$6.9 \cdot 10^{-9}$	$4.8 \cdot 10^{-9}$	0.9999
	($3.7 \cdot 10^{-9}$)	($3.9 \cdot 10^{-9}$)	($8.97 \cdot 10^{-5}$)
5	NA	NA	0.9999 (0.99988)
	NA	NA	
10	NA	NA	NA
	NA	NA	NA

7.4 Table A4

Table A4. Relative fitness values and statistics for the wild type and AZT-resistant HIV-1 RTase phenotypically mixed mutants in PBMC from Donor 3 (SEM: Standard Error of the Mean).

Variants	0µM AZT		1µM AZT		2µM AZT		5µM AZT		10µM AZT	
	Mean Fitness	SEM	Mean Fitness	SEM	Mean Fitness	SEM	Mean Fitness	SEM	Mean Fitness	SEM
100%WT	1	0.04404354	0.05281398	0.02097209	0.01493775	0.005984096	0.005873629	0.001503413	0	0
75%WT/25%MA1L	0.5689292	0.04874913	0.02837445	0.004744028	0.01289791	0.007849018	0.008402581	0.004139176	0.000337701	0.002336449
50%WT/50%MA1L	0.546052	0.008337315	0.01502498	0.009997628	0.008462962	0.007000396	0.008425961	0.004315841	0.000948914	0.001437645
25%WT/75%MA1L	0.5089615	0.07290415	0.03792289	0.01004998	0.009379138	0.01213582	0.008498534	0.002084463	0.000839671	0.008046423
100%MA1L	0.4705428	0.008838361	0.07215301	0.029596993	0.03750429	0.04594515	0.01210221	0.00484045	0.008615943	0.001984095
75%WT/25%T215Y	0.8832605	0.08127814	0.05177841	0.01394645	0.020366994	0.007253704	0.003413007	0.009590007	0.00083676	0.00121039
50%WT/50%T215Y	0.7086241	0.1011162	0.05247908	0.0098620215	0.0258261	0.003178915	0.004957592	0.001249703	0.000178498	0.00254415
25%WT/75%T215Y	0.698604	0.03666164	0.09236738	0.01026217	0.06813491	0.01150567	0.02919458	0.009753337	0.00482244	0.009097781
100%T215Y	0.5603107	0.1082984	0.1041139	0.01998594	0.07181243	0.02580053	0.031772	0.0153968	0.01126128	0.008782252
75%WT/25%MA1L/T215Y	0.8599299	0.07354484	0.08576999	0.02744549	0.05947848	0.00714825	0.01295623	0.01976435	0.000544379	0.009402538
50%WT/50%MA1L/T215Y	0.8278011	0.03319801	0.1453048	0.02086445	0.07762013	0.01150567	0.04405049	0.009753337	0.02022087	0.009097781
25%WT/75%MA1L/T215Y	0.6651542	0.0644123	0.1454315	0.02535958	0.09467709	0.08391032	0.05298696	0.04008622	0.02587813	0.008984441
100%MA1L/T215Y	0.6111014	0.1373881	0.2121919	0.1223786	0.1223021	0.1223786	0.08788782	0.01282479	0.05172885	0.04098069
75%MA1L/25%T215Y	0.4725479	0.05952987	0.07428817	0.05376913	0.04031248	0.02314785	0.01305036	0.01693531	0.006460901	0.004721322
50%MA1L/50%T215Y	0.5369338	0.1160907	0.07605389	0.04340458	0.04882629	0.0441241	0.01495862	0.003920514	0.00715202	0.009433345
25%MA1L/75%T215Y	0.5366505	0.03177311	0.0786752	0.06183594	0.05082021	0.01770496	0.02445375	0.01877801	0.00718401	0.01005693
75%MA1L/25%MA1L/T215Y	0.4814667	0.1597079	0.0881367	0.1062517	0.05154487	0.153986	0.0132301	0.007566699	0.007235159	0.02062931
50%MA1L/50%MA1L/T215Y	0.5910852	0.1496948	0.1214362	0.03391643	0.07505779	0.03274202	0.03716745	0.02629068	0.00878832	0.01539629
25%MA1L/75%MA1L/T215Y	0.5534797	0.2718719	0.1628188	0.02940801	0.1120546	0.08739694	0.06301503	0.04296213	0.02804992	0.05914909
75%T215Y/25%MA1L/T215Y	0.5600519	0.06355412	0.1061764	0.06275151	0.08202074	0.05399987	0.03219935	0.03298557	0.0115479	0.006445758
50%T215Y/50%MA1L/T215Y	0.5606163	0.06392162	0.1404335	0.06641655	0.0832504	0.02150463	0.03653479	0.03277564	0.01249282	0.008683193
25%T215Y/75%MA1L/T215Y	0.5622616	0.1082209	0.1669035	0.1039693	0.1107055	0.10401	0.07381325	0.04219854	0.0464285	0.02080273

7.5 Table A5

Table A5. % of infected cells for wild type and phenotypically mixed pseudotypes carrying up to a 1:4 ratio of wild type and T20^{Res} envelope proteins in PBMC from Donors 4 and 5 (SEM: Standard Error of the Mean)

PBMC	Variants	0 µg/ml T20		0.08 µg/ml T20		0.4 µg/ml T20		2 µg/ml T20		10 µg/ml T20	
		% Infected Cells	SEM	% Infected Cells	SEM						
	100% WT	100	3.076754	54.36134	4.990816	23.47171	3.335101	3.846244	0.6056673	0	0
	75% WT + 25% T20 ^{Res}	79.14925	8.361108	43.00667	10.94003	21.54305	0.333988	5.667526	0.08458702	0.3152763	0.3630468
	50% WT + 50% T20 ^{Res}	49.79912	3.038682	39.55836	9.507904	15.86469	6.120705	6.010878	0.1234311	1.099874	0.4850916
Donor 4	25% WT + 75% T20 ^{Res}	38.93894	4.887303	23.85419	3.788946	15.75987	2.323629	8.492281	0.1724702	3.434813	0.9394671
	100% T20 ^{Res}	12.49683	2.002919	9.890056	1.236346	9.750718	0.8649753	9.614284	0.8285527	4.258501	0.4050197
	100% WT	100	0.946191	58.73539	1.096511	19.09648	1.861947	1.077037	0.239028	0	0
	75% WT + 25% T20 ^{Res}	61.14094	6.740771	49.4929	5.404992	16.31021	0.711687	3.429438	0.5964896	0.5711613	0.2942498
	50% WT + 50% T20 ^{Res}	60.22849	0.8152806	35.31021	7.136646	16.26809	1.286958	3.352679	0.4144936	0.5649339	0.09882394
Donor 5	25% WT + 75% T20 ^{Res}	42.26957	8.375171	35.92802	1.433901	15.85109	2.985271	6.506673	0.7157134	2.350719	0.8656436
	100% T20 ^{Res}	14.5021	0.7809727	13.46215	0.8957732	11.16559	0.8396284	6.594039	0.2849459	4.579246	0.02292874

Table A6. Mean Relative fitness of variants carrying a combination of drug resistant RT and Envelope proteins from PBMC of Donors 6 and 7 (SEM: Standard Error of the Mean)

PBMC	Variants	0 Drug		0.1µM AZT + 0.1µg/ml T20		0.5µM AZT + 0.5µg/ml T20		2.5µM AZT + 0.5µg/ml T20		10µM AZT + 10µg/ml T20	
		Mean Relative Fitness	SEM	Mean Relative Fitness	SEM	Mean Relative Fitness	SEM	Mean Relative Fitness	SEM	Mean Relative Fitness	SEM
Donor 6	WT RT + WT ENV	1	0.035400395	0.2166359	0.08322736	0.008883047	0.01464777	0	0	0	0
	WT RT + T20 ^{Env} ENV	0.6366635	0.07664498	0.3594941	0.03042835	0.04598318	0.02433188	0.007140491	0.01012724	0	0
	T215Y RT + WT ENV	0.5739928	0.03456091	0.3398373	0.05652861	0.02689156	0.003458849	0	0	0	0
	T215Y RT + T20 ^{Env} ENV	0.2565475	0.06152567	0.479733	0.009178606	0.07438882	0.002234346	0.0201861	0.01354656	0.02014816	0.002824859
Donor 7	WT RT + WT ENV	1	0.021698958	0.1878458	0.1073189	0	0	0	0	0	0
	WT RT + T20 ^{Env} ENV	0.5487773	0.1472889	0.2454559	0.05454388	0.0298655	0.006738639	0	0	0	0
	T215Y RT + WT ENV	0.4936601	0.0187881	0.1842494	0.005719079	0.01457649	0.000981354	0	0	0	0
	T215Y RT + T20 ^{Env} ENV	0.07319191	0.03982785	0.2430201	0.03076634	0.03839329	0.01828801	0.0120552	0.001947546	0.005077221	0.006301713

7.6 Table A6

8. Acknowledgments

i) This thesis work was funded by the Deutscher Akademischer Austausch Dienst (DAAD). Doctoral Scholarship. Ref. A/06/04974 501 415

ii) I would like to specially thank my supervisor, Prof. Dr. Andreas Meyerhans for his support, guidance, interest, patience (lots of) and last, but not least, because he is a great individual. Thank you Sir.

iii) Without Prof. Bocharov and Anna Ignatovich involvement and dedication to this work, the statistical analysis would have been impossible to achieved. Thank you very much for the help and the beautiful time I spent in Moscow.

iv) I would like to thank my colleagues and the people of the Institute of Virology in Homburg. Thank you all!!

v) I thank Dr. Cecilia Galosi who introduced me to the field of virology.

vi) I would like to thank my friends. Specially Katharina and Martin, who were great supporters during my PhD period.

vii) I thank my Father, my Mother and my Sister. Even in the distance, without them I will be lost.

9. Curriculum Vitae

Personal Details

Name: Javier Pablo Martínez
Nationality: Argentinean / Spanish
Birth: October 4th of 1977, La Plata, BSAS, Argentina
Present Address: Kirrbergerstraße, Haus 47, 66421, Homburg (Saar), Germany.
Phone Number: 0049-0176-77028186
E-mail: vijmar@uniklinik-saarland.de
jmartinezvesga@yahoo.com.ar

University Education

2006-2010 **Ph.D. thesis. Title: “Consequences of HIV-1 Multinfection of Single Cells”** Institute of Virology, Department of Medical Microbiology, University of the Saarland, Germany. (**Submitted**)

1997-2004 **Bachelor in Biology.** Graduate Degree. Faculty Of Natural Sciences And Museum (FCNyM), National University Of La Plata (UNLP), Buenos Aires, Argentina.

Professional Education

2004-2006 **Graduate Assistant.** Project: Virological and Seroepidemiological Studies of Veterinary Interest, Isolation, Typification, Characterisation and Pathogenic Studies of Herpes viruses strains. Department Of

Virology, Faculty Of Veterinary Sciences, National University Of La Plata (UNLP), Buenos Aires, Argentina.

Short-Term Research Stays

- 01/2007 to 03/2007** Laboratory of Dr. Matthias T Dittmar, Department of Virology, Heidelberg University, Heidelberg, Germany.
- 08/2007** Laboratory of Prof. Dr. Utz Fischer, Department of Biochemistry, Theodor-Boveri-Institute, University of Würzburg, Würzburg, Germany.
- 02/2008 to 04/2008** Laboratory of Prof. Dr. Gennady Bocharov, Institute of Numerical Mathematics, Russian Academy of Sciences, Moscow, Russian Federation.
-

Teaching

- 2004-2006** **Instructor on Virological Methods.** Department Of Virology, Faculty Of Veterinary Sciences, National University Of La Plata (UNLP), Buenos Aires, Argentina.
-

Funding

- 2006-2010** **Deutscher Akademischer Austausch Dienst (DAAD).** Doctoral Scholarship. Ref. A/06/04974 501 415.

- 2009** **Individual grant** awarded for the International Bioinformatics Workshop on Virus Evolution and Molecular Epidemiology. Erasmus Postgraduate School of Molecular Medicine, Rotterdam, Netherlands.
- 2004-2006** **Subsidy of Research on Equine Production.** Project: Investigations on the pathogenic mechanisms of the Equine Herpes Virus 1 (EHV-1) in the production of abortions. Granted by the Direction of Equine Activities of the Secretariat of Agriculture, Cattle, Fishing and Food, and the Argentine Association of Equine Veterinary. Research Leader: Dr. Galosi CM. Research Team: **Javier P. Martínez**, Giselle M. Ocampos, Viviana Cid de la Paz, Maria E. Etcheverrygaray.
-

Workshops and Courses

- 2009** **International Bioinformatics Workshop on Virus Evolution and Molecular Epidemiology.** Erasmus Postgraduate School of Molecular Medicine, Rotterdam, Netherlands.
- 2008** **Russian-German Workshop on Systems Biology.** Helmholtz Association, Moscow, Russian Federation.
- 2005** **Postgraduate course on Applied Genetic Engineering.** National University of Quilmes, Bernal, Buenos Aires, Argentina. Hour Load: 130 hours theoretical-practical. With Test: Passed.
- 2004** **Postgraduate course on Laboratory Animals for Professionals and Researchers, FELASA (Federation Of European Laboratory Animal Science**

Associations), Category C. Central Bioterium, Veterinary Sciences, Buenos Aires University (UBA). Buenos Aires, Argentina. Hour Load: 80 hours theoretical-practical. With Test: Passed.

2004 **Postgraduate course on Gene Cloning and Expression By Recombinant DNA Techniques** Institute Of Experimental Biology and Medicine (IBYME) - Buenos Aires, Argentina. Hour Load: 32 hours theoretical-practical. With Test: Passed.

Scientific Meetings Attendance

2009 **The 16th International HIV Dynamics & Evolution Meeting.** Oxford University, Oxford, United Kingdom.
– Poster: Epistasis buffers HIV-1 fitness losses along an AZT-resistance pathway. **Martinez, JP**; Bocharov, G; Ignatovich, A; Reiter, J; Dittmar, MT; Wain-Hobson, S; Meyerhans, A.

2009 **German Society of Virology. Annual Meeting.** Leipzig, Germany.
- Poster: Epistasis buffers HIV-1 fitness losses along an AZT-resistance pathway. **Martinez, JP**; Bocharov, G; Ignatovich, A; Reiter, J; Dittmar, MT; Wain-Hobson, S; Meyerhans, A.

2006 **German Society of Virology. Annual Meeting.** Munich, Germany.
- Poster: Multi-infection and recombination in the intra-patient evolution of HIV. Bocharov, G; **Martinez, JP**; Breinig, T; Dittmar, MT; Wain-Hobson, S; Meyerhans, A.

- 2005** **VIII Argentinean Congress Of Virology.** Buenos Aires, Argentina.
- Poster: Molecular studies of the glycoprotein c (gC) codifying gene of the first Argentinean isolation of equine herpes virus type 1. Galosi, CM; **Martinez, JP**; Fernandez LC, Sguazza GH, Tizzano MA, Pecoraro MRI.
- Poster: Virulence study of a herpes virus type 1B strain in the Balb/C mouse experimental model. Ocampos GP, Barbeito CG, Cid de la Paz V, **Martinez JP**, Ayala MA, Gimeno EJ, Galosi CM.
- 2005** **The 12th International Symposium of the World Association of Veterinary Diagnostic Laboratories,** 7th OIE Seminar in Biotechnology, VIII Uruguayan Congress Of Veterinary Medicine. Buenos Aires, Argentina.
- Talk: First detection of genome 1B equine herpes virus type 1 in Argentina. **Martinez, JP**
- 2004** **Argentine Association of Veterinary Laboratory Diagnosticians (AAVLD) Meeting.** Buenos Aires, Argentina.
-Poster: DNA restriction patterns typification of equid herpes viruses strains isolated in Argentina between 1979 and 2003. Galosi CM, **Martinez, JP**, Fernandez LC, Martín Ocampos G, Vila Roza MV, Barrandeguy M, Fernandez F, Etcheverrigaray ME.
- 2002** **XXXI Congress of Genetic.** Argentinean Genetic Society (S.A.G) La Plata, Buenos Aires, Argentina. Auditor.
-

Publications

- 1) **Martinez, JP**; Bocharov, G; Ignatovich, A; Reiter, J; Dittmar, MT; Wain-Hobson, S; Meyerhans, A. Epistasis buffers HIV-1 fitness losses along an AZT-resistance pathway. *EMBO molecular medicine* SUBMITTED (2010)

- 2) **Martinez, JP**; Harnos, F; Jassoy, C; Meyerhans, A. Phenotypic mixing modulates the infectivity and fitness of HIV drug-resistant variants. IN PREPARATION (2010)

- 3) Herrmann, M; Ruprecht, K; Sauter, M; **Martinez, JP**; van Heteren, P; Glas, M; Best B; Meyerhans, A; Roemer K; Mueller-Lantzsch, N. Interaction of human immunodeficiency virus gp120 with the voltage-gated potassium channel BEC1. *FEBS Letters* 584, 3513-3518 (2010)

- 4) Markert, A; Grimm, M; **Martinez, JP**; Wiesner, J; Meyerhans, A; Meyuhas, O; Sickmann, A; Fischer, U. The La-related protein LARP7 is a component of the 7SK ribonucleoprotein and affects transcription of cellular and viral polymerase II genes. *EMBO reports* 9, 569–575 (2008)

- 5) **Martinez, JP**; Fernández, LC; Martín Ocampos GP; Cid de la Paz, V; Barrandeguy, M; Galosi, CM. Detection of equine herpesvirus 1 genome 1B in Argentina. *Rev. sci. tech. Off. int. Epiz.* 25 (3), 1075-1079 (2006)

- 6) Galosi CM, Cid de la Paz V, Fernandez LC, **Martínez, JP**, Craig MI, Barrandeguy M, Etcheverrigaray ME. Isolation of equine herpes virus 2 (EHV-2) from a lung of an aborted foetus. *J Vet Diagn Invest* 17:500–502 (2005)